

INFORMATION TO USERS

This manuscript has been reproduced from the microfilm master. UMI films the text directly from the original or copy submitted. Thus, some thesis and dissertation copies are in typewriter face, while others may be from any type of computer printer.

The quality of this reproduction is dependent upon the quality of the copy submitted. Broken or indistinct print, colored or poor quality illustrations and photographs, print bleedthrough, substandard margins, and improper alignment can adversely affect reproduction.

In the unlikely event that the author did not send UMI a complete manuscript and there are missing pages, these will be noted. Also, if unauthorized copyright material had to be removed, a note will indicate the deletion.

Oversize materials (e.g., maps, drawings, charts) are reproduced by sectioning the original, beginning at the upper left-hand corner and continuing from left to right in equal sections with small overlaps. Each original is also photographed in one exposure and is included in reduced form at the back of the book.

Photographs included in the original manuscript have been reproduced xerographically in this copy. Higher quality 6" x 9" black and white photographic prints are available for any photographs or illustrations appearing in this copy for an additional charge. Contact UMI directly to order.



University Microfilms International
A Bell & Howell Information Company
300 North Zeeb Road, Ann Arbor, MI 48106-1346 USA
313/761-4700 800/521-0600

Order Number 9132016

The optimal kinematic design of mechanisms

Park, Frank Chongwoo, Ph.D.

Harvard University, 1991

Copyright ©1991 by Park, Frank Chongwoo. All rights reserved.

U·M·I
300 N. Zeeb Rd.
Ann Arbor, MI 48106

HARVARD UNIVERSITY
THE GRADUATE SCHOOL OF ARTS AND SCIENCES



THESIS ACCEPTANCE CERTIFICATE
(To be placed in Original Copy)

The undersigned, appointed by the
Division of Applied Sciences
Department
Committee

have examined a thesis entitled
"The Optimal Kinematic Design of Mechanisms."

presented by Frank Chongwoo Park

candidate for the degree of Doctor of Philosophy and hereby
certify that it is worthy of acceptance.

Signature *Roger Brockett*
Typed name Professor R. Brockett

Signature *Jerry Clark*
Typed name Professor J. Clark

Signature *S.T. Yau*
Typed name Professor S.T. Yau (Mathematics)
Signature *J. Baillieul*
Professor J. Baillieul (B.U.)

Date April 25, 1991

The Optimal Kinematic Design of Mechanisms

A thesis presented

by

Frank Chongwoo Park

to

The Division of Applied Sciences

in partial fulfillment of the requirements

for the degree of

Doctor of Philosophy

in the subject of

Applied Mathematics

Harvard University

Cambridge, Massachusetts

May 1991

Copyright ©1991 by Frank Chongwoo Park

All rights reserved.

Abstract

In this thesis we develop a mathematical theory for optimizing the kinematic performance of robotic mechanisms, and as a main application obtain a collection of analytical tools for robot design. Judging from the sheer variety of kinematic chains found in nature, and given the wide range of robotic assembly tasks, it is unlikely that a single universal kinematic chain for robotics can be found. Nevertheless, two clearly desirable properties of general robotic mechanisms are that their workspace be large, and that they be able to generate motions and apply forces in arbitrary directions as easily as possible. This latter quality of a mechanism is generally what is meant by its *dexterity*. Clearly dexterity and workspace volume are intrinsic to a mechanism, so that any mathematical formulation of these properties should necessarily be independent of the particular coordinate representation of the kinematics.

Our focus in this thesis will be on the kinematic aspects of dexterity. By regarding the forward kinematics of a mechanism as defining a mapping between Riemannian manifolds, the coordinate-free language of differential geometry provides a natural setting for addressing the kinematic dexterity and workspace volume of a mechanism. An important consequence of this approach is that the geometric and topological structures of both the joint and work spaces are respected. One novel aspect of this thesis in this context is an engineering application of the theory of *harmonic maps*. Specifically, we show that the functional associated with harmonic mapping theory provides a natural measure of the kinematic dexterity of a mechanism; we call this measure the *kinematic distortion*. Extremizing this measure of dexterity then determines a unique design for the basic classes of mechanisms. We explore the relationship between kinematic dexterity and workspace volume, and compare this coordinate-free measure of kinematic dexterity with some other coordinate-free dexterity measures. Our results indicate that in order to fairly compare the kinematic dexterity between two mechanisms, the kinematic distortion of each mechanism should be normalized by the corresponding workspace volume. We also suggest some ways in which the dynamics of a mechanism might be included into a mathematical formulation of dexterity.

Acknowledgements

I gratefully acknowledge the support and guidance of my thesis advisor, Roger Brockett, whose impact on this thesis has made it a joint work in every sense. His intellectual guidance, generosity, and sense of humor have certainly made my experience as a graduate student rewarding and enjoyable. I would also like to acknowledge the other members of my thesis advisory committee, Shing-Tung Yau, Jim Clark, and John Baillieul, for their interest and useful commentary, in particular Shing-Tung Yau for his suggestion on applying harmonic mapping theory to kinematics. Fellow graduate students Ken Keeler, Yang Wang, and Wen Cebuhar deserve special mention for lending me their mathematical expertise, as well as for prolonging my stay in graduate school with endless discussions on topics of a decidedly unscientific nature. I would also like to acknowlege Bill Nowlin, Nicola Ferrier, Ed Rak, Steve Smith, and Ann Stokes for their friendship, as well as their valuable assistance throughout various stages of this work. Finally, special thanks to the Western Avenue crew (Sandy, Al, Ben, Bryan, Seung-Jin) for their close friendship and support these past few years.

Contents

1	Introduction	1
1.1	Understanding the Performance of a Mechanism	1
1.2	Previous Work	3
1.3	A Geometric Approach	5
1.4	Outline of Thesis	7
2	Kinematics: Geometric Theory	9
2.1	Mathematical Background	10
2.1.1	Lie Groups and Lie Algebras	10
2.1.2	Riemannian Metrics on Lie Groups	14
2.2	Euclidean Motions	17
2.2.1	$SO(3)$	18
2.2.2	$SE(3)$	22
2.3	Kinematic Mappings	24
2.3.1	The Product-of-Exponentials Kinematic Equations	24
2.3.2	Computational Aspects	28
2.4	Summary	32
3	Kinematic Performance	33
3.1	Workspace Volume	34
3.2	Kinematic Dexterity	35
3.2.1	Harmonic Maps and Kinematic Distortion	36
3.2.2	Other First-Order Measures	40

3.2.3	Second-Order Measures	43
3.2.4	The Configuration Space Metric and Actuator Strengths	45
3.2.5	Example: A 2R Spherical Mechanism	46
3.3	Summary	49
4	Planar Mechanisms	50
4.1	Open-Chain Planar Mechanisms	51
4.1.1	Link Lengths for Maximal Workspace Volume	52
4.1.2	Link Lengths for Minimum Kinematic Distortion	54
4.1.3	Optimal Joint Actuator Selection	57
4.2	A Planar Closed Chain	58
4.3	Summary	61
5	Spherical and Spatial Mechanisms	62
5.1	Spherical Mechanisms	62
5.1.1	Workspace Volume	63
5.1.2	Kinematic Distortion	68
5.1.3	Comparison with Other Dexterity Measures	73
5.2	Spatial Mechanisms	74
5.2.1	Workspace Volume	74
5.2.2	Kinematic Distortion	76
5.3	Summary	80
6	Conclusions	82
6.1	Summary	82
6.2	Dynamics	85
6.3	Concluding Remarks	89

List of Figures

3.1	A 2R spherical mechanism.	46
3.2	$f : T^2 \rightarrow S^2$ as a mapping from a cylinder to a sphere.	47
4.1	An n -link planar open-chain mechanism.	51
4.2	A planar closed-chain mechanism.	58
4.3	(a) A four-bar crank-rocker, and (b) a double-crank.	59
4.4	Distortion versus F_2 for the double-crank configuration.	61
5.1	A three-link spherical wrist mechanism.	63
5.2	The orienting region for an nR -wrist.	66
5.3	A 3R, two-link spatial chain.	76
5.4	Three designs for a 7R manipulator.	78
6.1	The pullback of a vector bundle.	88
6.2	A mechanical system.	88

Chapter 1

Introduction

1.1 Understanding the Performance of a Mechanism

The design of robotic mechanisms is best described as an eclectic discipline consisting of experience, human intuition, and a disparate set of analytical tools that are mostly *ad hoc*. The goal of this thesis is to develop a mathematical theory for optimizing the kinematic performance of mechanisms; we envisage our efforts as part of a broader program whose goal is to develop a theoretical foundation for the design of robot arms, end-effectors, and legs. Judging from the variety of mechanisms found in nature, however, and given the enormous space of possible designs, one can appreciate the formidability of developing such a theory. A typical robot design, for example, requires making choices between closed and open chains, rigid and flexible links, and various types of actuators, to list a few.

To maintain a tractable scope, we focus our attention on two specific but fundamental performance criteria for robotic mechanisms, the *workspace volume* and *kinematic dexterity*. Since the primary function of a robot is to generate forces and motions that cause objects to move in desired ways, a robot should have a large workspace, and also be able to move and apply forces in arbitrary directions as easily as possible. This latter quality of a mechanism is generally what is meant by its dexterity. A further distinction is made between *local* and *global* dexterity. Local dexterity measures a mechanism's dexterity at a particular configuration, and is useful for resolving redundancy or determining the optimal dexterous configuration of a mechanism. Global dexterity, on the other hand, measures the overall

dexterity of a mechanism in some average sense, and hence is useful for design purposes.

While the conceptual simplicity of our description of dexterity has obvious appeal, any attempt to formulate this notion mathematically makes it apparent that a more precise description is needed. What is also unclear is the exact level at which this mathematical formulation is to occur: the workspace volume of a mechanism is a purely kinematic property, but because physical motion of objects is governed by their dynamics, dexterity clearly involves both the kinematics and dynamics of a mechanism. Our main emphasis will be on the kinematic aspects of dexterity, which in some sense are fundamental to understanding the more complex effects of the dynamics. An interesting by-product of our kinematic analysis, however, provides some answers to questions concerning the actuators of a mechanism, such as what the relative strengths of the actuators should be, or, when choices for actuator placement exist (as in certain closed chains), which joint should be actuated. An investigation of the tradeoffs between global dexterity and workspace volume also suggests that these two measures should not be treated as separate entities. Rather, the workspace volume acts as a normalizing factor when comparing the global dexterity of different mechanisms.

Having hinted at the scope of the problem at hand, we now mention some of the performance and design issues not addressed. Foremost among these are the nonmechanical performance measures based on the electronics or software controlling the mechanism; these measures more aptly describe *controller* performance. In addition, a number of other non-kinematic design factors exist that also influence a mechanism's dexterity. For example, a designer can choose to actuate a joint directly, or through gearing and transmission systems. Also, the natural frequency associated with the structure of a mechanism, or the *mechanical bandwidth*, affects the "ease of controllability", and is an important consideration when designing mechanical structures in tandem with their control. This is but one aspect of a recently emergent trend toward an integrated approach to design, one that considers the effects of actuators, sensors, computational and communication elements on the overall performance of the mechanism. These approaches, as one might guess, are based largely on heuristics.

Before reviewing some previous research in the area of dexterity and workspace analysis

we clarify some terminology. A *mechanism* is defined as a set of rigid bodies, or *links*, connected by *joints* so that their relative motion is constrained. The two most common types of joints found in mechanisms are the *prismatic*, or sliding joint, and the *revolute* joint. More complex joints with additional degrees of freedom can be modelled as a connection of these basic joints by links of length zero. The notation ‘ nR ’ will mean a mechanism with n revolute joints; ‘ nP ’ similarly refers to mechanisms with n prismatic joints. *Mechanisms* have traditionally been identified with closed-chain linkages, such as the four-bar linkage, and *manipulators* with open-chain linkages. This distinction has recently become somewhat blurred, however. We therefore use these terms interchangeably, and where closed chains are discussed we describe their exact geometry.

1.2 Previous Work

Of the two kinematic performance criteria addressed in this thesis, the workspace volume has, beginning with the work of Roth[38], received the greater share of attention. One of the first notions of manipulator workspace is defined as the set of points in \mathbb{R}^3 reachable by the tip: this space is aptly denoted the *reachable workspace*. The subset of the reachable workspace at which the tip can assume any arbitrary orientation is termed the *dexterous workspace* (Kumar and Waldron[27]). The ratio of dexterous workspace volume to reachable workspace volume has been proposed as one measure of workspace quality (Gupta[20]).

A more geometric investigation of workspace volume was undertaken by Paden and Sastry in [32]. In their approach the workspace is considered not as a subset of \mathbb{R}^3 , but more naturally as a subset of the space of rigid-body motions. Unlike the previous notions of dexterous workspace, this notion of the workspace allows for a smooth tradeoff between position and orientation. It is moreover a natural measure in the sense that the volume is translation-invariant, *i.e.*, it does not change when the reference frame is translated and rotated. Using this natural measure of volume, they show that the geometry of a 6R open-chain mechanism which maximizes workspace volume is the elbow manipulator configuration; this is the anthropomorphic geometry common in many current industrial manipulator designs. We summarize their results in more detail in chapter 5.

Much of the previous work on dexterity has concentrated on measures for local dexterity,

usually by quantifying the “distance” from a singularity. Recall that a mechanism is at a singularity when its tip loses at least one degree of freedom of motion along some direction in the workspace, which also corresponds to a loss of rank in its Jacobian matrix. To fix notation in the following discussion let $f : N \rightarrow M$ denote the forward kinematic map from the n -dimensional joint space N to the m -dimensional tip space M , and let J be its Jacobian. Express the singular value decomposition of J as $J = U\Sigma V^T$, where the singular values σ_i are arranged along the principal diagonal of Σ (see, e.g., Golub and Van Loan[17]). In [45] Yoshikawa shows that for $n \geq m$, the image of the $(n - 1)$ -dimensional sphere $\{v \in \mathbb{R}^n | v_1^2 + \dots + v_n^2 = 1\}$ under J is an ellipsoid with principal axes $\sigma_1 u_1, \dots, \sigma_m u_m$, where u_i is the i th column of U . We call this ellipsoid the *velocity ellipsoid* associated with J . He defines the *manipulability* of a robotic mechanism with $n \geq m$ as

$$\eta = \sqrt{\det J(\theta)J^T(\theta)}$$

which can alternatively be expressed as the product of the singular values of the Jacobian, i.e., $\eta = \sigma_1 \sigma_2 \cdots \sigma_m$. For any fixed m and n the volume of the velocity ellipsoid is also proportional to this product. η can therefore be interpreted as a *local* measure of the kinematic map’s volume-preserving capability; it is useful for comparing the mechanism’s “volume gain” at different configurations.

While the zeros of η clearly mark the presence of singularities, numerical analysts have noted that its actual value is usually not an accurate indicator of a particular configuration’s proximity to a singularity. Instead, the *condition number* of the Jacobian, defined as $\text{cond}(J) = \frac{\sigma_{\max}}{\sigma_{\min}}$, has been applied by Salisbury and Craig[41] as a local dexterity measure. The condition number represents the spatial uniformity of the velocity ellipsoid, such that if $\text{cond}(J)$ attains the minimum value of one the velocity ellipsoid then assumes a spherical shape. This criterion can also be interpreted as a measure of the accuracy with which the mechanism can generate output forces from input torques. Since the singularities are also marked by the minimum singular values going to zero, one can alternatively consider the minimum singular value as a measure of local kinematic dexterity. A review of these and other local kinematic dexterity measures is provided in Klein and Blaho[26].

While Salisbury and Craig apply the condition number as a local dexterity measure, Gosselin and Angeles[18] extend it to a global dexterity measure for $n = m$. More specifi-

cally, they define the *global conditioning index* as the ratio D/V , where

$$D = \int_W \left(\frac{1}{\kappa}\right) dW$$

and

$$V = \int_W dW$$

Here V denotes the volume of the workspace W , and $\kappa(\cdot)$ is the condition number of the Jacobian. An alternative global dexterity measure can be obtained by substituting, in the expression for D , the reciprocal of the condition number by the minimum singular value. Observe that D should really be defined as a joint space integral, since its integrand $\frac{1}{\kappa}$ is a function defined over the joint space.

The dexterity measures considered thus far are based only on a mechanism's kinematics. In [3] Asada introduces the *generalized inertia ellipsoid* (GIE) as a dynamics-based dexterity measure, analogous to the velocity ellipsoid of kinematics. For a nonredundant mechanism with $n = m$ the GIE is determined by the eigenvalues and eigenvectors of $J^{-T} M J^{-1}$, where M is the inertia matrix of the mechanism. In a similar vein, Yoshikawa[46] defines the *dynamic manipulability measure* (DMM) for mechanisms with $n \geq m$ as $\det(J(M^T M)^{-1} J^T)$. A duality exists between these two concepts of dexterity: the DMM measures dexterity of the mechanism when it is regarded as a mapping from joint space to tip space, whereas the GIE measures dexterity in the reverse sense. Still another measure of dynamic dexterity is the *dynamic conditioning index* (DCI) proposed by Ma and Angeles[29]. The DCI indicates how close the inertia matrix is to being purely diagonal, and thus measures the extent of the interaction forces and torques between links.

1.3 A Geometric Approach

Although many of the proposed measures for dexterity and workspace volume are conceptually equivalent, it is evident that they can be formulated in a number of ways. The various dexterity measures, moreover, lead to some strikingly different conclusions about certain simple mechanisms. While they are in general intuitively reasonable, these measures in many cases do not respect the fundamental property of *coordinate-invariance*.

More specifically, the previous dexterity criteria are formulated in terms of an explicit coordinate representation of the kinematics. Although this approach is often accepted without question, it is often difficult to distinguish between properties of the particular coordinate representation with the kinematic properties of the mechanism. Dexterity obviously is a geometric property that should not depend on the choice of coordinates. Another drawback associated with these dexterity measures is that most are defined locally, and the global measures proposed unfortunately are defined only for mechanisms whose tip and configuration spaces have the same dimension. It must also be recognized that the space of positions and orientations is fundamentally different from \mathbb{R}^6 ; only locally can it be represented in this way. What is desirable, it seems, is a definition of dexterity that is intrinsic (*i.e.*, defined in a coordinate-invariant way), and that also takes into account the topological nature of the space of positions and orientations.

With these goals in mind we take the following approach. The forward kinematics of a mechanism are viewed as defining a mapping $f : N \rightarrow M$ between Riemannian manifolds. The tip space M is usually taken to be the group of *Euclidean motions* $SE(3)$, which in the robotics literature is often identified with the 4×4 homogeneous transformations. The principal tool for representing a mechanism's kinematics is the *product-of-exponentials* formula; this representation establishes the connection between the classical screw theory of rigid motions and the geometric methods of Lie groups and Lie algebras (Brockett[6]).

Although kinematic theory has evolved, for the most part, without modern geometry playing any direct role in its development, the commonly used coordinate-based approaches, which are quite cumbersome to work with, do not provide a global representation of the set of rigid-body motions. For example, the standard Euler angle representations for rotations are known to be degenerate at certain points. While true kinematic statements can be expressed in many ways, we argue that the intrinsic language of geometry offers the most natural means of representing the global kinematic properties of mechanisms; this in some sense parallels the motivation behind the recent geometric approach to classical mechanics (Arnold[2], Abraham and Marsden[1]). One can also take advantage of the large body of related mathematical theory, and one of the main ideas developed in this thesis is the characterization of the kinematic dexterity by the functional used in the definition of *harmonic*

mappings. Intuitively, the theory of harmonic maps is concerned with characterizing the maps of minimum distortion between Riemannian manifolds. We show that its associated functional provides a natural, coordinate-invariant way of defining global kinematic dexterity. The development of the theory of harmonic maps is fairly recent, and relatively little effort has been devoted to examining the potential applications of the theory to engineering problems. However, theoretical physicists have applied harmonic mapping theory to investigate the curvature of the spacetime bundle, as an alternative to Yang-Mills theory.

Although, from a certain point of view, the harmonic mapping functional is the most natural measure of the distortion of a mapping between Riemannian manifolds, there exist a number of other invariantly-defined functionals which merit investigation in the context of kinematic dexterity. Among these we will consider second-order measures based on the curvature of the joint and tip spaces, as well as some local first-order measures related to the velocity ellipsoid characterization of dexterity discussed above. These local measures in turn extend naturally to global measures, which we also discuss. It is also not surprising that in many cases these higher-order measures simplify to the harmonic mapping distortion.

1.4 Outline of Thesis

The material presented in this thesis should be readily accessible to engineers and applied mathematicians who are familiar with the basic concepts of calculus on manifolds and differential forms, at the level of Spivak's introductory text[42]. While these subjects are usually not standard mathematical fare for most engineers, the clarity with which one can express the kinematic and dynamic relationships of mechanisms using this language makes it worthwhile, we believe, to invest some effort in understanding the basic ideas. Accordingly, the development here is less terse than the style customary of modern abstract mathematics, but also reasonably complete.

The material is treated in the following order. In chapter 2 we present a geometric approach to the theory of kinematics, and in chapter 3 we formulate measures for the workspace volume and kinematic dexterity of a mechanism. In chapters 4 and 5 we apply these criteria to investigate the kinematic performance of the three basic classes of mechanisms. Chapter 4 studies the singularities, workspace volume, and kinematic dexterity of

planar open-chain mechanisms, as well as a simple closed-chain planar mechanism. The first half of chapter 5 covers these same topics for spherical mechanisms. With the insight drawn from the analysis of planar and spherical mechanisms, we then proceed to the most general class of mechanisms, the spatial mechanisms. In chapter 6 we summarize the main results and suggest some ways in which the dynamics of a mechanism might be included into a mathematical formulation of dexterity.

Chapter 2

Kinematics: Geometric Theory

In this chapter we review some facts about Lie groups and Riemannian geometry, and then show how these ideas may be used to model mechanisms as mappings between Riemannian manifolds. For our purposes The manifolds of most interest are the n -torus, T^n , and $SE(3)$, the group of rigid-body motions. $SE(3)$ can also be identified with the 4×4 homogeneous transformations appearing in the robotics literature. After introducing coordinate-free definitions and some basic properties of general Lie groups, we examine some particular aspects of $SE(3)$, expressing certain important quantities in the two fundamental coordinate systems defined on Lie groups. We will work almost exclusively with a particular matrix representation of $SE(3)$; not only does this unify the analysis, but it also identifies the geometric definitions with the standard treatments of kinematics.

The product-of-exponentials equations provide a general representation of the forward kinematics of open-chain mechanisms, through which the underlying connections with Lie groups and Lie algebras are made explicit. While this feature gives it geometric appeal, we show that it is also attractive from a computational viewpoint, and can serve as a useful alternative to the standard kinematic representations for a wide class of applications.

2.1 Mathematical Background

2.1.1 Lie Groups and Lie Algebras

Let \mathfrak{G} be a set which is simultaneously a manifold and a group. Then \mathfrak{G} is a *Lie group* provided the mappings defined by

$$\mathfrak{G} \times \mathfrak{G} \rightarrow \mathfrak{G}, \quad (a, b) \mapsto ab$$

and

$$\mathfrak{G} \rightarrow \mathfrak{G}, \quad a \mapsto a^{-1}$$

are smooth (*i.e.*, infinitely differentiable). In particular, given an element $a \in \mathfrak{G}$, the maps $L_a, R_a : \mathfrak{G} \rightarrow \mathfrak{G}$ taking $g \mapsto ag$ and $g \mapsto ga$, respectively, are diffeomorphisms of \mathfrak{G} onto itself, and are known as *left translation* and *right translation* by a , respectively.

There exist a number of ways of representing \mathfrak{G} by a set of linear transformations $\{\sigma_g : V \rightarrow V\}$ on a vector space V . Such a set is known as a *linear or matrix representation* of the Lie group.

Example 2.1 $Gl(n)$, the set of nonsingular $n \times n$ matrices, is an open submanifold of $\Re^{n \times n}$, and is a group with respect to matrix multiplication. The maps $(A, B) \mapsto AB$ and $A \mapsto A^{-1}$ are smooth, and $Gl(n)$ is therefore a Lie group.

Example 2.2 $SO(n)$, the set of $n \times n$ orthogonal transformations with unit determinant, is a Lie group under matrix multiplication.

Example 2.3 $SE(3)$, the special Euclidean group, has the standard linear representation

$$\left\{ \begin{bmatrix} \Theta & x \\ 0 & 1 \end{bmatrix} \mid \Theta \in SO(3), x \in \Re^3 \right\}$$

We will alternatively use the notation (Θ, x) for an element of $SE(3)$ in this representation, with group multiplication understood to be $(\Theta_1, x_1) \cdot (\Theta_2, x_2) = (\Theta_1 \Theta_2, \Theta_1 x_2 + x_1)$.

We now review the definition of a *Lie algebra*. A Lie algebra is a vector space, \mathfrak{g} , equipped with a bilinear map, $[,] : \mathfrak{g} \times \mathfrak{g} \rightarrow \mathfrak{g}$ called the *Lie bracket*, which is *anti-symmetric* (*i.e.*, $[\xi, \eta] = -[\eta, \xi]$) and satisfies Jacobi's identity:

$$[[\xi, \eta_1], \eta_2] + [[\eta_2, \xi], \eta_1] + [[\eta_1, \eta_2], \xi] = 0$$

Associated with every Lie group is its Lie algebra, which is defined in terms of vector fields; recall that a vector field ξ on a manifold M is a smooth function assigning to each point p of M a tangent vector $\xi_p \in T_p M$. A vector field ξ on a Lie group \mathfrak{G} is *left-invariant* if dL_a , the derivative of the left translation mapping L_a , satisfies $dL_a \xi = \xi$ for all $a \in \mathfrak{G}$. Although we do not show it here, the set of left-invariant vector fields on a manifold forms a Lie algebra; see, *e.g.*, Spivak[43] for details. From the definition of left-invariance it follows that the value of the left-invariant vector field ξ at a is determined by its value at the identity, e . Hence the map

$$\mathfrak{g} \rightarrow T_e \mathfrak{G}, \quad \xi \mapsto \xi(e)$$

is bijective, and for this reason the Lie algebra \mathfrak{g} of a Lie group \mathfrak{G} can be identified with the tangent space at the identity, $T_e \mathfrak{G}$. Henceforth we will take this to be the definition of the Lie algebra of a Lie group.

Given a matrix representation of a Lie group \mathfrak{G} , the corresponding matrix representation of its Lie algebra \mathfrak{g} can be easily obtained by differentiating the matrix-valued curves in \mathfrak{G} . \mathfrak{g} then forms a matrix Lie algebra, with the Lie bracket defined by $[A, B] = AB - BA$. We illustrate this technique with the following examples.

Example 2.4 $gl(n)$, the Lie algebra of $GL(n)$, consists of the real $n \times n$ matrices.

Example 2.5 We can determine the Lie algebra of $SO(3)$ by evaluating the tangent vectors to a smooth curve $\Theta(t)$ on $SO(3)$, where $\Theta(0) = I$. Differentiating both sides of the equality $\Theta(t)\Theta(t)^T = I$ with respect to t and evaluating at $t = 0$, we get $\dot{\Theta}(0) + \dot{\Theta}(0)^T = 0$. Thus, the Lie algebra $so(3)$ is the algebra of skew-symmetric 3×3 matrices, with the commutator defined by $[A, B] = AB - BA$. The standard ordered basis for $so(3)$ is formed by the set $\{\Omega_1, \Omega_2, \Omega_3\}$, where

$$\Omega_1 = \begin{bmatrix} 0 & -1 & 0 \\ 1 & 0 & 0 \\ 0 & 0 & 0 \end{bmatrix}, \quad \Omega_2 = \begin{bmatrix} 0 & 0 & 1 \\ 0 & 0 & 0 \\ -1 & 0 & 0 \end{bmatrix}, \quad \Omega_3 = \begin{bmatrix} 0 & 0 & 0 \\ 0 & 0 & -1 \\ 0 & 1 & 0 \end{bmatrix}$$

An inner product on $so(3)$ is defined in the standard way as

$$\langle \Omega, \Omega \rangle = \frac{1}{2} \text{Tr}(\Omega \Omega^T)$$

and its induced norm is $\|\Omega\| = \langle \Omega, \Omega \rangle^{\frac{1}{2}}$.

Example 2.6 By a derivation similar to the previous example it can be shown that $se(3)$, the Lie algebra of $SE(3)$, is the algebra of 4×4 matrices of the form

$$\begin{bmatrix} 0 & -\omega_3 & \omega_2 & v_1 \\ \omega_3 & 0 & -\omega_1 & v_2 \\ -\omega_2 & \omega_1 & 0 & v_3 \\ 0 & 0 & 0 & 0 \end{bmatrix}$$

Elements of $se(3)$ will alternatively be represented as (ω, v) . The standard ordered basis for $se(3)$ is defined in the usual way as the set

$$\Omega_1 = \begin{bmatrix} 0 & 0 & 0 & 1 \\ 0 & 0 & 0 & 0 \\ 0 & 0 & 0 & 0 \\ 0 & 0 & 0 & 0 \end{bmatrix} \quad \Omega_2 = \begin{bmatrix} 0 & 0 & 0 & 0 \\ 0 & 0 & 0 & 1 \\ 0 & 0 & 0 & 0 \\ 0 & 0 & 0 & 0 \end{bmatrix} \quad \Omega_3 = \begin{bmatrix} 0 & 0 & 0 & 0 \\ 0 & 0 & 0 & 0 \\ 0 & 0 & 0 & 1 \\ 0 & 0 & 0 & 0 \end{bmatrix}$$

$$\Omega_4 = \begin{bmatrix} 0 & -1 & 0 & 0 \\ 1 & 0 & 0 & 0 \\ 0 & 0 & 0 & 0 \\ 0 & 0 & 0 & 0 \end{bmatrix} \quad \Omega_5 = \begin{bmatrix} 0 & 0 & 1 & 0 \\ 0 & 0 & 0 & 0 \\ -1 & 0 & 0 & 0 \\ 0 & 0 & 0 & 0 \end{bmatrix} \quad \Omega_6 = \begin{bmatrix} 0 & 0 & 0 & 0 \\ 0 & 0 & -1 & 0 \\ 0 & 1 & 0 & 0 \\ 0 & 0 & 0 & 0 \end{bmatrix}$$

We now discuss the adjoint representation for Lie groups and algebras. Given $a \in \mathfrak{G}$, the identity element e is a fixed point of the inner automorphism, $g \mapsto aga^{-1}$. Its derivative mapping at e corresponds to an isomorphism of the Lie algebra, $Ad_a : \mathfrak{g} \rightarrow \mathfrak{g}$. The map Ad_a is called the *adjoint representation of the Lie group \mathfrak{G}* . Furthermore, given $\xi \in \mathfrak{g}$, let $ad_\xi : \mathfrak{g} \rightarrow \mathfrak{g}$ be the map $\eta \mapsto [\xi, \eta]$. The map sending ξ to ad_ξ is then called the *adjoint representation of the Lie algebra*.

Example 2.7 The adjoint representation of an element $G = (\Theta, x)$ of $SE(3)$, relative to the standard ordered basis of $se(3)$, is given by the 6×6 matrix

$$Ad_G = \begin{bmatrix} \Theta & [x]\Theta \\ 0 & \Theta \end{bmatrix}$$

where $[x]$ is the skew-symmetric matrix representation of the vector $x \in \mathbb{R}^3$:

$$[x] = \begin{bmatrix} 0 & -x_3 & x_2 \\ x_3 & 0 & -x_1 \\ -x_2 & x_1 & 0 \end{bmatrix}$$

The adjoint representation for an element $g = (\omega, v)$ of $se(3)$, relative to its standard ordered basis, has the 6×6 matrix representation

$$ad_g = \begin{bmatrix} [\omega] & [v] \\ 0 & [\omega] \end{bmatrix}$$

The *Killing form*, κ , of a Lie algebra \mathfrak{g} is defined to be the symmetric bilinear form $\kappa(x, y) = \text{Tr}(ad_x ad_y)$, where $x, y \in \mathfrak{g}$ and $\text{Tr}(\cdot)$ denotes the trace. Although in general κ need not be definite or even nondegenerate, for any compact semisimple Lie group (such as $SO(n)$) it is negative definite. We make use of this result in our later discussion of Riemannian metrics on $SO(3)$.

Example 2.8 The Killing form on $so(3)$ with respect to its standard basis is

$$\kappa = \begin{bmatrix} -2 & 0 & 0 \\ 0 & -2 & 0 \\ 0 & 0 & -2 \end{bmatrix}$$

As claimed, κ is indeed negative definite.

Another fundamental concept related to Lie groups is the *exponential mapping*. Given a matrix representation of a Lie group \mathfrak{G} and its corresponding matrix Lie algebra \mathfrak{g} , the exponential mapping is the smooth mapping $\exp : \mathfrak{g} \rightarrow \mathfrak{G}$ defined by the matrix exponential: $\exp A = I + A + \frac{1}{2!}A^2 + \dots$, where $A \in \mathfrak{g}$. A result of particular import which enables us to define a set of local coordinates on \mathfrak{G} is the following: let $\{\Omega_1, \dots, \Omega_n\}$ be a basis for the Lie algebra \mathfrak{g} , \mathcal{U} an open set in \mathbb{R}^n containing the origin, and $\phi : \mathcal{U} \rightarrow \mathfrak{G}$ a mapping defined as $\phi(x) = e^{\Omega_1 x_1 + \dots + \Omega_n x_n}$. It can be shown that ϕ is a diffeomorphism for some open neighborhood about $x = 0$, so that ϕ defines local coordinates for a neighborhood of e in \mathfrak{G} . An atlas for \mathfrak{G} can then be defined by either left or right translation of the open

sets in \mathfrak{G} to the neighborhood of e over which ϕ is diffeomorphic. Chevalley[11] calls these coordinates the *canonical coordinates* with respect to a particular basis; we also refer to these coordinates as *coordinates of the first kind*. Given a suitable set of $\{\Omega_1, \dots, \Omega_n\}$, it is also possible to obtain a local coordinate chart for \mathfrak{G} via the map $\psi : \mathcal{U} \rightarrow \mathfrak{G}$, defined this time as $\psi(x) = e^{\Omega_1 x_1} \dots e^{\Omega_n x_n}$; these coordinates will be called *coordinates of the second kind*, defined relative to the set $\{\Omega_1, \dots, \Omega_n\}$. It should be noted that the domain $\mathcal{U} \in \mathbb{R}^n$ of ψ as a coordinate chart will in general be different from the domain of the canonical coordinate chart given by ψ . Also, the set $\{\Omega_1, \dots, \Omega_n\}$ need not form a basis for \mathfrak{g} in order for the coordinates of the second kind to be well-defined. A familiar example of the coordinates of the second kind are the Euler angles for $SO(3)$, which we discuss later in this chapter.

The final concept we review related to Lie groups is the *left* and *right differential*. Let $f : N \rightarrow \mathfrak{G}$ be a smooth map from a manifold N into a Lie group \mathfrak{G} . The left differential of f is defined to be the map $f^{-1} \cdot df : T_p N \rightarrow T_e \mathfrak{G}$ such that for $v_p \in T_p N$,

$$f^{-1} \cdot df(v_p) = dL_{f(p)^{-1}}(f(p))(df_p(v_p))$$

where $df_p : T_p N \rightarrow T_{f(p)} \mathfrak{G}$ is the derivative mapping of f at p , and $dL_g(h) : T_h \mathfrak{G} \rightarrow T_{gh} \mathfrak{G}$ is the derivative of the left translation mapping $L_g : \mathfrak{G} \rightarrow \mathfrak{G}$, evaluated at h . The right differential is similarly defined as the linear mapping $df \cdot f^{-1} : T_p N \rightarrow T_e \mathfrak{G}$ sending v_p to $dR_{f(p)^{-1}}(f(p))(df_p(v_p))$. The left and right differentials can alternatively be interpreted as defining Lie-algebra-valued one forms on N . We make use of this interpretation in our later discussion on spherical mechanisms.

2.1.2 Riemannian Metrics on Lie Groups

Riemannian geometry allows us to extend the familiar Euclidean concepts of lengths and angles to curves on differentiable manifolds, by defining an inner product on the tangent space at each point of the manifold. A *Riemannian metric* on a manifold M is a function Φ which assigns to each $p \in M$ an inner product Φ_p on $T_p M$, which is continuous in the following sense: If s_1, s_2 are two continuous vector fields on M , then the function taking $p \mapsto \Phi_p(s_1(p), s_2(p))$ is also continuous. If (x, U) is a coordinate chart on a neighborhood

U of M , then on U the Riemannian metric can be written as

$$\Phi = g_{ij}(x)dx^i dx^j$$

or, in the more classical notation, as $ds^2 = g_{ij}(x)dx^i dx^j$, where we follow the Einstein convention of summation over repeated indices. Given a mapping $f : (N, h) \rightarrow (M, g)$ between Riemannian manifolds N and M with metrics h and g , respectively, we can also define a new metric on N by the *pullback* of g by f , denoted f^*g . If $X_p, Y_p \in T_p N$, then $f^*g(X_p, Y_p) = g(df_p(X_p), df_p(Y_p))$.

Example 2.9 The simplest example of a Riemannian manifold is \mathbb{R}^n with its usual inner product.

Example 2.10 Any imbedded or immersed submanifold of \mathbb{R}^n is endowed with a Riemannian metric by the imbedding $f : M \rightarrow \mathbb{R}^n$. In particular, all surfaces M of \mathbb{R}^3 have an induced Riemannian metric: if $i : M \rightarrow \mathbb{R}^3$ is the inclusion map and Φ is the standard inner product on \mathbb{R}^n , the pullback $i^*\Phi$ is the induced Euclidean metric on M . In the case of the unit sphere S^2 embedded in \mathbb{R}^3 , the inclusion map i is given by

$$\begin{aligned} x &= \cos \theta \sin \phi \\ y &= \sin \theta \sin \phi \\ z &= \cos \phi \end{aligned}$$

where (θ, ϕ) are spherical coordinates on S^2 . The induced Riemannian metric on S^2 can then be written in the classical notation as $ds^2 = \sin^2 \phi d\theta^2 + d\phi^2$.

On Riemannian manifolds there is a notion of infinitesimal volume determined by the Riemannian metric. It is given by an n -form Ω which is expressed in local coordinates as

$$\Omega = \sqrt{\det(g_{ij})} dx_1 \wedge \cdots \wedge dx_n$$

Using this volume form one can assign to some compact subset S of a Riemannian manifold a volume, given by $\int_S \Omega$. Integration of functions on S can now be defined using this volume element.

Because of their added algebraic structure, Lie groups have two special classes of Riemannian metrics, and both involve representing a tangent vector as an element of the Lie algebra. Given any finite-dimensional Lie group \mathfrak{G} , its tangent bundle $T\mathfrak{G}$ is isomorphic to $\mathfrak{G} \times \mathfrak{g}$ in two ways: by left translation λ , and by right translation ρ . For example, given $v \in T_g\mathfrak{G}$, left translation sends (g, v) to $(g, dL_{g^{-1}}(g)(v))$, whereas right translation sends it to $(g, dR_{g^{-1}}(g)(v))$. Any tangent vector $v \in T_g\mathfrak{G}$ can therefore be expressed as an element of \mathfrak{g} in one of two ways. The Lie algebraic representation of a tangent vector by left translation is called its *body coordinate velocity*, while right translation results in its *space coordinate velocity* (Abraham and Marsden[1]). This choice of terminology can be explained by the following observation. If $v_b \in \mathfrak{g}$ is the body coordinate velocity of some tangent vector $v \in T_g\mathfrak{G}$, then v_b is invariant under the action of a left translation by a , i.e., $\lambda \circ dL_a \circ \lambda^{-1}(h, v_b) = (ah, v_b)$. Under left translation the body coordinate velocity is therefore intrinsic in some sense, i.e., v_b is “attached” to the body. The space coordinate velocities, on the other hand, do not obey such a property. For a more physical interpretation, consider $SE(3)$ as the configuration space for a rigid body. The body coordinate velocities are then the generalized velocities expressed with respect to a reference frame attached to the body, whereas the space coordinate velocities are expressed with respect to a reference frame fixed in space. If $X(t)$ denotes a smooth curve in the matrix Lie group \mathfrak{G} , then its body coordinate velocity is given by $X^{-1}(t)\dot{X}(t)$, while its space coordinate velocity is $\dot{X}(t)X^{-1}(t)$.

Since any tangent vector to \mathfrak{G} can be represented as an element of \mathfrak{g} by either left or right translation, a Riemannian metric on \mathfrak{G} can be generated by simply defining an inner product on \mathfrak{g} . This inner product is applied to the body or space coordinate representation of tangent vectors. Metrics obtained in this way are called *left-* and *right-invariant* Riemannian metrics, respectively. More formally, a Riemannian metric Φ is said to be left-invariant if $\Phi_b = L_a^* \Phi_{ab}$, and right-invariant if $\Phi_b = R_a^* \Phi_{ba}$, where $a, b \in \mathfrak{G}$; Φ is bi-invariant if it is both left- and right-invariant. Specifying a symmetric positive-definite matrix (which corresponds to the inner product on \mathfrak{g} , with respect to some basis) therefore determines the unique left- and right-invariant Riemannian metrics on a Lie group.

For our purposes the Lie groups of most interest are $SO(3)$ and $SE(3)$, and on these groups we shall consider only the left-invariant Riemannian metrics. We do so not only because of the intrinsic nature of velocity vectors obtained by left translation, but also because the kinetic energy of rigid bodies is obtained from a left-invariant metric. That is, if ω_b represents the angular velocity of a rotating rigid body, expressed in terms of a frame attached to the body's center of mass, and I its rotational inertia matrix also expressed in this frame, the kinetic energy is then $\frac{1}{2}\omega_b^T I \omega_b$. In our Lie group framework, ω_b is the body coordinate velocity of the tangent vector ω , and the kinetic energy is given by $\frac{1}{2}\langle I\omega, \omega \rangle$, where $\langle \cdot, \cdot \rangle$ is the left-invariant Riemannian metric on $SO(3)$, and I is again the inertia tensor of the rigid body. We add that if \mathfrak{G} is a compact connected Lie group it is then well-known that \mathfrak{G} admits a bi-invariant Riemannian metric. This fact is especially useful in analyzing spherical mechanisms, whose range space $SO(3)$ is compact.

2.2 Euclidean Motions

For our purposes we consider physical space to be a flat, orientable three-dimensional manifold, with a family of Euclidean metrics parametrized by a choice of length scale; most often physical space is regarded as the Euclidean space E^3 with the metric $ds^2 = c(dx_1^2 + dx_2^2 + dx_3^2)$, $c > 0$ denoting the length scale. The group $SE(3)$ can then be viewed as the set of orientation-preserving isometries (with respect to a fixed length scale) of physical space. Alternatively, recall that the location of any rigid object in physical space can be described, with respect to a reference frame, by a point in $SE(3)$ describing the rigid object's position and orientation. Since robot manipulation primarily involves moving objects around in space, we will take this latter viewpoint of $SE(3)$ as a rigid object's configuration space, and regard a mechanism abstractly as a mapping into $SE(3)$.

In order to actually obtain numerical values for the intrinsic kinematic properties of mechanisms, local coordinates for $SO(3)$ and $SE(3)$ are required. In section 2.1.1 we mentioned the coordinates of the first and second kind as two basic coordinate systems for Lie groups. On $SO(3)$ these coordinates can also be identified with the zero-pitch screws and Euler angles, respectively. We work out in detail the explicit form of these coordinate systems, and compute the translation-invariant Riemannian metrics on $SO(3)$ and $SE(3)$.

using these coordinates.

2.2.1 $\text{SO}(3)$

We begin by describing the canonical coordinates of the first kind on $SO(3)$. First, define the Euclidean inner product on $so(3)$ in the usual way as $\langle \Omega_1, \Omega_2 \rangle = \frac{1}{2}\text{Tr}(\Omega_1 \Omega_2^T)$, and let $\|\cdot\|$ denote the norm induced from this metric. The following formula for the exponential mapping $\exp : so(3) \rightarrow SO(3)$ is well-known, and can alternatively be derived from Cayley's formula and Rodrigues' equation for rotations (see [30]).

Proposition 2.1 *Given $\omega \in so(3)$,*

$$\exp[\omega] = I + \frac{\sin \|\omega\|}{\|\omega\|} \cdot [\omega] + \frac{1 - \cos \|\omega\|}{\|\omega\|^2} \cdot [\omega]^2$$

where $[\omega]$ is the skew-symmetric matrix representation, and $\|\omega\|$ is the standard Euclidean norm.

Proof: The characteristic polynomial of $[\omega]$ is $s^3 + \|\omega\|^2 s$, and by the Cayley-Hamilton theorem, $[\omega]^3 = -\|\omega\|^2 [\omega]$. The result then follows from application of this identity to the series expression for $\exp[\omega]$. \square

This proposition suggests one of the standard visualizations of $SO(3)$ as a solid ball of radius π , centered at the origin with the antipodal points identified; a point p on the ball represents a rotation about the axis from the origin through p by the amount $\|p\|$ radians. Any $\omega \in so(3)$ such that $\|\omega\| \leq \pi$ can be viewed via the exponential mapping as a rotation about the ω -axis by $\|\omega\|$ radians, a positive rotation being defined in the right-hand sense.

The exponential map, recall, acts as a local parametrization via coordinates of the first kind. On $SO(3)$, this parametrization is given by $\exp : \mathcal{U} \rightarrow \mathcal{V}$, where \mathcal{U} is the open ball of radius π in \mathbb{R}^3 centered at the origin, and $\mathcal{V} = \exp(\mathcal{U})$ is the set $\{\Theta \in SO(3) | \text{Tr}(\Theta) \neq -1\}$; this is at once obvious from the solid ball picture of $SO(3)$. Note furthermore that the set $SO(3) - \mathcal{V}$ is of measure zero, so that the volume of $SO(3)$ can be computed in terms of this exponential coordinate chart alone. The inverse of the exponential mapping, or *logarithm*, is well-defined on \mathcal{V} , and is given by the following proposition.

Proposition 2.2 Suppose $\Theta \in SO(3)$ such that $\text{Tr}(\Theta) \neq -1$. Then

$$\log \Theta = \frac{\phi}{2 \sin \phi} (\Theta - \Theta^T)$$

where ϕ satisfies $1 + 2 \cos \phi = \text{Tr}(\Theta)$, $|\phi| < \pi$. Furthermore, $\|\log \Theta\|^2 = \phi^2$.

Proof: First recall Euler's theorem, which states that for any $\Theta \in SO(3)$ there exists $Q \in SO(3)$ and $0 < \phi < 2\pi$ such that

$$\Theta = Q \begin{bmatrix} \cos \phi & -\sin \phi & 0 \\ \sin \phi & \cos \phi & 0 \\ 0 & 0 & 1 \end{bmatrix} Q^T \quad (2.1)$$

The eigenvalues of Θ are $1, e^{\pm i\phi}$, and it follows that the condition $\text{Tr}(\Theta) \neq -1$ is equivalent to $\phi \neq \pi$. Then clearly

$$\Theta - \Theta^T = \frac{2 \sin \phi}{\phi} Q \begin{bmatrix} 0 & -\phi & 0 \\ \phi & 0 & 0 \\ 0 & 0 & 0 \end{bmatrix} Q^T$$

From the matrix identity $Q(\exp \Omega)Q^T = \exp(Q\Omega Q^T)$, it follows that $\log \Theta = \frac{\phi}{2 \sin \phi} (\Theta - \Theta^T)$. Finally, $\|\log \Theta\|^2 = -\frac{1}{2} \text{Tr}[\log \Theta]^2 = -\frac{1}{2} \frac{\phi^2}{4 \sin^2 \phi} \text{Tr}(\Theta - \Theta^T)^2$. Substituting for Θ from equation 2.1 then establishes that $\|\log \Theta\|^2 = \phi^2$. \square

We now discuss coordinates of the second kind on $SO(3)$. Given a suitable choice of the set $\{\Omega_1, \Omega_2, \Omega_3\}$, where each $\Omega_i \in so(3)$, we can obtain these coordinates on $SO(3)$ by the map $e^{\Omega_1 x_1} e^{\Omega_2 x_2} e^{\Omega_3 x_3}$, where x belongs to some open set \mathcal{U} in \mathbb{R}^3 . For example, when $\{\Omega_1, \Omega_2, \Omega_3\}$ is chosen to be the standard ordered basis on $so(3)$ (see example 2.5), then (x_1, x_2, x_3) in the mapping $e^{\Omega_1 x_1} e^{\Omega_2 x_2} e^{\Omega_3 x_3} = \Theta$ corresponds to the z - y - x Euler angles for Θ . As a coordinate chart this mapping covers all of $SO(3)$ (minus the identity) once when the domain \mathcal{U} of x is defined to be $0 < x_1, x_3 < 2\pi$ and $-\frac{\pi}{2} < x_2 < \frac{\pi}{2}$. However, if instead Ω_3 above is replaced by Ω_1 , we get the z - y - z Euler angle representation of Θ , which is now defined over the range $0 < x_1, x_3 < 2\pi$, $0 < x_2 < \pi$. More generally, any choice of $\{\Omega_1, \Omega_2, \Omega_3\}$ with unit norm such that $\langle \Omega_1, \Omega_2 \rangle = 0$ and $\langle \Omega_2, \Omega_3 \rangle = 0$ yields an Euler angle representation for $SO(3)$ in some reference frame. An atlas can be constructed with a collection of coordinate charts based on Euler angles (see, e.g., Choquet-Bruhat[12]).

As mentioned before, because $SO(3)$ is compact it admits a bi-invariant Riemannian metric. Let Φ denote such a metric, and suppose Φ_e is its inner product on $so(3)$. Applying the theorem which states that Φ is bi-invariant if and only if $Ad_{\Theta}^* \Phi_e = \Phi_e$ for any $\Theta \in SO(3)$, we must have $\Phi_e(\omega_1, \omega_2) = \Phi_e(Ad_{\Theta}(\omega_1), Ad_{\Theta}(\omega_2)) = \Phi_e(\Theta\omega_1, \Theta\omega_2)$, for all $\omega_1, \omega_2 \in so(3)$. This can only be true if Φ_e is simply cI , the Euclidean inner product scaled by a constant $c > 0$. The bi-invariant metrics are therefore obtained by either left or right translation of the inner product cI on $so(3)$. If we scale the metric so that the length of a circle, viewed as a submanifold of $SO(3)$, is 2π , c should then be set to one. Note that this inner product on $so(3)$ corresponds to $-\frac{1}{2}\kappa$, where κ is the Killing form (see example 2.8). κ can therefore be said to define a bi-invariant Riemannian metric on $SO(3)$.

The bi-invariant Riemannian metric on $SO(3)$ is now expressed in the coordinates of the first and second kind. Before doing so we need to establish the following lemma.

Lemma 2.1 *Let $x(t)$ be a smooth curve in $gl(n)$. Then $X(t) = e^{x(t)}$ is a smooth curve in $Gl(n)$, and $X^{-1}(t)\dot{X}(t)$ is given by*

$$X^{-1}\dot{X} = \int_0^1 e^{-x(t)s} \dot{x}(t) e^{x(t)s} ds$$

When $x(t)$ is a curve in $so(3)$, $X(t)$ is a curve in $SO(3)$, and $X^{-1}(t)\dot{X}(t) = [Ax]$, where

$$A = I - \frac{1 - \cos \|x\|}{\|x\|^2} \cdot [x] + \frac{\|x\| - \sin \|x\|}{\|x\|^3} \cdot [x]^2$$

Proof: By Taylor expansion with respect to h ,

$$\begin{aligned} \frac{d}{dt} e^{x(t)} &= \lim_{h \rightarrow 0} \left(\frac{1}{h} e^{x(t+h)} - e^{x(t)} \right) \\ &= \lim_{h \rightarrow 0} \frac{1}{h} (e^{x(t)+h\dot{x}(t)+O(h^2)} - e^{x(t)}) \end{aligned}$$

The $O(h^2)$ terms go to zero in the limit, and hence can be ignored. The above equation then reduces to

$$\begin{aligned} \frac{d}{dt} e^{x(t)} &= \lim_{h \rightarrow 0} \frac{1}{h} (e^{x(t)} + h \frac{d}{dh} e^{x(t)+h\dot{x}(t)+O(h^2)} - e^{x(t)}) \\ &= \lim_{h \rightarrow 0} \frac{d}{dh} e^{x(t)+h\dot{x}(t)} \end{aligned}$$

Now if A, B are matrices and ϵ, t are scalars, it is well known that $\frac{d}{d\epsilon} e^{(A+\epsilon B)t}|_{\epsilon=0} = \int_0^t e^{As} Be^{A(t-s)} ds$ (see, e.g., Brockett[5]). From this result it is clear that

$$\frac{d}{dt} e^{x(t)} = e^{x(t)} \int_0^1 e^{-x(t)s} \dot{x}(t) e^{x(t)s} ds \quad (2.2)$$

This proves the first part. Now, given an arbitrary $\Theta \in SO(3)$ and $\omega \in so(3)$, a simple calculation shows that $\Theta[\omega]\Theta^T = [\Theta\omega]$. It is now easy to verify that $\int_0^1 e^{-x(t)s} ds = A$ as given above, from which the second part follows. \square

An expression for $\dot{X}(t)X^{-1}(t)$ can also be derived similarly. With this result the bi-invariant Riemannian metric can be expressed in coordinates of the first kind straightforwardly. Let $x \in \mathcal{U}$ denote these coordinates, where as before \mathcal{U} is the open ball of radius π in \mathbb{R}^3 , and suppose $X = \exp[x]$. Because this metric is bi-invariant its coordinate representation should be the same regardless of whether the tangent vectors are expressed in body or space coordinates; to apply the lemma in its present form body coordinates are used. Now, if $x(t)$ is a curve in \mathcal{U} , then $X(t)$ is a curve in $SO(3)$, and according to the lemma, the body coordinate velocity $X^{-1}(t)\dot{X}(t) = [A\dot{x}]$, where A is defined as

$$A = I - \frac{1 - \cos \|x\|}{\|x\|^2} \cdot [x] + \frac{\|x\| - \sin \|x\|}{\|x\|^3} \cdot [x]^2$$

Setting $\Phi_e = I$, where Φ_e once again denotes the bi-invariant metric on $so(3)$, we can express the metric in coordinates of the first kind as $g_{ij} = A^T \Phi_e A = A^T A$, which simplifies to

$$g_{ij} = I + \frac{\|x\|^2 + 2 \cos \|x\| - 2}{\|x\|^4} \cdot [x]^2$$

The volume form on $SO(3)$ induced from this metric is

$$\Omega = \frac{2 \cos \|x\| - 2}{\|x\|^2} dx_1 \wedge dx_2 \wedge dx_3$$

Integrating Ω over \mathcal{U} , we find that the volume of $SO(3)$ is $8\pi^2$.

We now express the bi-invariant Riemannian metric for $SO(3)$ in coordinates of the second kind. Let its local parametrization $f : \mathcal{U} \rightarrow SO(3)$ be defined as $f(x_1, x_2, x_3) = e^{\Omega_1 x_1} e^{\Omega_2 x_2} e^{\Omega_3 x_3}$, where \mathcal{U} is an open set in \mathbb{R}^3 (different from the one above), and $\{\Omega_i\}$ forms an orthonormal basis of $so(3)$. Its left differential $f^{-1} \cdot df$ is

$$f^{-1} \cdot df = \Omega_3 dx_3 + e^{-\Omega_3 x_3} \Omega_2 e^{\Omega_3 x_3} dx_2 + e^{-\Omega_3 x_3} e^{-\Omega_2 x_2} \Omega_1 e^{\Omega_2 x_2} e^{\Omega_3 x_3} dx_1$$

The bi-invariant metric is then equal to $ds^2 = \langle f^{-1} \cdot df, f^{-1} \cdot df \rangle$; choosing $\{\Omega_1, \Omega_2, \Omega_3\}$ to be the standard ordered basis for $so(3)$, ds^2 is given in z-y-x Euler angle coordinates by

$$ds^2 = dx_1^2 + dx_2^2 + dx_3^2 - 2 \sin x_2 dx_1 dx_3$$

and the bi-invariant volume form induced from this metric is

$$\Omega = |\cos x_2| dx_1 \wedge dx_2 \wedge dx_3$$

Integrating Ω over the region $0 \leq x_1, x_3 \leq 2\pi$ and $-\frac{\pi}{2} \leq x_2 \leq \frac{\pi}{2}$, we confirm that the volume of $SO(3)$ is once again $8\pi^2$. In z - y - x Euler angles the metric could also have been expressed as $ds^2 = dx_1^2 + dx_2^2 + dx_3^2 + 2 \cos x_2 dx_1 dx_3$.

2.2.2 SE(3)

We now discuss coordinates of the first and second kind on $SE(3)$. As in $SO(3)$, computational formulas for the exponential mapping from $se(3)$ onto $SE(3)$ can be explicitly derived.

Proposition 2.3 *Let $(\omega, v) \in se(3)$. Then*

$$\exp \begin{bmatrix} [\omega] & v \\ 0 & 0 \end{bmatrix} = \begin{bmatrix} \exp[\omega] & Av \\ 0 & 1 \end{bmatrix}$$

where

$$A = I + \frac{1 - \cos \|\omega\|}{\|\omega\|^2} \cdot [\omega] + \frac{\|\omega\| - \sin \|\omega\|}{\|\omega\|^3} \cdot [\omega]^2$$

Proof: Writing out the series expansion for the exponential,

$$\exp \begin{bmatrix} [\omega] & v \\ 0 & 0 \end{bmatrix} = \begin{bmatrix} \exp[\omega] & (\sum_{n=1}^{\infty} \frac{[\omega]^{n-1}}{n!})v \\ 0 & 1 \end{bmatrix}$$

$A = \sum_{n=1}^{\infty} \frac{[\omega]^{n-1}}{n!}$ can also be written as $\int_0^1 e^{[\omega]s} ds$, which reduces to the above. \square

As before, the exponential map defines coordinates of the first kind on $SE(3)$, and its domain of definition \mathcal{U} in \mathfrak{R}^6 is $\{(\omega, v) | \omega, v \in \mathfrak{R}^3, \|\omega\| < \pi\}$. Its inverse mapping can be calculated by the following proposition.

Proposition 2.4 *Suppose $\Theta \in SO(3)$ such that $\text{Tr}(\Theta) \neq -1$, and let $x \in \mathfrak{R}^3$. Then*

$$\log \begin{bmatrix} \Theta & x \\ 0 & 1 \end{bmatrix} = \begin{bmatrix} \log \Theta & A^{-1}x \\ 0 & 0 \end{bmatrix}$$

where

$$A^{-1} = I - \frac{1}{2} \cdot [\omega] + \frac{2 \sin \|\omega\| - \|\omega\|(1 + \cos \|\omega\|)}{2\|\omega\|^2 \sin \|\omega\|} \cdot [\omega]^2$$

and $\log \Theta$ is as in proposition 2.2.

Proof: Since by the Cayley-Hamilton theorem $[\omega]^3 = -\|\omega\|^2[\omega]$, it's clear that A^{-1} is a quadratic matrix polynomial in $[\omega]$. An elementary calculation then establishes the result.

□

The coordinates of the second kind on $SE(3)$ are constructed by a parametrization of the form $e^{\Omega_1 x_1} \dots e^{\Omega_6 x_6}$, where the Ω_i are elements of $se(3)$. For our purposes we assume that the set $\{\Omega_1, \dots, \Omega_6\}$ forms the standard ordered basis for $se(3)$ (as given by example 2.6). $SE(3)$ is then parametrized over the range $x_1, x_2, x_3 \in \mathbb{R}$, $0 \leq x_4, x_6 \leq 2\pi$, and $-\frac{\pi}{2} \leq x_5 \leq \frac{\pi}{2}$.

As is well known, the group $SE(3)$ does *not* admit a bi-invariant Riemannian metric (see Loncaric[28] for references). Our main interest will instead be in the left-invariant metrics on $SE(3)$ whose matrix representation on $se(3)$ (with respect to its standard ordered basis) is

$$\Phi_e = \begin{bmatrix} dI & 0 \\ 0 & cI \end{bmatrix}$$

Here I is the 3×3 identity matrix, and c and d are positive constants such that $\frac{d}{c}$ represents the length scale for physical space; the choice of constants reflects the tradeoff between orientation and position. This metric not only employs the bi-invariant metric on $SO(3)$, but also preserves the isotropy of \mathbb{R}^3 . It is expressed in coordinates of the second kind, with respect to the standard ordered basis, as

$$ds^2 = d(dx_1^2 + dx_2^2 + dx_3^2) + c(dx_4^2 + dx_5^2 + dx_6^2 - 2 \sin x_5 dx_4 dx_6)$$

The metric can also be expressed in coordinates of the first kind following the same procedure as outlined for the $SO(3)$ case, but the resulting expression is quite complex and not particularly insightful.

Although $SE(3)$ does not admit a bi-invariant Riemannian metric, it does possess a bi-invariant volume form.

Proposition 2.5 *A bi-invariant volume form exists on $SE(3)$.*

Proof: Suppose Ω is a left-invariant volume form on $SE(3)$. To show that it is also right-invariant it suffices to show that $Ad_G^* \Omega_e = \Omega_e$ for all $G \in SE(3)$. If the matrix representation for G is (Θ, x) , then

$$Ad_G^* \Omega_e = (\det \begin{bmatrix} \Theta & [x]\Theta \\ 0 & \Theta \end{bmatrix}) \cdot \Omega_e = (\det \Theta)^2 \cdot \Omega_e = \Omega_e$$

from which the result follows. \square

This proposition states that the bi-invariant volume forms on $SE(3)$ can be induced from the Riemannian metric generated by left or right translation of an inner product Φ_e on $se(3)$. They can be written in coordinates of the second kind, with respect to the standard basis on $se(3)$, as

$$\Omega = \det(\Phi_e) \cdot |\cos x_5| dx_1 \wedge \dots \wedge dx_6$$

where (x_4, x_5, x_6) represent the *z-y-x* Euler angles, and the constant $\det(\Phi_e)$ is identified with the choice of length scale in physical space.

2.3 Kinematic Mappings

2.3.1 The Product-of-Exponentials Kinematic Equations

In this section the product-of-exponentials formula is introduced as a general representation for the kinematics of open chains. We first define some terminology used informally in chapter 1. Recall that a *mechanism* is a set of rigid bodies, or *links*, connected by joints so that their relative motion is constrained. Mechanisms are typically categorized into three fundamental classes, according to the motion of any arbitrary point on the mechanism. If the motion is restricted to lie on a plane, the mechanism is called a *planar mechanism*, while if the motion lies on a sphere, it is called a *spherical mechanism*. Mechanisms satisfying neither of these properties are generically referred to as *spatial mechanisms*. If we associate with each mechanism a tip, the planar, spherical, and spatial mechanisms can be characterized as those which have as tip configuration spaces open subsets of $SE(2)$, $SO(3)$, and $SE(3)$, respectively. A further distinction is made between *open-chain* and *closed-chain* mechanisms. The links of an open-chain mechanism are arranged in serial order, and in

most cases there is a concrete notion of base and tip. On the other hand, closed-chain mechanisms have one or more internal loops formed by the links, and subsequently limits often exist on the range of motion of certain joints. This distinction made between open and closed chains is not entirely satisfactory, since in a robotics context certain closed-chain designs have the same kinematics as open chains. Our focus in this section will be on open-chain mechanisms.

The configuration space for a prismatic joint is \mathbb{R} (or more accurately, some subinterval of \mathbb{R} because of joint limits), while for revolute joints it is the circle S^1 . For an n -link open chain containing m revolute joints and $n - m$ prismatic joints, its configuration space can be regarded as the product manifold $T^m \times \mathbb{R}^{n-m}$, where $T^m = S^1 \times \cdots \times S^1$ (m copies) is the m -dimensional torus. T^m can be coordinatized by identifying it with the m -dimensional cubic lattice in \mathbb{R}^m , such that corresponding points among the cubes are identified. For example, T^2 can be thought of as a square grid in \mathbb{R}^2 , with any point on the edge of a square identified with the corresponding point on any opposite edge. As a Riemannian manifold, T^m is said to be a *flat torus* if its Riemannian metric $ds^2 = \epsilon_1 dx_1^2 + \epsilon_2 dx_2^2 + \dots + \epsilon_n dx_n^2$. When $\epsilon_i = 1$ for all i this metric corresponds to the standard Euclidean metric. For our purposes we take the flat torus to be the configuration space for revolute-joint mechanisms. The particular choice of flat metric (*i.e.*, choice of $\{\epsilon_i\}$) can then be interpreted physically as determining the relative “strengths” of the actuators; this is discussed further in the next chapter. So that we may assign a length of 2π (with respect to the Euclidean metric) to the circle S^1 , regarded here as a submanifold of T^m , we will henceforth coordinatize T^m as \mathbb{R}^m modulo $2\pi\mathbb{Z} \times \cdots \times 2\pi\mathbb{Z}$; its volume with respect to the volume form induced from the flat metric $ds^2 = \epsilon_1 dx_1^2 + \dots + \epsilon_n dx_n^2$ is then $(\epsilon_1 \cdots \epsilon_m)^{\frac{1}{2}}(2\pi)^n$.

The standard convention for describing the kinematics of open chains is to relate coordinate frames attached to each link in terms of the coordinate frame attached to the previous link. The links are usually numbered in ascending order from the base to the tip, and a coordinate frame is simply a point in $SE(3)$. In robotics a coordinate transformation between links is usually described in terms of the Denavit-Hartenberg parameters, which are defined using Paul’s notation[36] as follows: θ_i is the joint angle, a_i is the link length, d_i is the offset distance, and α_i is the twist angle. A frame at link i can be expressed in

terms of the frame at link $i - 1$ as

$${}^{i-1}T_i = \exp(H_1\theta_i) \cdot \exp(H_2d_i) \cdot \exp(H_3a_i) \cdot \exp(H_4\alpha_i)$$

where

$$H_1 = \begin{bmatrix} 0 & -1 & 0 & 0 \\ 1 & 0 & 0 & 0 \\ 0 & 0 & 0 & 0 \\ 0 & 0 & 0 & 0 \end{bmatrix}, \quad H_2 = \begin{bmatrix} 0 & 0 & 0 & 0 \\ 0 & 0 & 0 & 0 \\ 0 & 0 & 0 & 1 \\ 0 & 0 & 0 & 0 \end{bmatrix}$$

$$H_3 = \begin{bmatrix} 0 & 0 & 0 & 1 \\ 0 & 0 & 0 & 0 \\ 0 & 0 & 0 & 0 \\ 0 & 0 & 0 & 0 \end{bmatrix}, \quad H_4 = \begin{bmatrix} 0 & 0 & 0 & 0 \\ 0 & 0 & -1 & 0 \\ 0 & 1 & 0 & 0 \\ 0 & 0 & 0 & 0 \end{bmatrix}$$

and $\exp : se(3) \rightarrow SE(3)$ is the matrix exponential mapping.

By this convention the joint variables for revolute and prismatic joints are θ_i and d_i , respectively. The forward kinematics for obtaining the tip frame in terms of the base frame is then given by ${}^0T_n = {}^0T_1T_2 \dots {}^{n-1}T_n$. Let (x_1, \dots, x_n) denote the joint configuration variables for an n -link open chain. By a repeated application of the matrix identity $P(\exp M)P^{-1} = \exp(PMP^{-1})$ we can rewrite each link transformation ${}^{i-1}T_i$ as $M_i e^{S_i x_i}$ or $e^{U_i x_i} N_i$. Further application of this matrix identity allows us to write the forward kinematic equations as

$$f(x_1, \dots, x_n) = M e^{A_1 x_1} \dots e^{A_n x_n}$$

or

$$f(x_1, \dots, x_n) = e^{B_1 x_1} \dots e^{B_n x_n} N$$

where each $A_i, B_i \in se(3)$, and $M, N \in SE(3)$. These two representations of the kinematics will be called the *product-of-exponentials (POE) kinematic equations* in *body* and *space coordinates*, respectively.

The POE kinematic equations are closely related to the screw representation of rigid motions (see Paden and Sastry[32], McCarthy[30]). In screw theory a rigid motion is represented as a rotation about a screw axis, represented by a directed line in space, accompanied by a translation along this axis by an amount equal to the screw pitch times the rotation

angle. Given $(\omega, v) \in se(3)$ we can derive from it a screw whose pitch h and screw axis $l_{\hat{u}}$ are given by

$$h = \begin{cases} \frac{\omega^T v}{\|\omega\|^2} & \text{if } \|\omega\| \neq 0 \\ \infty & \text{if } \|\omega\| = 0 \end{cases}$$

$$l_{\hat{u}} = \begin{cases} \frac{\omega \times v}{\|\omega\|^2} + \lambda \omega & \text{if } \|\omega\| \neq 0 \\ \lambda v & \text{if } \|\omega\| = 0 \end{cases}$$

where $\lambda \in \mathbb{R}$ parametrizes the position along the screw axis; the rotation angle about the screw axis is $\|\omega\|$ radians. The screw representation of rigid motions can be traced to a fundamental theorem by Chasles, which states that any rigid motion can be achieved by a rotation and a translation which commute. The actual screw motion defined by (ω, v) is then realized by taking the exponential mapping of (ω, v) . In Lie group terminology each $e^{A_i x_i}$ forms a one-parameter subgroup on $SE(3)$ generated by A_i . In the POE equations above the tip frame is obtained by a concatenation of screw motions, with the amount of rotation about the screw axes determined by the joint variables x_i .

Part of the appeal of the POE equations, apart from its inherent identification with Lie theory, is the visualization of the joint axes as the screw axes in the POE formula. The Denavit-Hartenberg parameters constitute the minimum set required to describe the forward kinematics; unlike the POE equations, however, they do not afford an easy to visualize, physical interpretation. Although we chose to derive the POE equations from the Denavit-Hartenberg representation to make explicit contact with current kinematic practice, one can in fact obtain the POE formula quite easily by identifying the screws representing the joint axes. There does not, however, appear to be a natural way to define a unique forward kinematic map based on the POE equations; the relationship between equivalent POE representations also has not been addressed in the literature. It is immediately clear that if joint i is revolute, the pitch of the corresponding screw, determined in body coordinates from A_i (or in space coordinates from B_i), should be zero, whereas for prismatic joints the pitch should be infinite. The usual convention for mechanisms also assigns to each revolute joint a 2π range of motion, and in this case we see that the ω_i associated with A_i in the POE equations must be of unit norm.

Clearly the POE equations provide a general representation of the forward kinematics

through a mapping $f : N \rightarrow SE(3)$, where N is a flat Riemannian manifold. The left and right differentials of f are given respectively by

$$f^{-1} \cdot df = A_n dx_n + e^{-A_n x_n} A_{n-1} e^{A_n x_n} dx_{n-1} + \dots$$

and

$$df \cdot f^{-1} = B_1 dx_1 + e^{B_1 x_1} B_2 e^{-B_1 x_1} dx_2 + \dots$$

In kinematics the Jacobian of a mechanism is thought of as the linear transformation relating joint velocities to the generalized Cartesian velocities of the tip, expressed with respect to some reference frame. By this convention the left and right differentials can be identified with the Jacobian expressed in the tip and base frames, respectively. To make this identification more explicit, one could rearrange $f^{-1} \cdot df$ or $df \cdot f^{-1}$ into a six-vector, and similarly rearrange the right-hand side as a linear transformation of the joint velocity vector (dx_1, \dots, dx_n) by the $6 \times n$ matrix $J(x)$. For the left differential we label this matrix with the subscript $J_L(x)$; the right differential matrix is labelled $J_R(x)$.

2.3.2 Computational Aspects

While the product-of-exponentials formula clearly has geometric and visual appeal, its usefulness as a computational tool for practical applications has, with few exceptions (*e.g.*, Salam and Yoon[40]), not been addressed. In this section we show that the POE equations can in fact provide a practical alternative for applications involving the computation of the forward kinematics and the corresponding Jacobian. The particular scheme we consider, first suggested in Brockett[7], is based on table lookup of the matrix exponentials $e^{A_i x_i}$ in the POE formula. The scheme is intermediate between methods which are based on real-time computation and those which are entirely memory-based. By generating, for each A_i , a table of values for $e^{A_i x_i}$ at regular intervals of x_i , the forward kinematics can be determined by multiplying the matrix exponentials in the POE formula. This method is to be compared with the standard approach using link transformations defined by the

Denavit-Hartenberg parameters, where each link transformation is given by

$${}^i T_{i+1} = \begin{bmatrix} \cos \theta_i & -\sin \theta_i \cos \alpha_i & \sin \theta_i \sin \alpha_i & a_i \cos \theta_i \\ \sin \theta_i & \cos \theta_i \cos \alpha_i & -\cos \theta_i \sin \alpha_i & a_i \sin \theta_i \\ 0 & \sin \alpha_i & \cos \alpha_i & d_i \\ 0 & 0 & 0 & 1 \end{bmatrix}$$

For a revolute joint the computation of this link transformation involves six multiplications and the evaluation of $\sin \theta_i$ and $\cos \theta_i$; for a prismatic joint, which has d_i as the joint variable, this computation is trivial. It is important to note that the algorithm which evaluates ${}^i T_{i+1}$ must know beforehand the joint type in order to avoid unnecessary computation involving the $\cos \alpha_i$ and $\sin \alpha_i$ terms. The table lookup scheme based on the POE equations, however, handles both prismatic and revolute joints in a uniform way, and thus adds a measure of device-independence *vis-a-vis* the standard Denavit-Hartenberg scheme, albeit at the expense of efficiency. Computationally the table lookup method substitutes the six multiplication operations and evaluation of $\sin \theta_i$ and $\cos \theta_i$ in the Denavit-Hartenberg method with the overhead of looking up twelve numbers. A fundamental tradeoff between computation and memory therefore exists between these two methods.

We now turn our attention to the computation of the Jacobian (or more accurately, the left and right differentials). The Jacobian in the base frame, recall, is given by the right differential

$$df \cdot f^{-1} = A_1 dx_1 + e^{A_1 x_1} A_2 e^{-A_1 x_1} dx_2 + \dots$$

While at first this expression may seem to require an inordinate amount of computation, because of the special structure of the matrices, the number of operations required to compute the Jacobian is considerably less than straightforward multiplication of arbitrary matrices. Each term, first of all, is an element of $se(3)$, and with the exception of the dx_1 term, consists of a multiplication of the form

$$\begin{bmatrix} \Theta & x \\ 0 & 1 \end{bmatrix} \begin{bmatrix} [\omega] & v \\ 0 & 0 \end{bmatrix} \begin{bmatrix} \Theta^T & -\Theta x \\ 0 & 1 \end{bmatrix} = \begin{bmatrix} [\Theta \omega] & \Theta v - [\Theta \omega]x \\ 0 & 0 \end{bmatrix}$$

where $\Theta \in SO(3)$ and $x, \omega, v \in \mathbb{R}^3$. Much of the computation for each term can also be reused for subsequent terms. Given these considerations, we see that for an n -link open

chain, $n - 2$ multiplications of $SE(3)$ matrices and $n - 1$ manipulations of the form above are required to compute the Jacobian. These figures also apply to the Jacobian expressed in the tip frame.

In [31] Orin and Schrader investigate various methods of computing the Jacobian for an open-chain mechanism. Their analysis concentrates on a particular class of recursive methods based on transforming the angular and translational velocities from one end of the chain to the other. We describe what they conclude to be the most computationally efficient algorithm for evaluating the Jacobian in terms of the base frame. Let ${}^i\Theta_j$ and ${}^i\boldsymbol{x}_j$ denote the 3×3 orientation matrix and position vector of the link transformation iT_j , and let $({}^i\omega_j, {}^i\boldsymbol{v}_j)$ represent the angular and translational velocities of frame j with respect to frame i , respectively. The recursive equations used to compute the Jacobian are then given by

$$\begin{aligned} {}^0\Theta_i &= {}^0\Theta_{i-1}{}^{i-1}\Theta_i, \quad i = 1, \dots, n-1 \text{ and } {}^0\Theta_0 = I \\ {}^0\omega_i &= \begin{cases} {}^0\Theta_{i-1} \begin{bmatrix} 0 \\ 0 \\ 1 \end{bmatrix}, & i = 1, \dots, n \text{ for a revolute joint} \\ 0, & i = 1, \dots, n \text{ for a prismatic joint} \end{cases} \\ {}^0p_i &= {}^0p_{i-1} + {}^0\Theta_{i-1}{}^{i-1}\boldsymbol{x}_i, \quad i = 1, \dots, n-1 \text{ and } {}^0p_0 = 0 \\ {}^0\boldsymbol{v}_i &= \begin{cases} {}^0\omega_i \times ({}^0p_n - {}^0p_{i-1}), & i = 1, \dots, n \text{ for a revolute joint} \\ {}^0\Theta_{i-1} \begin{bmatrix} 0 \\ 0 \\ 1 \end{bmatrix}, & i = 1, \dots, n \text{ for a prismatic joint} \end{cases} \end{aligned}$$

For the Jacobian with respect to the tip (or tool) frame, Orin and Schrader propose a similar recursive method, but this time iterating from the tip to the base. The following table compares the number of operations required in computing the Jacobian of an n degree-of-freedom open chain for the three methods discussed:

	multiplications	additions/subtractions.	overhead
POE Formula	$60n - 96$	$45n - 72$	$12n$ lookup values
Recursive – Base Frame	$42n + 9$	$30n + 12$	$2n$ trig. functions
Recursive – Tool Frame	$42n$	$30n$	$2n$ trig. functions

For six, seven, and eight link chains, the number of operations are given by

	$n = 6$	$n = 7$	$n = 8$
POE Formula	264 mult, 198 add	324 mult, 243 add	384 mult, 288 add
Recursive – Base Frame	261 mult, 192 add	303 mult, 222 add	345 mult, 252 add
Recursive – Tool Frame	252 mult, 180 add	294 mult, 210 add	336 mult, 240 add

We see, first of all, that for $n \leq 8$ the number of operations required for the POE Jacobian, while greater than that required for the recursive methods, is certainly comparable for most applications. However, as Orin and Schrader point out in [31], extra computational overhead is incurred in transforming the recursively obtained Jacobian in terms of one frame to a different reference frame, *e.g.*, expressing the base frame Jacobian in terms of the tip frame. The POE Jacobian, meanwhile, can be expressed in terms of both the tip and base frames by the same computational algorithm, and hence the number of operations is identical for both cases. The POE method is therefore more appealing for applications where coordinate changes between the base and tip frames are involved.

More significantly, the recursive methods, like the Denavit-Hartenberg link transformation for forward kinematics, need to know in advance whether a joint is prismatic or revolute before the algorithm can be reduced to a strictly arithmetic computation. Hence, the POE formula also adds a certain measure of device independence in the computation of the Jacobian. The lookup-based POE scheme may also prove useful in calculating a manipulator's forward and inverse dynamics, since these also require knowledge of the Jacobian at some stage of the computation process.

It has also been pointed out in the literature on kinematic calibration, notably by Hayati[21], that the four parameter Denavit-Hartenberg representation of link transformations can cause singularities in the calibration algorithms that are based on minimizing a least-squares error measure (see Hollerbach's survey paper[24] on kinematic calibration). Specifically, singularities in the Denavit-Hartenberg representation occur when adjacent joint axes are nearly parallel, and because the common normal between the axes is quite sensitive to small changes in the orientation of the axis, the Denavit-Hartenberg parameters are ill-conditioned. Some approaches have therefore abandoned the Denavit-Hartenberg parameters altogether in favor of five- and six-parameter representations of link transformations. Although these representations are redundant, they can in some cases avoid the

algorithmic singularities of kinematic calibration. Some six-parameter representations also have the ability to model higher-order kinematic pairs, such as bent prismatic joints. The POE equations belong to this class of six-parameter kinematic representations, and it would be of interest to investigate the performance of kinematic calibration methods based on the POE equations.

2.4 Summary

In this chapter we review particular aspects of Riemannian geometry and Lie groups that form the basic tools for our subsequent analysis of mechanisms. The two fundamental local coordinate systems for Lie groups, the coordinates of the first and second kind, are discussed for $SO(3)$ and $SE(3)$, and Riemannian metrics and volume forms for these two Lie groups are displayed in these coordinates. We then discuss the product-of-exponentials formula for open kinematic chains, and argue that it has both geometric and practical appeal.

Chapter 3

Kinematic Performance

In this chapter we shall develop coordinate-invariant, geometrically-defined measures for the kinematic dexterity and workspace volume of a mechanism. The geometry of $SE(3)$, especially the choice of a Riemannian metric, enters into our analysis in a crucial way, and we show that the existence of a bi-invariant volume form on $SE(3)$ permits a natural definition of a mechanism's workspace volume; this is the definition employed by Paden and Sastry[32].

The kinematic dexterity measures that we consider are distinguished by the following two attributes: global versus local, and first-order versus second-order; by the latter we mean that the measure contains either first or second derivatives of the forward kinematic map. There exists a natural global measure of the distortion of a mapping $f : N \rightarrow M$ between Riemannian manifolds, given by a certain functional $D(f)$. *Harmonic maps*, which are the critical points of $D(f)$, have recently been the object of significant mathematical research; here we survey some basic notions of harmonic mapping theory, and discuss the suitability of $D(f)$ as a measure of kinematic dexterity. The physical meaning of $D(f)$ for mechanisms is determined in large part by the choice of Riemannian metric on N and M , and some of the physical implications of this choice are also discussed.

While $D(f)$ serves as a natural measure of global dexterity, it is not applicable for measuring local dexterity, and in addition there exist other geometrically-defined dexterity measures which, while not as basic as $D(f)$, still merit consideration. Of these we investigate a number of first-order measures that can be interpreted physically in terms of the

velocity ellipsoid generated by the Jacobian. These measures permit both a local and global coordinate-invariant definition of kinematic dexterity. A class of second-order global measures based on the Ricci curvature tensor of a manifold are also considered. All these ideas are illustrated by a simple but nontrivial example of a basic mechanism whose kinematics defines a mapping from the torus to the sphere.

3.1 Workspace Volume

Let (N, h) be a Riemannian manifold representing the configuration space of a mechanism, and let the forward kinematics of the mechanism be given by the map $f : N \rightarrow SE(3)$. We define the workspace of the mechanism to be $\text{Im}(f)$, the image of this mapping, and the workspace volume, $W(f)$, as

$$W(f) = \int_{\text{Im}(f)} \Omega$$

where Ω is the bi-invariant volume form on $SE(3)$ parametrized by a choice of length scale (see proposition 2.5). Volumes on $SE(3)$ defined with respect to Ω are natural in the following sense: if \mathcal{U} is a compact subset in $SE(3)$, its volume is invariant under left and right translations of \mathcal{U} , i.e.,

$$\int_{\mathcal{U}} \Omega = \int_{g\mathcal{U}} \Omega = \int_{\mathcal{U}g} \Omega$$

for any $g \in SE(3)$. If \mathcal{U} is the workspace of a mechanism, left translation invariance then implies that the workspace volume does not change when the base is moved or reoriented; any reasonable notion of workspace volume must obviously obey this property. A nontrivial consequence of the right translation invariance property, moreover, is that adding any fixed attachment to a mechanism's tip, such as a broom handle, does not change the workspace volume. For these reasons the bi-invariant volume form Ω will also be referred to as the *natural volume form* on $SE(3)$.

One of the obviously desirable properties of a manipulator is that, subject to some reach constraint, its workspace volume be maximized. As outlined in chapter 1, previous studies on workspaces have considered alternative definitions of workspace volume based on the *reachable* and *dexterous* workspaces. The reachable workspace is defined as the set of all points in physical space that can be reached by the manipulator's tip. The dexterous

workspace is the subset of the reachable workspace in which the tip can assume any arbitrary orientation. According to this definition workspace volumes are measured as the volume of subsets in E^3 . The dexterous workspace volume moreover does not include points of the reachable workspace at which the mechanism's tip can assume only a partial set of orientations. On the other hand, the volume measured with respect to the natural volume form includes these intermediate points, and therefore allows for smooth tradeoffs between the tip's orientation and position freedoms.

One possible objection to our definition of workspace volume is that it does not, roughly speaking, count the “number of times” each point in the workspace is covered by the mechanism’s tip. For example, it may seem inequitable to assign the same workspace volume to a 2-link and 3-link planar chain which both cover the same disk in the plane. However, the fact that a mechanism has multiple ways of reaching a particular workspace point is in some sense a measure of its dexterity, and in fact the *volume* of a mapping, which we describe below, attempts to capture this property. Based on these considerations, $W(f)$ as a measure of workspace volume is reasonable from both a physical and analytical point of view.

3.2 Kinematic Dexterity

Before specifying any kinematic dexterity measures, we first establish some notation for mappings between Riemannian manifolds, and show how to construct coordinate-invariant integral measures on manifolds. Let N and M denote Riemannian manifolds of dimension n and m , respectively. Let (x^1, \dots, x^n) denote local coordinates on N , and (f^1, \dots, f^m) local coordinates on M . We denote the Riemannian metrics on N and M by $h_{\alpha\beta}dx^\alpha dx^\beta$ and $g_{ij}df^i df^j$, respectively, where we use the Einstein convention of summation over repeated indices. Define $(h^{\alpha\beta})$ and (g^{ij}) to be $(h_{\alpha\beta})^{-1}$ and $(g_{ij})^{-1}$, respectively. Mappings between Riemannian manifolds will then be denoted by $f : (N, h) \rightarrow (M, g)$.

The general integral measures that we consider are defined in terms of tensor fields on manifolds. Let $\{dx^\alpha\}$ be a basis for the cotangent bundle T^*N , and let $\omega = \omega_{\alpha\beta} dx^\alpha \wedge dx^\beta$, $\xi = \xi_{\alpha\beta} dx^\alpha \wedge dx^\beta$ be two two-tensors on N , *i.e.*, $\omega(p)$ and $\xi(p)$ are real-valued functions of pairs of tangent vectors on $T_p N$, where $p \in N$. An inner product on this space can be

defined as

$$\langle \omega, \xi \rangle = \omega_{\alpha\beta} h^{\alpha p} \xi_{pq} h^{\beta q}$$

This inner product is invariantly-defined with respect to coordinate changes. Now, given any two-tensor ω on N , fix a point $p \in N$, and form the proper values of ω relative to the metric tensor of N , i.e., the n real roots of the equation $\det(h_{\alpha\beta}(p)\lambda - \omega_{\alpha\beta}(p)) = 0$. Apart from their order, these values are intrinsically associated with ω and $p \in N$.

Now let σ be any symmetric function¹ of n variables, and define $\sigma(\omega) : N \rightarrow \mathbb{R}$ to be the function such that $\sigma(\omega)p$ is the symmetric function σ with the proper values of $\omega(p)$ as its arguments. With these constructs we can specify an invariant functional $L(\omega)$ on N as

$$L(\omega) = \int_N \sigma(\omega) \Omega_N$$

where Ω_N is the volume measure on N induced by its Riemannian metric, expressible in coordinates as $\Omega_N = [\det(h_{\alpha\beta})]^{\frac{1}{2}} dx^1 \wedge \cdots \wedge dx^n$. Specific choices for ω and σ lead to variational problems of geometric interest. We will mainly be interested in tensors ω obtained by pulling back various two-tensors on M by f , and in functions σ defined in terms of the *elementary symmetric functions* σ_k , $k = 1, \dots, n$. The elementary symmetric functions are defined as follows: given an n -vector $\lambda = (\lambda_1, \dots, \lambda_n)$,

$$\sigma_k(\lambda) \triangleq \sum_{i_1 < i_2 < \dots < i_k} \lambda_{i_1} \lambda_{i_2} \cdots \lambda_{i_k}$$

In particular, $\sigma_1(\lambda) = \lambda_1 + \dots + \lambda_n$, and $\sigma_n(\lambda) = \lambda_1 \lambda_2 \cdots \lambda_n$.

3.2.1 Harmonic Maps and Kinematic Distortion

In this section we review the basic concepts of harmonic maps, and discuss the suitability of the integral functional of harmonic mappings as a first-order global measure of kinematic dexterity. Let $f : N \rightarrow M$ be a C^1 map between Riemannian manifolds as above. Define the *distortion density*² of f to be

$$d(f) = \frac{1}{2} h^{\alpha\beta}(x) g_{ij}(f(x)) \frac{\partial f^i}{\partial x^\alpha} \frac{\partial f^j}{\partial x^\beta}$$

¹A function is *symmetric* if its value is invariant under any permutation of its arguments.

²What we call the distortion is usually called the *energy* in the harmonic mapping literature. Unfortunately, the way the term energy is used in the harmonic mapping literature leads to some ambiguity, since in our context energy has a different meaning.

If we denote the Jacobian matrix of the map f by J , and the Riemannian metrics (g_{ij}) and $(h_{\alpha\beta})$ by G and H , respectively, an equivalent expression for the distortion density is

$$d(f) = \frac{1}{2} \text{Tr}(J^T G J H^{-1})$$

The *distortion* of the map f is defined in terms of $d(f)$ as

$$\begin{aligned} D(f) &= \int_N d(f) \Omega_N \\ &= \frac{1}{2} \int_N g_{ij} \frac{\partial f^i}{\partial x^\alpha} \frac{\partial f^j}{\partial x^\beta} h^{\alpha\beta} [\det(h_{\alpha\beta})]^{\frac{1}{2}} dx^1 \wedge \dots \wedge dx^n \end{aligned}$$

where $\Omega_N = [\det(h_{\alpha\beta})]^{\frac{1}{2}} dx^1 \wedge \dots \wedge dx^n$ is the volume element in N induced from its metric. If f is of class C^2 , the distortion $D(f)$ is finite, and f is a critical point of $D(f)$, then the map f is called *harmonic*.

Since harmonic maps are extremals of the distortion integral, they must satisfy a corresponding set of Euler-Lagrange equations. These are

$$\frac{1}{\sqrt{|h_{\alpha\beta}|}} \frac{\partial}{\partial x^\alpha} (\sqrt{|h_{\alpha\beta}|} h^{\alpha\beta} \frac{\partial f^i}{\partial x^\beta}) + h^{\alpha\beta} \Gamma_{jk}^i \frac{\partial f^j}{\partial x^\alpha} \frac{\partial f^k}{\partial x^\beta} = 0, \quad i = 1, 2, \dots, m.$$

where $|h_{\alpha\beta}|$ denotes the determinant of the metric $h_{\alpha\beta}$, and Γ_{jk}^i are the Christoffel symbols of the second kind on M . In coordinates the Christoffel symbols are given in terms of the metric by

$$\Gamma_{jk}^i = \frac{1}{2} g^{is} \left(\frac{\partial g_{sk}}{\partial f^j} + \frac{\partial g_{sj}}{\partial f^k} - \frac{\partial g_{jk}}{\partial f^s} \right)$$

We thus obtain a nonlinear elliptic system of m partial differential equations, where the first term on the left is the Laplace-Beltrami operator on N , and the second term is quadratic in the gradient of the solution. Note that if M is a flat space, so that (g_{ij}) is a constant diagonal matrix, the Euler-Lagrange equations then specialize to Laplace's equation. The individual terms in these equations are generally very tedious to compute, and in many of our applications it is more convenient to write the Euler-Lagrange equations for multiple integrals using the standard calculus of variations in local coordinates. Specifically, given any integral functional $P(f)$ of the form

$$P(f) = \int_N L(x, f(x), \nabla f(x)) dx$$

where $\nabla f(x) \in \mathfrak{X}^{mn}$ is $\left(\frac{\partial f^1}{\partial x^1}, \dots, \frac{\partial f^1}{\partial x^n}, \dots, \frac{\partial f^m}{\partial x^1}, \dots, \frac{\partial f^m}{\partial x^n}\right)$, and assuming that N is a manifold with fixed boundaries, a routine derivation then shows that the Euler-Lagrange equations are

$$\frac{\partial L}{\partial f^i} - \sum_{j=1}^m \frac{d}{dx^j} \frac{\partial}{\partial (\frac{\partial f^i}{\partial x^j})} L = 0, \quad i = 1, \dots, m$$

We now present some familiar examples of harmonic maps.

Example 3.1 Suppose $M = N = [0, 1]$. The distortion functional in this case is $\int_0^1 \dot{f}^2 dt$, and its Euler-Lagrange equation is $\ddot{f} = 0$; the minimum distortion maps are therefore linear. If we identify the endpoints of the interval with each other, problem can then be regarded as a mapping from S^1 into itself. If f is required to cover S^1 exactly once, the identity map then corresponds to the harmonic mapping solution.

Example 3.2 If $M = \mathbb{E}$, the Euler-Lagrange equations reduce to Laplace's equation, $\nabla^2 \Phi(x) = 0$, whose solutions are the *harmonic functions*. A well-known physical example is the problem of determining the equilibrium temperature distribution in a metal plate, subject to a set of thermal boundary conditions at the edges of the plate. In this case the distortion is

$$D(\Phi) = \int \int_A \left(\frac{\partial \Phi}{\partial x} \right)^2 + \left(\frac{\partial \Phi}{\partial y} \right)^2 dx dy$$

The solution is given by the function $\Phi(x, y)$ which satisfies the Euler-Lagrange equation $(\frac{\partial^2}{\partial x^2} + \frac{\partial^2}{\partial y^2})\Phi = 0$ and the given boundary conditions.

Example 3.3 If N is of dimension 1, the Euler-Lagrange equations for the distortion are the familiar equations for geodesics on M . Recall that geodesics generalize the notion of straight lines in flat spaces: the great circles on the two-sphere are a familiar example. If N is the interval $[0, 1]$, then $D(f) = \int_0^1 \langle \dot{f}, \dot{f} \rangle dt$, and the Euler-Lagrange equations are

$$\frac{d^2}{dt^2} f^i + \Gamma_{jk}^i \frac{df^j}{dt} \frac{df^k}{dt} = 0, \quad i = 1, \dots, m$$

This example shows the sense in which harmonic maps can be thought of as a generalization of geodesics to mappings between arbitrary Riemannian manifolds.

The distortion can also be formulated invariantly in the tensor field setting discussed above. Specifically, let σ_1 denote the first symmetric function given by the sum of its

arguments, and choose on N the pullback metric f^*g . Then

$$D(f) = \frac{1}{2} \int_N \sigma_1(f^*g) \Omega_N$$

is the corresponding coordinate-free definition of a mapping's distortion.

Eells and Sampson[14] offer the following physical interpretation of $D(f)$ as a measure of distortion associated with f . Suppose N were made of elastic and M of marble, and it was desired to cover M by N . One can then associate with each point in N an elastic tension, and harmonic maps can be thought of as the maps which result in an elastic equilibrium of minimum average tension. This intuitive notion is made more precise by their concept of *infinitesimal dispersion*. Specifically, let $d(P, Q)$ denote the geodesic distance between two points P, Q in M , and suppose p, q are two points in N such that $f(p) = P, f(q) = Q$. Given a fixed p we consider $d(P, \cdot)$ to be the function $q \mapsto d(P, Q)$; for q sufficiently near p this function is smooth. Suppose that $B_\epsilon = \{q \in N | r(p, q) \leq \epsilon\}$, where $r(\cdot, \cdot)$ is the geodesic distance metric on N , and let $V(B_\epsilon)$ be its volume. Eells and Sampson then show that

$$\frac{2\epsilon^2}{n+2} d(f(p)) + O(\epsilon^3) = \frac{1}{V(B_\epsilon)} \int_{B_\epsilon} d^2(P, Q) \Omega_N$$

The distortion $D(f)$ therefore estimates the mean-square infinitesimal dispersion of the image points on N produced by f , integrated over the domain with respect to its volume form.

Another useful interpretation applicable to mechanisms involves probability. As is well-known, the Jacobian of the forward kinematic map can be viewed as defining the velocity gain from joint space to tip space, and its inverse transpose as defining the force-torque gain; a large velocity gain results in a small force-torque gain. By controlling the size of the velocity gains one can then control the force-torque gain. Now, if the velocity vector is randomly distributed in joint space according to a zero mean, unity variance Gaussian, and if the average velocity gain is defined to be the expected value of the length of the velocity vector in tip space, then the harmonic map minimizes the “mean” velocity gain, averaged over the entire set of joint values; this average is computed relative to the natural volume measures in both the range and domain.

Finally, when $n \leq m$ (*i.e.*, for nonredundant mechanisms), $D(f)$ can also be interpreted as a measure of the proximity of f to an isometry: recall that f is an isometry if $h = f^*g$.

A simple calculation shows that the distortion density $d(f) = \frac{n}{2}$ when f is an isometry; Ells and Sampson further show that any isometry $f : N \rightarrow N$ is harmonic. When $D(f)$ is regarded as a measure of kinematic dexterity it will henceforth be referred to as the *kinematic distortion*.

3.2.2 Other First-Order Measures

While the harmonic mapping distortion provides a natural global measure of kinematic dexterity, one can also define other invariant measures based on the local first-order kinematic properties of a mechanism. In this section we examine some of these first-order measures, which are closely related to the velocity ellipsoid-based measures of Yoshikawa[45] and Salisbury and Craig[41]. The proper invariant formulation of any such measure, recall, requires constructing symmetric functions of the proper values of f^*g , i.e., the roots of $\det(H\lambda - J^T G J) = 0$. One might expect that the distortion density $d(f)$ could also serve as a local dexterity measure, but unfortunately this is not the case. Any candidate local dexterity measure must, first of all, penalize singular configurations, but in general $d(f)$ fails to do so. The simplest illustrative example is given by a map $f : [0, 1] \rightarrow [0, 1]$. For this case the distortion density $d(f) = \dot{f}^2$, and the singularities of f are precisely those points at which $d(f)$ also vanishes. The reason that a global measure of distortion can be obtained from $d(f)$ is because of the boundary condition requirements that the map cover a certain portion of the range.

Since kinematic singularities clearly play an important role in the formulation of any local dexterity measure, as a preliminary step we recount some facts from differential topology on the singularities of mappings. More precisely, the *critical points* of a mapping $f : N \rightarrow M$ in which $n \geq m$, recall, are those points x in N at which the derivative mapping df_x fails to be onto; their image points are called *critical values*. If a point is not critical then it is *regular*, and its image points are correspondingly called *regular values*. By Sard's theorem (see Guillemin[19]) it is known that the critical values of f form a set of measure zero in M . Moreover, if y is a regular value in M , it is well-known that $f^{-1}(y)$ is an $(n-m)$ -dimensional submanifold of N . This submanifold can be assigned a volume in terms of the volume form naturally induced from the one on N .

Because the derivative of f has maximal rank at a regular point, the pullback metric f^*g has exactly m nonzero proper values (again assuming that $n \geq m$); we label these in descending order as $\lambda_1, \lambda_2, \dots, \lambda_m$. Now, the critical points of f are marked by the minimum proper value λ_m going to zero. Maximizing λ_m is therefore one possibility for a local kinematic dexterity measure that penalizes singular configurations. The nonzero proper values can still be visualized as the lengths of the principal axes associated with the velocity ellipsoid, however. This interpretation allows us to generalize the local dexterity measures of Yoshikawa[45] and Salisbury and Craig[41] to mappings between Riemannian manifolds. Specifically, the condition number-based local dexterity measure is defined as

$$c(f) = \frac{\lambda_1(f^*g)}{\lambda_m(f^*g)}$$

This local measure can be extended to a global measure $C(f)$ by

$$C(f) = \int_N c(f) \Omega_N$$

$c(f)$ can be maximized as a criterion for redundancy resolution, while $C(f)$ can be maximized with respect to the kinematic parameters for optimal design synthesis. Similarly, we define the *volume density* of $f : N \rightarrow M$ to be

$$v(f) = \begin{cases} [\sigma_n(f^*g)]^{\frac{1}{2}} & \text{if } n \leq m \\ [\sigma_m(f^*g)]^{\frac{1}{2}} & \text{if } n > m \end{cases}$$

where σ_k is the k th elementary symmetric function defined earlier in this chapter. The *volume* of f , $V(f)$, is then

$$V(f) = \int_N v(f) \Omega_N$$

In the case when $n \leq m$, $v(f)$ can be equivalently represented in terms of the Jacobian J and the metrics G and H as

$$v(f) = [\det(J^T G J H^{-1})]^{\frac{1}{2}}$$

Since $\Omega_N = [\det(H)]^{\frac{1}{2}} dx^1 \wedge \cdots \wedge dx^n$, $V(f)$ can also be expressed as

$$V(f) = \int_N [\det(J^T G J)]^{\frac{1}{2}} dx^1 \wedge \cdots \wedge dx^n$$

i.e., $V(f)$ is the volume of N measured with respect to the volume form induced by the pullback metric, f^*g . Eells and Sampson have observed that if f is an *immersion*³, then the minima of $V(f)$ are the *minimal immersions*. Minimal surfaces, which are surfaces of minimal area formed, for example, by soap film spanning a given wire frame, are the most familiar examples of this class of maps. In connection with harmonic mappings, Chern[10] has shown that if f is an isometry, then f is harmonic if and only if it is a minimal immersion.

When $n \geq m$, $v(f)$ is proportional to the volume of the velocity ellipsoid in M generated by the derivative of f . By infinitesimalizing this picture and integrating $v(f)$ over the domain N , $V(f)$ can be regarded as a measure of the volume of $f(N)$, but with each point in $f(N)$ counted according to the number of its preimages in N . This is also analogous to summing up, over all regular values of f , the signed volume of the preimage manifold assigned to each regular value. Since one of the principal advantages of redundant mechanisms over their nonredundant counterparts is their ability to reach a point in the workspace in many different ways, thereby avoiding workspace obstacles and singularities, by this interpretation one would clearly want to maximize $V(f)$. In the subsequent chapters we show that, not surprisingly, $V(f)$ is closely related to the workspace volume $W(f)$. By our interpretation of $V(f)$, it follows that the normalized ratio $V(f)/W(f)$ measures the “mean volume gain” of the mechanism represented by f ; one can argue that a key motivation behind adding redundancy is to increase this volume gain.

What distinguishes $c(f)$ and $v(f)$ from Yoshikawa’s manipulability index $\det(JJ^T)$ and the condition number $\text{cond}(J)$ of Salisbury and Craig is that in their prior work, J is implicitly identified with the right differential of the forward kinematic map f , and furthermore the metric chosen is the right-invariant Riemannian metric on $SE(3)$ corresponding to the identity on $se(3)$. We must emphasize again that $SE(3)$ has no natural metric. The left-invariant metric parametrized by the length scale, meanwhile, is invariant with respect to translations of the base, as any legitimate kinematic performance measure ought to be. $c(f)$ is a measure of how nearly uniform (or how nearly spherical) the velocity ellipsoid in the tip space M is; $v(f)$, meanwhile, measures the extent to which f locally preserves volume. Since

³Recall that $f : N \rightarrow M$ is an *immersion* if $n \leq m$ and its derivative df_x is of maximal rank at all points x in N .

the class of metric-preserving maps (*i.e.*, isometries) is a subset of the volume-preserving maps (*i.e.*, maps for which $\det(J^T G J) = \det(H)$), $c(f)$ is a more restrictive measure than $v(f)$.

3.2.3 Second-Order Measures

All of the first-order distortion measures discussed above are based on the pullback metric f^*g . The well-known *Theorema Egregium* of Gauss, which states that two surfaces are locally isometric if and only if their Gaussian curvatures at corresponding points are equal, suggests that distortion might be formulated in terms of the “curvature” associated with the spaces N and M . In this section we formalize this idea and propose a set of global distortion measures for f that are based on the Ricci curvature tensor of a manifold.

The notion of a *connection* plays an essential role in differential geometry, and provides an intrinsic means of differentiating a vector field in the direction defined by another vector field. Formally, a connection on a manifold M is a mapping ∇ which associates a vector field, $\nabla_X Y$, to any two vector fields X and Y , and which satisfies, for any function $f : M \rightarrow \mathbb{R}$, the following properties:

1. $\nabla_{X_1+X_2} Y = \nabla_{X_1} Y + \nabla_{X_2} Y$
2. $\nabla_X(Y_1 + Y_2) = \nabla_X Y_1 + \nabla_X Y_2$
3. $\nabla_f X = f \cdot \nabla_X Y$
4. $\nabla_X(fX) = f \cdot \nabla_X Y + X(f) \cdot Y$

With the connection one can introduce the notion of *parallel transport* of a tangent vector along a curve on a manifold. To do so, first consider a smooth vector field V along a curve $p : [a, b] \rightarrow M$, *i.e.*, a smooth function V on $[a, b]$ such that $V_t \in T_{p(t)}M$. The mapping $t \mapsto \nabla_{\frac{dp}{dt}} V$ is a smooth vector field along p , called the *covariant derivative* of V *along p*, and is also denoted by the symbol $\frac{DV}{dt}$. V is said to be *parallel along p* (with respect to ∇) if $\frac{DV}{dt} = 0$ along p . Expressed in local coordinates, the equation $\frac{DV}{dt} = 0$ reduces to a set of linear differential equations, and thus has a unique solution for any initial condition. Hence, given a curve $p : [a, b] \rightarrow M$ and a vector $V_a \in T_{p(a)}M$, there is a unique vector field V

along p which is also parallel along p . This vector field V_t is said to be generated from V_a by *parallel translation along p* . Clearly parallel translation determines a linear transformation $\tau_t : T_{p(a)}M \rightarrow T_{p(t)}M$ taking $V_a \mapsto V_t$; this transformation is one-one, since its inverse is given by parallel translating V_t in the reverse direction from t to a . The connection thus establishes an isomorphism between the tangent spaces $T_{p(t_1)}M$ and $T_{p(t_2)}M$ along any curve p . In short, the connection ∇ allows us to compare, or “connect”, tangent spaces at different points along a curve.

It must be emphasized that parallel transport depends on the choice of path: if two different paths connect a point x to another point y , there is no reason for parallel transport along these paths to agree at y . In fact, one can intuitively imagine this difference as being the total “curvature” of M in the region enclosed by the two paths. This picture can be infinitesimalized in Newtonian style to obtain an infinitesimal notion of curvature at a point in M .

A connection can be defined on any differentiable manifold M ; if we specialize to the case where M is a Riemannian manifold, then a particular connection on M is said to be *compatible* with the metric $\langle \cdot, \cdot \rangle$ if the parallel translations $\tau_t : T_{p(a)}M \rightarrow T_{p(t)}M$ along any curve $p : [a, b] \rightarrow M$ are isometric, i.e., given $X_{p(a)}, Y_{p(a)} \in T_{p(a)}M$, then $\langle X_{p(a)}, Y_{p(a)} \rangle_{p(a)} = \langle \tau_t(X_{p(a)}), \tau_t(Y_{p(a)}) \rangle_{p(t)}$. It is known (see Spivak[43], vol. 2) that a connection ∇ is compatible with $\langle \cdot, \cdot \rangle$ if and only if

$$X_p(Y, Z) = \langle \nabla_{X_p}Y, Z_p \rangle + \langle Y_p, \nabla_{X_p}Z \rangle$$

for all vector fields Y, Z and tangent vectors $X_p \in T_pM$. A connection ∇ is said to be *symmetric* if $[X, Y] = \nabla_X Y - \nabla_Y X$, where $[X, Y]$ denotes the Lie bracket between vector fields on M . The fundamental lemma of Riemannian geometry then states that any Riemannian manifold has a unique symmetric connection compatible with its Riemannian metric. Given a coordinate system $\{x^i\}$ for the manifold, with $\{x^i, \frac{\partial}{\partial x^i}\}$ the corresponding set of coordinates for the tangent bundle, this symmetric connection ∇ , called the *Levi-Civita connection*, is expressible in terms of the Christoffel symbols as

$$\nabla_{\frac{\partial}{\partial x^i}} \frac{\partial}{\partial x^j} = \Gamma_{ij}^k \frac{\partial}{\partial x^k}$$

For a general connection ∇ , the *curvature tensor* is defined as follows: if X, Y , and Z are

vector fields, the curvature tensor R defines another vector field given by

$$R(X, Y)Z = \nabla_X(\nabla_Y Z) - \nabla_Y(\nabla_X Z) - \nabla_{[X, Y]}Z$$

On a Riemannian manifold M with Levi-Civita connection ∇ the *Ricci tensor* S is defined as a symmetric two-tensor on M , whose components are given in coordinates by

$$S_{ik} = \frac{\partial}{\partial f^k} \Gamma_{ji}^j - \frac{\partial}{\partial f^j} \Gamma_{ki}^j + \Gamma_{km}^j \Gamma_{ji}^m - \Gamma_{jm}^j \Gamma_{ki}^m$$

Here the Christoffel symbols Γ_{ij}^k again represent the connection ∇ , and f^i are local coordinates on M . The connection, and consequently the Ricci tensor, is determined uniquely by the metric on M . Note further that the expression for S_{ik} contains second derivatives of the metric: it is this feature which gives rise to the “second-order” description of measures based on curvature.

Second-order distortion measures for a mapping $f : N \rightarrow M$ based on the Ricci tensor S of M can be defined in a number of ways, and also admit a useful physical interpretation via the following fact: if $f : N \rightarrow M$ is an isometry, then $f^*R_M = R_N$, where R_M and R_N are the curvature tensors on M and N given by their Levi-Civita connections, respectively, and f^*R_M is the pullback of R_M by f . The particular second-order measures that we consider are

$$K_1(f) = \int_N \sigma_1(f^*S) \Omega_N$$

and

$$K_n(f) = \int_N [\sigma_n(f^*S)]^{\frac{1}{2}} \Omega_N$$

For our applications the configuration space N of a mechanism is usually a flat space, so that R_N is zero. Hence, minimizing $|K_1(f)|$ and $|K_n(f)|$ is equivalent to making f^*R_M as close to zero as possible, or to finding the f that is “closest” to being an isometry.

3.2.4 The Configuration Space Metric and Actuator Strengths

The physical interpretation of the kinematic dexterity measures proposed above clearly depends on the choice of Riemannian metrics for the domain and range manifolds. Earlier we argued that the configuration space for revolute-joint mechanisms is most naturally identified with the flat torus T^n . In this space the Euclidean metric $ds^2 = dx_1^2 + \dots + dx_n^2$ is

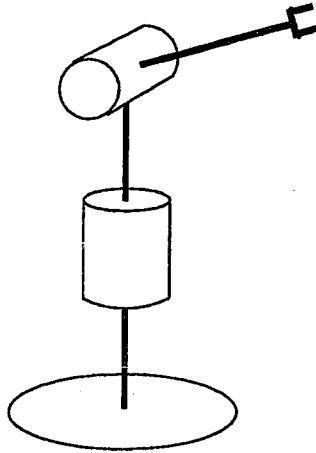


Figure 3.1: A 2R spherical mechanism.

generally the most common choice of flat metric, but for our purposes there is no physically compelling reason to favor this choice. We offer the following physical interpretation for a flat metric on T^n of the form $ds^2 = \epsilon_1 dx_1^2 + \dots + \epsilon_n dx_n^2$. First of all, since the volume of T^n should be constant whatever the choice of ϵ_i , we require that $\epsilon_1 \epsilon_2 \dots \epsilon_n$ be constant. We arbitrarily set this constant to one, so that with T^n coordinatized as \mathbb{R}^n modulo $2\pi\mathbb{Z} \times \dots \times 2\pi\mathbb{Z}$, its volume is $(2\pi)^n$. Now, suppose that all of the joint actuators are identical, and we wish to place single gears between each actuator and the corresponding joint. Clearly we see that $\sqrt{\epsilon_i}$ then corresponds to the gear ratio between joint i and its actuator. If the joint actuators are no longer assumed to be identical, each $\sqrt{\epsilon_i}$ can then be regarded as representing the maximum velocity attainable by the corresponding actuator of joint x_i . By choosing the ϵ_i that minimize the kinematic distortion, the relative strengths of a mechanism's actuators can be uniquely determined. We illustrate this and other ideas with the following example.

3.2.5 Example: A 2R Spherical Mechanism

Consider the 2R spherical mechanism of figure 3.1, whose kinematics can be regarded as a mapping from the two-torus T^2 to the two-sphere S^2 . Coordinatize T^2 as \mathbb{R}^2 modulo $2\pi\mathbb{Z} \times 2\pi\mathbb{Z}$, with local coordinates (u_1, u_2) , and metric $ds^2 = \epsilon_1 du_1^2 + \epsilon_2 du_2^2$, $\epsilon_1 \epsilon_2 = 1$. Let S^2 be the unit sphere embedded in \mathbb{R}^3 , with local spherical coordinates (θ, ϕ) , so that the

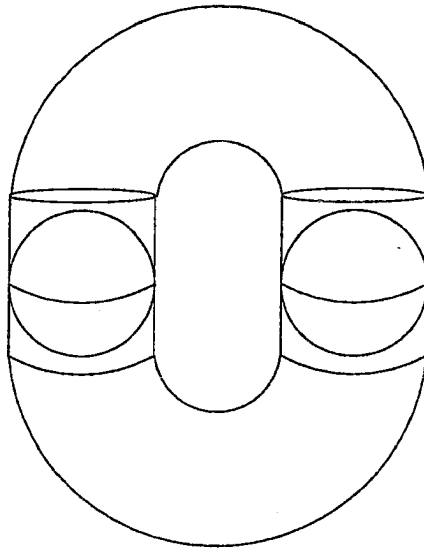


Figure 3.2: $f : T^2 \rightarrow S^2$ as a mapping from a cylinder to a sphere.

embedding is given by $x = \cos \theta \sin \phi$, $y = \sin \theta \sin \phi$, $z = \sin \phi$; the induced metric is then $ds^2 = d\phi^2 + \sin^2 \phi d\theta^2$ (see example 2.10). The kinematic equations are given in coordinates as

$$\begin{aligned}\theta &= u_1 \\ \phi &= u_2\end{aligned}$$

The expression for the distortion of f , $D(f)$, is

$$D(f) = \int_0^{2\pi} \int_0^{2\pi} \frac{1}{\epsilon_1} \left(\left(\frac{\partial \phi}{\partial u_1} \right)^2 + \sin^2 \phi \left(\frac{\partial \theta}{\partial u_1} \right)^2 \right) + \frac{1}{\epsilon_2} \left(\left(\frac{\partial \phi}{\partial u_2} \right)^2 + \sin^2 \phi \left(\frac{\partial \theta}{\partial u_2} \right)^2 \right) du_1 du_2$$

For the 2R mechanism $D(f)$ reduces to $\pi^2(\epsilon_1 + 2\epsilon_2)$, and a minimal value of $2\sqrt{2}\pi^2$ is attained when $\epsilon_1 = \sqrt{2}$, $\epsilon_2 = (\sqrt{2})^{-1}$. The physical interpretation of the metric constants ϵ_1 and ϵ_2 as relative peak velocities of the actuators suggests that the base actuator's maximum velocity should be $\sqrt{2}$ times as large as that of the elbow actuator. Intuitively this makes sense, since for trajectories which pass near either of the sphere's poles, movement in the θ direction for a given velocity of the base actuator takes much longer than movement in the ϕ direction for the same velocity applied to the elbow actuator.

Which kinematic design results in minimum kinematic distortion? We can get a lower bound on the performance of such a mechanism by looking at the harmonic maps from T^2

to S^2 . In this case the corresponding Euler-Lagrange equations are

$$\begin{aligned} \frac{1}{\epsilon_1} \left(\frac{\partial^2 \phi}{\partial u_1^2} - \sin \phi \cos \phi \left(\frac{\partial \theta}{\partial u_1} \right)^2 \right) + \frac{1}{\epsilon_2} \left(\frac{\partial^2 \phi}{\partial u_2^2} - \sin \phi \cos \phi \left(\frac{\partial \theta}{\partial u_2} \right)^2 \right) &= 0 \\ \frac{1}{\epsilon_1} \left(2 \cot \phi \frac{\partial \phi}{\partial u_1} \cdot \frac{\partial \theta}{\partial u_1} + \frac{\partial^2 \theta}{\partial u_1^2} \right) + \frac{1}{\epsilon_2} \left(2 \cot \phi \frac{\partial \phi}{\partial u_2} \cdot \frac{\partial \theta}{\partial u_2} + \frac{\partial^2 \theta}{\partial u_2^2} \right) &= 0 \end{aligned}$$

A theorem by Eells and Wood (cited in [15]) states that there are no harmonic maps of degree one from T^2 to S^2 ; we thus direct our search to maps of degree two or higher. By a symmetry argument we assume that θ is linear in u_1 , i.e., $\theta = u_1$, and ϕ depends on u_2 alone. These assumptions are plausible if the T^2 to S^2 mapping is regarded equivalently as mapping a cylinder to a sphere, where the cylinder represents half of a torus (see figure 3.2). Under these assumptions the Euler-Lagrange equations now reduce to a single pendulum equation of the form

$$\frac{d^2}{du_2^2} \phi(u_2) - \frac{\epsilon_2}{\epsilon_1} \sin \phi(u_2) \cos \phi(u_2) = 0$$

The boundary conditions for the double-covering solution are $\phi(0) = 0$, $\phi(2\pi) = 2\pi$. For these particular set of boundary conditions the pendulum equation has a unique periodic solution which can be determined numerically. We have thus reduced the Euler-Lagrange equations by a series of symmetry arguments to a single pendulum equation. Baird[4] provides a more general reduction theorem describing conditions under which the Euler-Lagrange equations for harmonic mappings between manifolds of constant curvature can be reduced to a single nonlinear equation of the pendulum type, of which our example is one case.

Given a numerically obtained solution to the pendulum equation above, one can vary the ratio $r = \frac{\epsilon_2}{\epsilon_1}$, and determine the behavior of $D(f)$ as a function of r for the harmonic mapping. We discover that as r approaches zero, $D(f)$ decreases monotonically to the minimum value of 8π . In fact, this is in accordance with a theorem which states that the infimum of the distortion in the class of maps of degree k from T^2 to S^2 is $|k| \cdot \text{Volume}(S^2)$.

We now consider the kinematic dexterity of this 2R mechanism using the second-order curvature-based measure $K_1(f) = \int_{T^2} \sigma_1(f^* S) \Omega_{T^2}$, discussed in section 3.2.3. For simplicity take the identity metric $ds^2 = du_1^2 + du_2^2$ on T^2 . On S^2 the Christoffel symbols are given by $\Gamma_{22}^1 = -\sin \phi \cos \phi$, $\Gamma_{12}^2 = \Gamma_{21}^2 = \cot \phi$, and $\Gamma_{ij}^k = 0$ otherwise, and the Ricci

tensor S_{ik} on S^2 is $S_{11} = -1$, $S_{22} = -\sin^2 \phi$, and $S_{12} = S_{21} = 0$. The Ricci tensor is simply the Riemannian metric scaled by -1 , and the extrema of this functional are clearly identical to the harmonic mapping solution. By choosing our dexterity measure to be $|K_1|$, we see that for this example the optimal solutions agree for the particular first and second-order measures of kinematic dexterity chosen.

By a simple calculation we can show that, under the above assumptions of $\theta = u_1$ and ϕ depending on u_2 alone, the proper values of f^*g are $\lambda_1 = (\frac{d\phi}{du_2})^2$ and $\lambda_2 = \sin^2 \phi$. Hence, the volume density $v(f)$ is $(\frac{d\phi}{du_2})^2 \sin^2 \phi$, and the corresponding Euler-Lagrange equations for $V(f)$ are

$$\frac{d^2\phi}{du_2^2} + \left(\frac{d\phi}{du_2}\right)^2 \cot \phi = 0$$

There does not exist an admissible solution to these equations for the double-covering boundary conditions given by $\phi(0) = 0$, $\phi(2\pi) = 2\pi$, and consequently a minimal solution for $V(f)$ cannot be determined. The condition number measure $C(f)$ leads to an even more complicated set of Euler-Lagrange equations, and for this particular example we cannot obtain a useful lower bound on these two measures.

3.3 Summary

In this chapter we have proposed a set of geometrically-defined measures for a mechanism's kinematic dexterity and workspace volume. The workspace volume of a mechanism can be defined in a natural way using the bi-invariant volume form on $SE(3)$. After introducing the functional of harmonic mapping theory, we argue that this functional provides a natural means of measuring the kinematic dexterity of a mechanism. In addition we propose a number of other coordinate-invariant, first-order dexterity measures that admit a physical interpretation in terms of the velocity ellipsoids generated by the forward kinematic map. A set of second-order measures of distortion based on the Ricci curvature of a manifold have also been constructed. The key ideas are illustrated by a simple example of a 2R spherical mechanism, considered as a mapping from the two-torus to the two-sphere.

Chapter 4

Planar Mechanisms

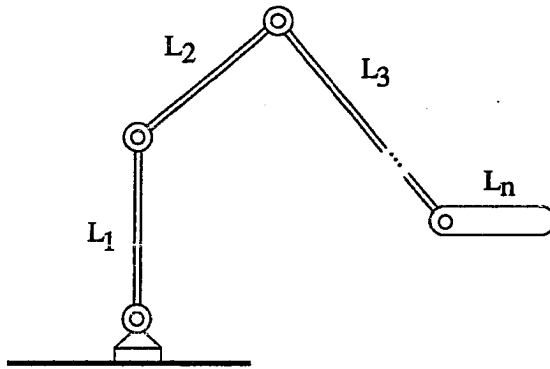
This chapter is concerned with the kinematic distortion and workspace volume of planar mechanisms. While in conventional treatments planar mechanisms are regarded as strictly translating devices, we will also consider the orientation and take the range of these mechanisms to be the Euclidean group of planar motions, denoted $SE(2)$. The particular matrix representation of $SE(2)$ we work with has the form

$$\begin{bmatrix} \cos \theta & -\sin \theta & x_1 \\ \sin \theta & \cos \theta & x_2 \\ 0 & 0 & 1 \end{bmatrix}$$

where $0 \leq \theta \leq 2\pi$, and $x_1, x_2 \in \mathbb{R}$. The corresponding Lie algebra, $se(2)$, then has the matrix representation

$$\begin{bmatrix} 0 & -\omega & v_1 \\ \omega & 0 & v_2 \\ 0 & 0 & 0 \end{bmatrix}$$

where $\omega, v_1, v_2 \in \mathbb{R}$. Since the planar mechanisms studied in this chapter have exclusively revolute joints, their forward kinematics will be represented as mappings from T^n to $SE(2)$. After classifying the kinematic singularities of a planar nR open chain, we derive the link lengths that minimize the kinematic distortion, as well as the link lengths that maximize the workspace volume for the $n = 3$ case. We then investigate the kinematic performance of a particular three degree-of-freedom closed-chain mechanism.

Figure 4.1: An n -link planar open-chain mechanism.

4.1 Open-Chain Planar Mechanisms

The kinematic equations for an open-chain planar mechanism are expressed by a special form of the product-of-exponentials formula: for an n -link chain with link lengths L_1, L_2, \dots, L_n (see figure 4.1) they are given by

$$f(x_1, \dots, x_n) = e^{Sx_1} M_1 e^{Sx_2} M_2 \dots e^{Sx_n} M_n$$

where the x_i are the local coordinates on $T^n = \mathbb{R}^n$ modulo $2\pi\mathbb{Z} \times \dots \times 2\pi\mathbb{Z}$ representing the joint variables, and

$$S = \begin{bmatrix} 0 & -1 & 0 \\ 1 & 0 & 0 \\ 0 & 0 & 0 \end{bmatrix}, \quad M_i = \begin{bmatrix} 1 & 0 & L_i \\ 0 & 1 & 0 \\ 0 & 0 & 1 \end{bmatrix}$$

Repeatedly applying the identity $P^{-1}(\exp A)P = \exp(P^{-1}AP)$, we get the body coordinate representation of the kinematics

$$f(x_1, \dots, x_n) = M e^{A_1 x_1} \dots e^{A_n x_n}$$

where

$$A_i = \begin{bmatrix} 0 & -1 & 0 \\ 1 & 0 & \sum_{k=i}^n L_k \\ 0 & 0 & 0 \end{bmatrix}, \quad M = \begin{bmatrix} 1 & 0 & \sum_{i=1}^n L_i \\ 0 & 1 & 0 \\ 0 & 0 & 1 \end{bmatrix}$$

Observe that the A_i are elements of $se(2)$. The left differential of f is

$$f^{-1} \cdot df = A_n dx_n + e^{-A_n x_n} A_{n-1} e^{A_n x_n} dx_{n-1} + \dots$$

The left differential can alternatively be expressed in matrix form as $J_L(x)dx$, where $dx \triangleq (dx_1, \dots, dx_n)$ is the n -vector representing the joint velocities, and $J_L(x)$ is the $3 \times n$ matrix with elements

$$\begin{aligned} j_{1n} &= \dots = j_{11} = 1 \\ j_{2n} &= 0 \\ j_{2k} &= j_{2,k+1} + L_k \sin\left(\sum_{i=k+1}^n x_i\right), k = 1, \dots, n-1 \\ j_{3n} &= L_n \\ j_{3k} &= j_{3,k+1} + L_k \cos\left(\sum_{i=k+1}^n x_i\right), k = 1, \dots, n-1 \end{aligned}$$

In particular, for the three-link case $n = 3$,

$$J_L(x) = \begin{bmatrix} 1 & 1 & 1 \\ L_2 \sin x_3 + L_1 \sin(x_2 + x_3) & L_2 \sin x_3 & 0 \\ L_3 + L_2 \cos x_3 + L_1 \cos(x_2 + x_3) & L_3 + L_2 \cos x_3 & L_3 \end{bmatrix}$$

4.1.1 Link Lengths for Maximal Workspace Volume

We now derive the link lengths of a planar open chain for maximal workspace volume. Recall that the workspace volume of a planar chain f is defined to be

$$W(f) = \int_{\text{Im}(f)} \Omega$$

where Ω is the bi-invariant volume form on $SE(2)$; this volume element is naturally induced from the bi-invariant volume form on $SE(3)$. Since $SE(2)$ is a three-dimensional manifold our primary interest in this section will be in three-link chains. Before examining their workspace volume, however, we first identify the set of critical points for general n -link planar chains.

Proposition 4.1 *Let $f : T^n \rightarrow SE(2)$ be the kinematic mapping of an nR planar open-chain mechanism. The critical points of f are*

$$\mathcal{C}_n = \{(x_1, \dots, x_n) \in T^n \mid x_2 = \dots = x_{n-1} = 0, \pi\}$$

Furthermore, the derivative of f has rank 2 at the critical points.

Proof: The critical points of f coincide with those points at which the left differential (or the right differential) is not onto. For the $n = 3$ case, $\det(J_L(x)) = L_1 L_2 \sin x_2$, which is singular at $x_2 = 0, \pi$. An induction argument establishes the proposition for the general case. By inspection of the expression for $J_L(x)$ it is easily verified that at the critical points the derivative is of rank two. \square

The critical points for the three-link chain occur when x_2 is 0 or π , and in these configurations the mechanism cannot execute a pure rotation or a pure translation of the tip in some particular direction (e.g., when the arm is completely outstretched, or when link one and link two overlap each other). If in the above proposition we had instead regarded the planar chain's range as \mathbb{R}^2 rather than $SE(2)$, the critical points then would be $\{(x_1, \dots, x_n) \in T^n \mid x_2 = \dots = x_n = 0, \pi\}$.

With this result in hand we now return to the original problem of determining the link lengths of a three-link planar chain that maximize the workspace volume. By Sard's theorem (see Guillemin[19]) we know that the critical values of f form a set of measure zero, and hence do not contribute to the volume of $\text{Im}(f)$. Moreover it's clear that each regular value in $SE(2)$ has exactly two inverse kinematic solutions, corresponding to an elbow-up and elbow-down configuration of the first two links. The set of critical points of the three-link chain

$$\mathcal{C}_3 = \{(x_1, x_2, x_3) \in T^3 \mid x_2 = 0, \pi\}$$

partitions T^3 into two open sets, \mathcal{U}_1 and \mathcal{U}_2 , each of which corresponds to one of the two elbow configurations. Hence, both $f(\mathcal{U}_1)$ and $f(\mathcal{U}_2)$ cover all of the regular values of $\text{Im}(f)$, and the workspace volume is determined by evaluating either $\int_{f(\mathcal{U}_1)} \Omega$ or $\int_{f(\mathcal{U}_2)} \Omega$, where Ω is the natural volume form on $SE(2)$. If we now regard f strictly as a map from \mathcal{U}_1 (respectively \mathcal{U}_2) onto its image $f(\mathcal{U}_1)$ (respectively $f(\mathcal{U}_2)$), the degree of f is then one. The workspace volume $W(f)$ now follows from a straightforward application of the degree formula (see Guillemin[19]):

$$\int_{\mathcal{U}_1} f^* \Omega = \deg(f) \cdot \int_{f(\mathcal{U}_1)} \Omega$$

With this formula $W(f)$ can be expressed as

$$\begin{aligned} W(f) &= \int_{\mathcal{U}_f} f^* \Omega \\ &= \int_0^{2\pi} \int_0^\pi \int_0^{2\pi} L_1 L_2 |\sin x_2| dx_1 dx_2 dx_3 \end{aligned}$$

Observe that the length scale for physical space is embodied in our choice of unit for L_1 and L_2 . Suppose we impose the constraint that the maximum *reach* of the planar chain is L , where reach is defined to be the Euclidean distance in \mathbb{R}^2 between the tip's position and the origin. By inspection the set of link lengths for maximal volume is clearly $L_1 = L_2 = \frac{1}{2}L$, $L_3 = 0$. Our discussion can be summarized by the following:

Proposition 4.2 *Let L_1, L_2 , and L_3 be the link lengths of a planar three-link open chain whose forward kinematics are represented as a map from T^3 to $SE(2)$. The link lengths which maximize the workspace volume of the chain, subject to the maximum reach constraint $L_1 + L_2 + L_3 = L$, are $L_1 = L_2 = \frac{1}{2}L$ and $L_3 = 0$.*

4.1.2 Link Lengths for Minimum Kinematic Distortion

Because no natural Riemannian metric exists on $SE(2)$, it is first necessary to choose a physically meaningful metric before the issue of kinematic distortion can be addressed. For reasons outlined in chapter 2 we consider the left-invariant Riemannian metric whose inner product on $se(2)$ is, with respect to its standard ordered basis, given by $ds^2 = c d\omega^2 + d(dv_1^2 + dv_2^2)$, which in matrix form is

$$Q = \begin{bmatrix} c & 0 & 0 \\ 0 & d & 0 \\ 0 & 0 & d \end{bmatrix}$$

Here c and d are positive constants such that $\frac{d}{c}$ represents the length scale of physical space. Assume initially the metric on T^n to be the Euclidean metric, i.e., $ds^2 = dx_1^2 + \dots + dx_n^2$. For the n -link planar chain represented by the mapping $f : T^n \rightarrow SE(2)$, the distortion density with respect to this metric is

$$d(f) = \frac{1}{2} \text{Tr}(J_L^T Q J_L)$$

$$= nc + d \left(\sum_{k=1}^n k L_k^2 + \sum \sum_{i \neq j} A_{ij} \cos x_i \cos x_j + B_{ij} \sin x_i \sin x_j \right)$$

where J_L is the left differential of f , and A_{ij} , B_{ij} are constants determined by the link lengths. Integrating the distortion density over the domain T^n , the total distortion reduces to

$$D(f) = (L_1^2 + 2L_2^2 + \dots + nL_n^2) d + nc$$

The set of link lengths which minimize $D(f)$ subject to some reach constraint can now be determined straightforwardly. It is immediately clear from the above expression that the optimal link lengths in no way depend on the choice of c or d . The variational equations for $D(f)$ in terms of the link lengths (L_1^*, \dots, L_n^*) , subject to the constraint that the reach is 1, can be reduced to the linear system

$$\begin{bmatrix} 3 & 1 & \cdots & 1 & 1 \\ 1 & 4 & \cdots & 1 & 1 \\ \vdots & \vdots & \ddots & \vdots & \vdots \\ 1 & 1 & \cdots & n & 1 \\ 1 & 1 & \cdots & 1 & n+1 \end{bmatrix} \begin{bmatrix} L_2^* \\ \vdots \\ L_n^* \end{bmatrix} = \begin{bmatrix} 1 \\ \vdots \\ 1 \end{bmatrix}$$

Since $D(f)$ is quadratic, the solution to this linear system is clearly a global minimum. Rewriting the above symmetric $(n-1) \times (n-1)$ matrix as $A + bb^T$, where $b = [1, \dots, 1]^T$, and A is the square matrix above consisting of just the diagonal elements, the well-known matrix inversion formula $(A + bb^T)^{-1} = A^{-1} - A^{-1}b(b^TA^{-1}b + 1)^{-1}b^TA^{-1}$ can be applied to obtain $L_k^* = \frac{1}{k}(1 + \frac{1}{2} + \dots + \frac{1}{n})^{-1}$. Normalizing the link lengths so that $L_1^* = 1$, the optimal solution is given by the harmonic sequence

$$(L_1^*, \dots, L_n^*) = (1, \frac{1}{2}, \frac{1}{3}, \dots, \frac{1}{n})$$

For the three-link case the optimal link lengths are in the ratio $L_1 = 6$, $L_2 = 3$, and $L_3 = 2$. Note that for this particular set of lengths the set of reachable points in the plane forms an annulus, so that the tip is unable to reach points whose distance from the origin (which coincides with the base joint) is less than one. The requirement that the chain be able to reach all points in the disk whose radius is $L_1 + L_2 + L_3$ can be expressed by the

inequality

$$\text{length of longest link} \leq \text{sum of lengths of other links}$$

If $n > 3$ the optimal link lengths given by the harmonic sequence satisfy this inequality. If $n = 3$ the link lengths that minimize the kinematic distortion and at the same time satisfy this constraint are $(L_1, L_2, L_3) = (5, 3, 2)$.

We observed above that the optimal link lengths did not depend on our choice of the scale factors c and d in the Riemannian metric. One consequence of this length scale-invariance is that these link lengths also minimize the kinematic distortion when the planar chain is regarded as a mapping into \mathbb{R}^2 rather than $SE(2)$. A further observation of interest is that the link lengths of human fingers are more or less in the optimal ratio of $(5, 3, 2)$ obtained above. We summarize these results as follows:

Proposition 4.3 *The link lengths of an n -link planar open chain which minimize the kinematic distortion are, up to constant scaling factor,*

$$(L_1, L_2, \dots, L_n) = \left(1, \frac{1}{2}, \dots, \frac{1}{n}\right)$$

With these link lengths, the planar chain's set of reachable points for $n > 3$ forms a disk in \mathbb{R}^2 with radius equal to the maximum reach. For $n = 3$, the link lengths which minimize the kinematic distortion, subject to the constraint that the reachable points cover a disk in \mathbb{R}^2 , are in the ratio $L_1 = 5, L_2 = 3, L_3 = 2$.

For comparison we now consider $V(f)$ and $C(f)$ (see section 3.2.2) as our kinematic dexterity measures. To simplify matters we will just consider three-link chains subject to the constraint that their maximum reach is one. In addition, their range is taken as \mathbb{R}^2 ; we noted above that the link lengths which minimize $D(f)$ in this case are also in the ratio $(5, 3, 2)$. A straightforward calculation reveals that $V(f)$ is proportional to $L_1^2 L_2^2 + 2L_3^2(L_1^2 + L_2^2)$, so that the link lengths (L_1, L_2, L_3) which maximize $V(f)$ are $(\frac{1}{2}, 0, \frac{1}{2})$ and $(0, \frac{1}{2}, \frac{1}{2})$. To see if these results agree with our physical intuition, recall the visualization of $V(f)$ given in section 3.2.2 for redundant mechanisms: $V(f)$ is obtained by summing, over all regular values in the workspace, the volume of the preimage manifold associated with each regular value; the volume is measured in terms of the volume form naturally induced from the

domain. From this interpretation it is evident that these two optimal sets of link lengths do in fact afford the greatest volume, since in both cases the preimage manifold at each regular point in the workspace has a maximal volume of 2π .

For the two-link planar chain Gosselin and Angeles[18] have shown that the link lengths (L_1, L_2) which maximize $C(f)$ are in the ratio $(1, \sqrt{2})$. A numerical analysis of the three-link case shows that $C(f)$ is maximized when the link lengths are approximately in the ratio $(0.625, 0, 0.375)$. Contrary to expectations, the ratio between link one and link three is not equal to the $\sqrt{2} : 1$ ratio of the two-link case. These results are in marked contrast to the optimal link lengths obtained via the kinematic distortion measure.

4.1.3 Optimal Joint Actuator Selection

As in the 2R spherical mechanism example of chapter 3, we can also determine the optimal actuator sizes for an nR open-chain planar mechanism, by choosing on the torus the flat metric which minimizes the kinematic distortion. Let the metric on $T^n = \mathbb{R}^n$ modulo $2\pi\mathbb{Z} \times \dots \times 2\pi\mathbb{Z}$ be of the form

$$ds^2 = \epsilon_1 dx_1^2 + \dots + \epsilon_n dx_n^2$$

where each $\epsilon_i > 0$ represents the maximum actuator velocity of joint x_i , and $\epsilon_1 \epsilon_2 \dots \epsilon_n = 1$. Once again applying the left-invariant Riemannian metric on $SE(2)$ with scale factors c and d , the kinematic distortion simplifies to

$$D(f) = \frac{(2\pi)^n}{2} \left(\frac{\rho_1}{\epsilon_1} + \dots + \frac{\rho_n}{\epsilon_n} \right)$$

where

$$\rho_i = c + d(L_i^2 + L_{i+1}^2 + \dots + L_n^2)$$

Given the above constraints on ϵ_i , and excluding negative values for the link lengths and scale factors, $D(f)$ has a unique critical point $\epsilon^* = (\epsilon_1^*, \dots, \epsilon_n^*)$ given by

$$\epsilon_i^* = \left(\frac{\rho_i^{n-1}}{\rho_1 \rho_2 \dots \rho_{i-1} \rho_{i+1} \dots \rho_{n-1} \rho_n} \right)^{\frac{1}{n}}$$

After an elementary but involved calculation, one can verify by examining the Hessian of $D(f)$ that ϵ^* is indeed a global minimum. In order to minimize kinematic distortion, the

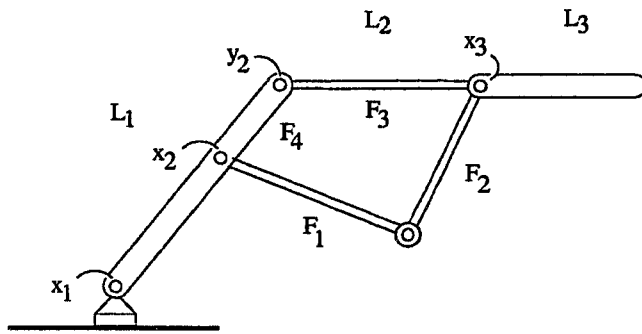


Figure 4.2: A planar closed-chain mechanism.

square of the maximum actuator velocities of the nR planar open chain should therefore be chosen in the ratio given by ϵ^* above. For the three-link example with equal link lengths and c, d set to one, the optimal actuator peak velocities are, proceeding from the base to the tip, in the ratio $(2, \sqrt{3}, \sqrt{2})$. For the general case, it is clear that $\rho_1 \geq \rho_2 \geq \dots \geq \rho_n$ for all feasible values of c, d , and L_i , and this further implies that $\epsilon_1^* \geq \dots \geq \epsilon_n^*$, i.e., the actuators should decrease in peak velocities as we progress outwardly from the base to the tip. This result agrees with most current practices in manipulator design, although the motivation behind using more powerful actuators for the base joints can usually be traced to other nonkinematic considerations.

4.2 A Planar Closed Chain

In this section we investigate the kinematic performance of the closed-chain mechanism of figure 4.2. Closed-chain mechanisms are recognized to have some practical advantages over their open-chain counterparts: in many cases they can lead to the elimination of drive transmissions like gear trains or chains, or avoid having undesirably heavy links, like those found on direct-drive open chains. The kinematic equations of general closed-chain mechanisms are typically specified by a forward mapping $f : N \rightarrow M$, along with a set of algebraic constraints. Both the joint space and workspace, as well as the Jacobian, of such mechanisms are in general difficult to characterize. Such mechanisms moreover present a choice among the joints which can be actuated. To circumvent many of these difficulties

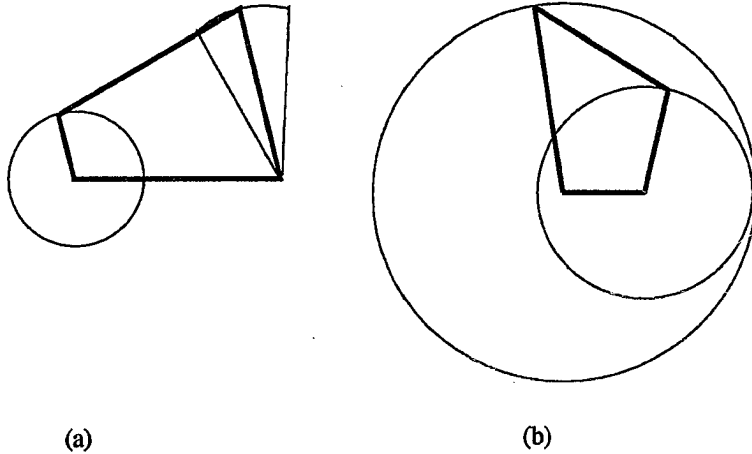


Figure 4.3: (a) A four-bar crank-rocker, and (b) a double-crank.

while at the same time preserving the essential features of closed chains, we will consider a particular closed-chain design with three degrees of freedom. The mechanism of figure 4.2 is similar to the three-link open chain of our previous analysis, but its kinematic behavior depends on the choice of link lengths for the closed-chain portion. Note that this closed-chain portion formed by $\{F_1, F_2, F_3, F_4\}$ constitutes a four-bar linkage¹. We consider only values of $\{F_i\}$ which satisfy the *Grashof* inequality, *i.e.*,

$$\text{longest link} + \text{shortest link} < \text{sum of other links}$$

Only if this inequality is satisfied can the closed-chain mechanism function as a *crank-rocker* or a *double-crank* (see figure 4.3), which are the only two types of four-bar linkages allowing the full 2π range of motion for joint x_2 .

Let (x_1, x_2, x_3) denote the local coordinates on $T^3 = \mathbb{R}^3$ modulo $2\pi\mathbb{Z} \times 2\pi\mathbb{Z} \times 2\pi\mathbb{Z}$, which also correspond to the actuated joints of the closed-chain mechanism of figure 4.2. The kinematic equations are given by

$$f(x_1, x_2, x_3) = M e^{A_1 x_1} e^{A_2 y_2(x_2)} e^{A_3 x_3}$$

where M, A_1, A_2 , and A_3 are the same as in the 3R open chain case, and

$$y_2(x_2) = 2 \tan^{-1} \frac{2F_1F_3 \sin x_2 - \sqrt{4F_1^2F_2^2 - (F_3^2 + F_4^2 - F_1^2 - F_2^2 + 2F_3F_4 \cos x_2)^2}}{F_3^2 + F_4^2 + F_1^2 - F_2^2 - 2F_1F_4 + 2F_3(F_4 - F_1) \cos x_2}$$

¹See [25], [13] for a review of four-bar linkages.

To examine the qualitative behavior of this mechanism's kinematic distortion, choose the link lengths (L_1, L_2, L_3) , to be $(5, 3, 2)$ (recall that these values also minimize the kinematic distortion for the 3R open chain case), and fix $F_4 = 2$, $F_3 = L_2 = 3$. Depending on our choice of F_1 and F_2 , then, the forward kinematics of the mechanism will differ according to a "warping" $y_2(x_2)$ of x_2 ; observe that if $y_2 = x_2$ the closed chain is kinematically identical to the 3R open chain.

The kinematic distortion and workspace volume of this mechanism are now evaluated for different values of F_1 and F_2 . First note that the left differential is

$$f^{-1} \cdot df = A_3 dx_3 + e^{-A_3 x_3} A_2 e^{A_3 x_3} \frac{dy_2}{dx_2} dx_2 + e^{-A_3 x_3} e^{-A_2 y_2(x_2)} A_1 e^{A_2 y_2(x_2)} e^{A_3 x_3} dx_1$$

As before, we apply the usual left-invariant metric on $SE(2)$ parametrized by the length scale factor $\frac{d}{c}$, and take the flat Euclidean metric on T^3 . In this case the distortion density $d(f)$ is

$$d(f) = c \left(2 + \left(\frac{dy_2}{dx_2} \right)^2 \right) + d \left(L_1^2 + L_2^2 + 2L_3^2 + \left(\frac{dy_2}{dx_2} \right)^2 (L_2^2 + L_3^2) + 2L_1 L_2 \cos y_2 \right)$$

Consider first the crank-rocker case: F_1 and F_2 must satisfy the inequality $F_1 + 1 < F_2 < 5 - F_1$. A numerical study of $D(f)$ as a function of F_1 and F_2 reveals that for any positive scale factors c and d , $D(f)$ has a unique global maximum at $(F_1, F_2) = (3, 2)$. In this case $y_2 = x_2$, and the kinematic equations are identical to the equations of the corresponding 3R open chain. The minimum distortion occurs when $(F_1, F_2) = (0, 1)$, i.e., when joint y_2 is fixed. For crank-rocker configurations of this closed chain, a tradeoff therefore exists between workspace volume and kinematic distortion: among the set of link lengths which result in the same workspace, the set with the shortest link F_2 will have the smallest kinematic distortion.

Suppose now that the closed chain functions as a double-crank. Fix F_1 to be 3, so that the allowable range of F_2 is $2 < F_2 < 4$. Figure 4.4 plots the distortion as a function of F_2 , for $c = d = 1$. An interesting observation is that the distortion is minimal when $F_2 = 2.6$. Since $F_2 = 2$ corresponds to the kinematics for the corresponding 3R open chain, we see that the closed chain with $F_2 = 2.6$ actually has a lower value of kinematic distortion than its open chain counterpart. The workspace volume of all double-crank configurations is, of course, identical to that of the corresponding 3R open chain.

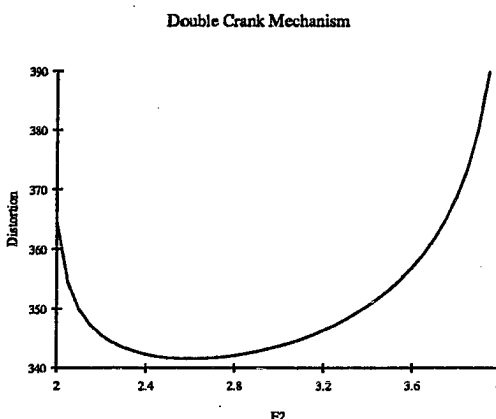


Figure 4.4: Distortion versus F_2 for the double-crank configuration.

4.3 Summary

In this chapter we have investigated the kinematic distortion and workspace volume of planar open chains, as well as a certain three degree-of-freedom closed chain. After classifying the singularities of nR open chains, we show that the workspace volume of a 3R open chain is maximized when the outer link is of length zero, and the two inner links are of equal length. The link lengths which minimize the kinematic distortion of an arbitrary nR open chain, on the other hand, are given by the harmonic sequence $(L_1, L_2, \dots, L_n) = (1, \frac{1}{2}, \dots, \frac{1}{n})$. Investigation of the actuator sizes for the nR open chain further reveals that, in order to minimize kinematic distortion for a given fixed product of the actuator peak velocities, the actuators should have decreasing peak velocities as the joints progress outwardly from the base to the tip.

An interesting result of our closed-chain analysis is that there exists a closed-chain version of the three-link open chain which actually has lower kinematic distortion than its open chain counterpart. We also observe tradeoffs between distortion and workspace volume for these closed-chain mechanisms.

Chapter 5

Spherical and Spatial Mechanisms

5.1 Spherical Mechanisms

A *spherical mechanism* is a revolute-joint kinematic chain all of whose joint-axes intersect at a single point. The motion of any point on a link of such a mechanism is constrained to lie on some sphere centered at the intersection point. Mathematically, the kinematics of an n -link open-chain spherical mechanism defines a map $f : T^n \rightarrow SO(3)$, expressed by the usual product-of-exponentials

$$f(x_1, \dots, x_n) = e^{A_1 x_1} \cdots e^{A_n x_n}$$

where the $A_i \in so(3)$ and x_i are the joint variables. Define T^n to be \mathbb{R}^n modulo $2\pi\mathbb{Z} \times \cdots \times 2\pi\mathbb{Z}$ with the flat Euclidean metric. In addition, define the inner product on the matrix Lie algebra $so(3)$ in the usual way as

$$\langle A, B \rangle = \frac{1}{2}\text{Tr}(AB^T)$$

and let $\|\cdot\|$ denote the norm induced from this metric. Now, in order for f to be well-defined as a mapping from T^n to $SO(3)$, each $\|A_i\|$ must be integer valued: only then will f be multiperiodic in each variable x_i , with period $\frac{2\pi}{\|A_i\|}$ (see the discussion on the POE equations in chapter 2).

As we pointed out earlier, $SO(3)$ is a compact Lie group and therefore admits a bi-invariant Riemannian metric. The kinematic results we obtain on spherical mechanisms

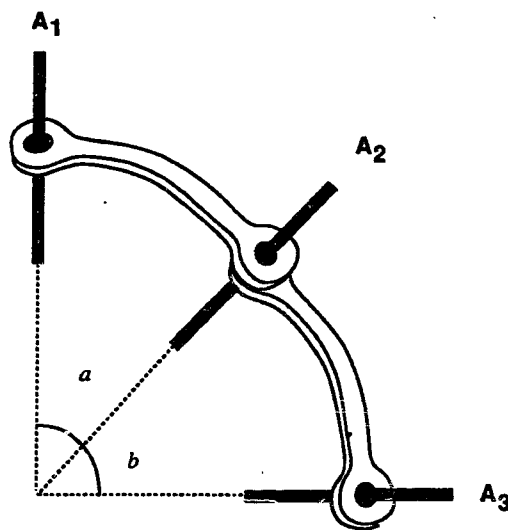


Figure 5.1: A three-link spherical wrist mechanism.

assume a particularly simple and concise form with respect to this metric. Furthermore, some previously established theorems on harmonic maps into compact Lie groups can be applied to our analysis of kinematic distortion. We begin by first calculating the workspace volume of spherical mechanisms.

5.1.1 Workspace Volume

Since $SO(3)$ is a three-dimensional group, any spherical mechanism must possess at least three degrees of freedom to cover $SO(3)$. We begin by determining the workspace volume of 3R spherical mechanisms, then generalize the resulting volume formula to nR spherical mechanisms. The kinematics of the 3R mechanism of figure 5.1 is completely specified by the angles α and β between the adjacent joint axes. To see this, note that any desired angle γ between joint axes A_1 and A_3 can be achieved by a simple rotation of the mechanism about axis A_2 , while still preserving the angles α and β ; specifying γ is therefore no more than simply defining a zero configuration for the mechanism. Note that $SO(3)$ is covered in its entirety when the axes are orthogonal, *i.e.*, when α and β are both $\frac{\pi}{2}$.

Given a reference frame, choose the A_i in the forward kinematic equations of the mech-

anism, $f(x_1, x_2, x_3) = e^{A_1 x_1} e^{A_2 x_2} e^{A_3 x_3}$, to be

$$A_1 = \begin{bmatrix} 0 & -\sin \alpha & \cos \alpha \\ \sin \alpha & 0 & 0 \\ -\cos \alpha & 0 & 0 \end{bmatrix}$$

$$A_2 = \begin{bmatrix} 0 & 0 & 1 \\ 0 & 0 & 0 \\ -1 & 0 & 0 \end{bmatrix}$$

$$A_3 = \begin{bmatrix} 0 & 0 & \cos \beta \\ 0 & 0 & -\sin \beta \\ -\cos \beta & \sin \beta & 0 \end{bmatrix}$$

The forward kinematic mapping, it turns out, also acts as a local chart in coordinates of the second kind for the region of $SO(3)$ that f covers. This fact greatly simplifies our evaluation of the workspace volume, as we shall see.

Lemma 5.1 *Let $\mathcal{V} = (0, 2\pi) \times (-\frac{\pi}{2}, \frac{\pi}{2}) \times (0, 2\pi)$ be an open set in \mathbb{R}^3 , and $f : \mathcal{V} \rightarrow SO(3)$ be the map $f(x_1, x_2, x_3) = e^{\Omega_1 x_1} e^{\Omega_2 x_2} e^{\Omega_3 x_3}$, with $\|\Omega_1\| = \|\Omega_2\| = \|\Omega_3\| = 1$, and $\langle \Omega_1, \Omega_2 \rangle = \cos \alpha$, $\langle \Omega_2, \Omega_3 \rangle = \cos \beta$, $\langle \Omega_1, \Omega_3 \rangle = \cos \alpha \cos \beta$ for some $0 < \alpha, \beta < \pi$. Then f is a homeomorphism, and its inverse is a coordinate chart for $\mathcal{U} = f(\mathcal{V})$.*

Proof: Clearly f is smooth, so it suffices to show that f is 1-1 on \mathcal{V} . Suppose initially that $\Omega_i = A_i$, $i = 1, 2, 3$, where A_i is as given above, and $f(x) = f(y)$ for some $x, y \in \mathcal{V}$. By equating the elements in the matrix identity $e^{A_1 x_1} e^{A_2 x_2} e^{A_3 x_3} = e^{A_1 y_1} e^{A_2 y_2} e^{A_3 y_3}$, it follows that $x = y$. Now, note that any arbitrary set of $\{\Omega_i\}$ satisfying the hypothesis of the lemma can be expressed as $\Omega_i = Q A_i Q^T$, $i = 1, 2, 3$, for some $Q \in SO(3)$. If we suppose $f(x) = f(y)$ for this general case, then because $e^{Q A_i Q^T x_i} = Q e^{A_i x_i} Q^T$ it again follows that x must equal y . f is therefore a homeomorphism on \mathcal{V} , and defines a coordinate chart. \square

Remark: Note that when $\alpha = \beta = \frac{\pi}{2}$ the map $f = e^{A_1 x_1} e^{A_2 x_2} e^{A_3 x_3}$ describes the kinematics of a roll-pitch-yaw wrist. A_3 could just as easily have been chosen to be

$$A_3 = \begin{bmatrix} 0 & -\sin \beta & \cos \beta \\ \sin \beta & 0 & 0 \\ -\cos \beta & 0 & 0 \end{bmatrix}$$

so that f , when $\alpha = \beta = \frac{\pi}{2}$, now describes a roll-pitch-roll wrist. If the hypothesis of the lemma is altered so that now $\langle \Omega_1, \Omega_3 \rangle$ is $\cos(\alpha - \beta)$, the domain \mathcal{V} of f (as a coordinate chart) would then be $(0, 2\pi) \times (0, \pi) \times (0, 2\pi)$. The range over which x_2 is defined (as a local coordinate) always forms an open interval of width π , its endpoints varying continuously with $\langle \Omega_1, \Omega_3 \rangle$.

By treating the forward kinematic map as a coordinate chart for $SO(3)$, the workspace volume of f , or more precisely the volume of $\text{Im}(f)$ in terms of the bi-invariant volume form on $SO(3)$, can now be determined by a straightforward application of the degree formula (again, see Guillemin[19]): if $f : N \rightarrow M$ is a smooth map between two compact, n -dimensional manifolds, and Ω is an n -form on M , then

$$\int_N f^* \Omega = \deg(f) \int_M \Omega$$

where $\deg(f)$ is the (Brouwer) degree of f ; this result was also applied in our earlier analysis on the workspace volume of planar open chains. For our purposes we take N to be T^3 , M as $\text{Im}(f)$, and Ω to be the bi-invariant volume form on $SO(3)$. The workspace volume $W(f)$ is then

$$W(f) = \frac{1}{\deg(f)} \cdot \int_{T^3} f^* \Omega$$

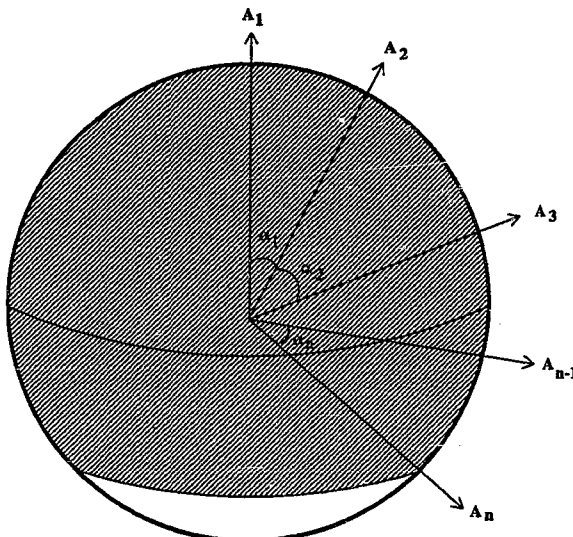
To determine the degree of f it suffices to simply count the number of preimage points of any regular value, except that each preimage point makes a contribution of +1 or -1, according to whether f preserves or reverses orientation.

For the map $f = e^{A_1 x_1} e^{A_2 x_2} e^{A_3 x_3}$ above, any regular value of f has two preimage points: if (x_1^*, x_2^*, x_3^*) is one solution, the other solution is $(x_1^*, 2\pi - x_2^*, x_3^*)$. We next evaluate the bi-invariant volume form on $SO(3)$. The left differential $J_L(x)$, recall, is obtained from

$$f^{-1} \cdot df = A_3 dx_3 + e^{-A_3 x_3} A_2 e^{A_3 x_3} dx_2 + e^{-A_3 x_3} e^{-A_2 x_2} A_1 e^{A_2 x_2} e^{A_3 x_3} dx_1$$

and the bi-invariant metric g_{ij} is given in the local coordinates provided by the forward kinematic map as $J_L^T(x) J_L(x)$, or

$$g_{ij} = \begin{bmatrix} 1 & \cos \alpha & \cos \alpha \cos \beta - \sin \alpha \sin \beta \sin x_2 \\ \cos \alpha & 1 & \cos \beta \\ \cos \alpha \cos \beta - \sin x_2 \sin \alpha \sin \beta & \cos \beta & 1 \end{bmatrix}$$

Figure 5.2: The orienting region for an nR -wrist.

Observe that if α and β are $\frac{\pi}{2}$, the expression for the metric agrees with that obtained in chapter 2 for the z - y - x Euler angle coordinates of $SO(3)$. The volume form induced from this metric is

$$\Omega = \sin \alpha \sin \beta \cos x_2 dx_1 \wedge dx_2 \wedge dx_3$$

Since $\cos x_2 = \cos(2\pi - x_2)$, Ω retains the same sign at both preimage points of a regular value of f . Clearly f is of degree two, and after a simple calculation the workspace volume reduces to

$$W(f) = \sin \alpha \sin \beta \cdot \text{Volume}(SO(3))$$

The workspace volume of 3R spherical mechanisms is given by this simple formula which depends only on the angles between adjacent joint axes. Not surprisingly, the workspace volume of nR spherical mechanisms, derived by generalizing the 3R formula, also depends only on the angles between adjacent joint axes, as we now show.

The local diffeomorphism of $SO(3)$ with the fiber bundle S^1 (the fiber) over S^2 (the base) suggests a useful spatial analogy between $SO(3)$ and the workspace of a spherical mechanism. Specifically, any element of $SO(3)$ can be characterized as a rotation about some line in \mathbb{R}^3 containing the origin. Each element of $SO(3)$ can therefore be identified with a pair, consisting of a point on S^2 representing the axis of rotation, and a point on

S^1 specifying the amount of rotation about this axis. For the nR spherical chain whose kinematic mapping is $f(x_1, \dots, x_n) = e^{A_1 x_1} \dots e^{A_n x_n}$, a set of prescribed joint values for the first $n - 1$ joints x_1, \dots, x_{n-1} fixes a line in \mathbb{R}^3 , corresponding to a point on S^2 , of the last joint axis A_n (see figure 5.2). The angles between the adjacent joint axes are labelled $\alpha_1, \dots, \alpha_{n-1}$, and satisfy $\langle A_i, A_{i+1} \rangle = \cos \alpha_i$. The set of points on S^2 reachable by the joint axis A_n then forms a band about the sphere determined by the angles θ_{min} and θ_{max} , which are called the *minimum* and *maximum orienting angles*. For the 3R chain with angles α_1 and α_2 , these orienting angles are given by $\theta_{min} = |\alpha_1 - \alpha_2|$ and $\theta_{max} = |\alpha_1 + \alpha_2|$. The workspace volume can alternatively be expressed in terms of these angles as

$$\begin{aligned} W(f) &= \sin\left(\frac{\theta_{max} + \theta_{min}}{2}\right) \sin\left(\frac{\theta_{max} - \theta_{min}}{2}\right) \cdot \text{Volume}(SO(3)) \\ &= \frac{1}{2}(\cos \theta_{min} - \cos \theta_{max}) \cdot \text{Volume}(SO(3)) \end{aligned}$$

For $n \geq 3$ it is not too difficult to see that the maximum and minimum orienting angles are given by

$$\theta_{max} = \begin{cases} \pi & \text{if } \sum \alpha_i \geq \pi \\ \sum \alpha_i & \text{otherwise} \end{cases}$$

and

$$\theta_{min} = \begin{cases} 0 & \text{if largest } \alpha_i \leq \text{sum of other } \alpha_i \\ \text{largest } \alpha_i - \text{sum of other } \alpha_i & \text{otherwise} \end{cases}$$

We see clearly that from this geometric picture of $SO(3)$ as the circle bundle over the two-sphere, the workspace volume of an nR spherical chain is completely determined by θ_{min} and θ_{max} . The formula for the 3R chain extends directly to the general nR case as follows.

Theorem 5.1 *Let $A_1, \dots, A_n \in so(3)$, and let*

$$f(x_1, \dots, x_n) = e^{A_1 x_1} \dots e^{A_n x_n}$$

be a map from T^n to $SO(3)$ representing the forward kinematics of an nR spherical open chain. Let $\alpha_1, \dots, \alpha_{n-1}$ be the angles between adjacent joint axes such that $\langle A_i, A_{i+1} \rangle = \cos \alpha_i$. Then the workspace volume, $W(f)$, is given by

$$W(f) = \frac{1}{2}(\cos \theta_{min} - \cos \theta_{max}) \cdot \text{Volume}(SO(3))$$

where θ_{min} and θ_{max} are the minimum and maximum orienting angles of f .

In particular, note that f covers all of $SO(3)$ if and only if $\theta_{min} = 0$ and $\theta_{max} = \pi$.

5.1.2 Kinematic Distortion

In this section we examine the kinematic distortion of spherical nR chains, and compare these results with those obtained for other dexterity measures discussed in section 3.2.2. Unlike planar mechanisms, some strong assertions can be made about spherical mechanisms because of the compactness of $SO(3)$. Of particular relevance is a theorem by Pluzhnikov[37], which characterizes the harmonic maps into any Lie group admitting a bi-invariant Riemannian metric. We begin by first reviewing some necessary basic concepts, and then stating these specific harmonic mapping results.

Recall first the definition of *homotopy*: two maps $f_0 : N \rightarrow M$ and $f_1 : N \rightarrow M$ are said to be homotopic if there exists a smooth map $F : N \times [0, 1] \rightarrow M$ such that $F(x, 0) = f_0(x)$ and $F(x, 1) = f_1(x)$. In [44] Toth shows that any harmonic mapping between compact manifolds is of minimum distortion in its homotopy class. Now, given a Lie group \mathfrak{G} , the *Maurer-Cartan form* μ on \mathfrak{G} is a one-form with values in the Lie algebra given by the relation

$$\mu(v_g) = dL_g^{-1}(v_g) \in T_e(\mathfrak{G})$$

where v_g is an arbitrary element in $T_g\mathfrak{G}$, L_g^{-1} denotes left-translation by the element $g^{-1} \in \mathfrak{G}$, and dL_g^{-1} is its derivative. When \mathfrak{G} is the linear group $Gl(n)$ or one of its subgroups (*e.g.*, $SO(3)$ or $SE(3)$), the Maurer-Cartan form μ is defined through the equation $\mu(v_g) = g^{-1}v_g$, since the derivative of a linear mapping can be identified with the mapping itself. Also recall that for any n -dimensional Riemannian manifold N with metric h , the linear operator d^* maps p -forms to $(p-1)$ -forms, and is defined in terms of the exterior derivative d and Hodge $*$ operator by $d^*\omega = (-1)^{p+p(n-p)}\text{sign}(\det h_{ij}) * d * \omega$, where ω is any p -form on N . See Choquet-Bruhat[12] for a more complete discussion of these concepts.

The theorem by Pluzhnikov can now be stated in terms of these definitions as follows: let N be a Riemannian manifold, G a Lie group which admits a bi-invariant Riemannian metric, μ the Maurer-Cartan form on GG , and $f : N \rightarrow \mathfrak{G}$ a smooth map. Then f is harmonic if and only if $d^*(f^*\mu) = 0$, where $f^*\mu$ is the pullback of μ by f .

Since T^n and $SO(3)$ are both compact, and $SO(3)$ furthermore admits a bi-invariant

metric, these results can be directly applied to the class of mappings $f(x_1, \dots, x_n) = e^{A_1 x_1} \dots e^{A_n x_n}$ from T^n to $SO(3)$. Before characterizing these minimum distortion harmonic maps, let us introduce the notation $\text{Ad}_k : so(3) \rightarrow so(3)$ to represent the adjoint action

$$\text{Ad}_k(\Omega) = e^{A_k x_k} \Omega e^{-A_k x_k}$$

Once again, let T^n be \mathbb{R}^n modulo $2\pi\mathbb{Z} \times \dots \times 2\pi\mathbb{Z}$ with the usual Euclidean metric given by $ds^2 = dx_1^2 + \dots + dx_n^2$, and let $\|A_i\| \in \mathbb{Z}$, $i = 1, \dots, n$. The pullback of the Maurer-Cartan form on $SO(3)$ by f is just the left differential

$$f^{-1} \cdot df = A_n dx_n + e^{-A_n x_n} A_{n-1} e^{A_n x_n} dx_{n-1} + \dots$$

Note that here $f^{-1} \cdot df$ is regarded as a $so(3)$ -valued 1-form on T^n . Now, if $\alpha = a_i dx^i$ were a 1-form in \mathbb{R}^n , one can easily show that $d^*\alpha = -\text{div}(V)$, where V is a vector with components $(\alpha_1, \dots, \alpha_n)$, and $\text{div}(\cdot)$ is the divergence operator. Since locally T^n is the same as \mathbb{R}^n , the necessary condition $d^*(f^*\mu) = 0$ is equivalent to

$$-\text{div}(V_i) = 0, \quad i = 1, \dots, n$$

where each V_i is the three-vector determined by

$$[V_i] = \text{Ad}_n^{-1} \circ \text{Ad}_{n-1}^{-1} \circ \dots \circ \text{Ad}_{i+1}^{-1}(A_i)$$

Since each V_i is a function only of (x_{i+1}, \dots, x_n) , the necessary condition $d^*(f^*\mu) = 0$ for harmonic mappings is clearly satisfied. Combined with Toth's result, we therefore conclude the following:

Theorem 5.2 *Let A_1, \dots, A_n be elements of $so(3)$ such that $\|A_i\| \in \mathbb{Z}$, $i = 1, \dots, n$, and let $T^n = \mathbb{R}^n$ modulo $2\pi\mathbb{Z} \times \dots \times 2\pi\mathbb{Z}$ be the flat torus with local coordinates (x_1, \dots, x_n) . Then the map $f : T^n \rightarrow SO(3)$ taking $(x_1, \dots, x_n) \mapsto e^{A_1 x_1} \dots e^{A_n x_n}$ is a minimum distortion harmonic map in its homotopy class.*

We now classify the homotopy classes of the product-of-exponentials mappings from T^n to $SO(3)$. While these mappings form only a restricted class of mappings from T^n to $SO(3)$, our primary interest is in mechanisms, and for purposes of kinematic analysis it suffices to consider only this limited class. We first establish the following lemma.

Lemma 5.2 Let $A_1, \dots, A_n, B_1, \dots, B_n \in so(3)$ with $\|A_i\|, \|B_i\| \in \mathbb{Z}$, $i = 1, \dots, n$. If $e^{A_1 x_1} \dots e^{A_n x_n} = e^{B_1 x_1} \dots e^{B_n x_n}$ for all $x \in T^n$, then $A_i = B_i$, $i = 1, \dots, n$.

Proof: Differentiating both sides of $e^{A_1 x_1} \dots e^{A_n x_n} = e^{B_1 x_1} \dots e^{B_n x_n}$ with respect to x_i and evaluating at $x = 0$ for $i = 1, \dots, n$ establishes this result. \square

The homotopy classes of the product-of-exponentials mappings can now be classified as follows:

Proposition 5.1 Let $A_1, \dots, A_n, B_1, \dots, B_n \in so(3)$ with $\|A_i\|, \|B_i\| \in \mathbb{Z}$, $i = 1, \dots, n$, and let $f_a(x) = e^{A_1 x_1} \dots e^{A_n x_n}$ and $f_b(x) = e^{B_1 x_1} \dots e^{B_n x_n}$ be two maps from T^n to $SO(3)$. Then f_a is homotopic to f_b if and only if $\|A_i\| = \|B_i\|$, $i = 1, \dots, n$.

Proof: We prove the forward direction first. Suppose f_a is homotopic to f_b , and let $F : T^n \times [0, 1] \rightarrow SO(3)$ be the homotopy map $e^{C_1(t)x_1} \dots e^{C_n(t)x_n}$ such that $F(x, 0) = f_a(x)$ and $F(x, 1) = f_b(x)$. Then clearly $C_i(0) = A_i$ and $C_i(1) = B_i$ from the lemma. Moreover, since each $\|C_i(t)\|$ must be integer-valued in order for $F(t, x)$ to be well-defined as a map from T^n to $SO(3)$, it follows that $\|A_i\| = \|B_i\| \forall i$. The reverse direction can be shown by a direct construction of the homotopy F . \square

Mechanically, the homotopy classes of spherical mechanisms admits an interpretation in terms of gearing ratios. If $f(x_1, \dots, x_n) = e^{A_1 x_1} \dots e^{A_n x_n}$ denotes the forward kinematics of the mechanism, then each joint motor x_i is geared according to the ratio $1 : \|A_i\|$, where each $\|A_i\|$ is integer-valued. By the proposition, two spherical nR mechanisms belong to the same homotopy class if and only if the gear ratios of the corresponding joint motors are identical. Since the choice of a Riemannian metric on T^n also fixes the gear ratios for each joint, we will eliminate this redundant parametrization and assume henceforth that each $\|A_i\| = 1$ in the forward kinematic equations.

Since gear ratios can also be interpreted as the maximum actuator velocities, the preceding discussion naturally raises the question of what the peak velocities of the joint actuators should be in order to minimize the kinematic distortion. Thus far we have assumed identical peak velocities by taking the Euclidean metric $ds^2 = dx_1^2 + \dots + dx_n^2$ on T^n . Suppose now

that the metric is of the form $ds^2 = \epsilon_1 dx_1^2 + \dots + \epsilon_n dx_n^2$, where $\epsilon_1 \epsilon_2 \dots \epsilon_n = 1$. With this metric the distortion density becomes

$$\begin{aligned} d(f) &= \frac{1}{2} \left\{ \frac{1}{\epsilon_1} \langle A_1, A_1 \rangle + \frac{1}{\epsilon_2} \langle A_2, A_2 \rangle + \dots + \frac{1}{\epsilon_n} \langle A_n, A_n \rangle \right\} \\ &= \frac{1}{2} \left(\frac{1}{\epsilon_1} + \frac{1}{\epsilon_2} + \dots + \frac{1}{\epsilon_n} \right) \end{aligned}$$

$D(f)$ is therefore a symmetric function of the ϵ_i , minimized when $\epsilon_1 = \dots = \epsilon_n = 1$. The joint actuators of a spherical mechanism should therefore have the same peak velocities in order for the kinematic distortion to be minimal. For fixed n , all nR spherical mechanisms whose actuators all have the same peak velocity will have the same kinematic distortion regardless of their geometry, *i.e.*, $D(f)$ is invariant with respect to the angles between the adjacent joint axes. The principal tradeoffs in kinematic performance therefore occur in the workspace volume. It would seem natural to favor spherical mechanisms with maximal workspace volume, which for the 3R case corresponds to the joint axes being orthogonal.

One might, based on a purely intuitive and informal understanding of dexterity, object to the fact that a 3R spherical mechanism's kinematic distortion is constant regardless of the angles between the joint axes. A 3R mechanism with its joint axes colinear should, according to this argument, be less dexterous than one with orthogonal axes, which can assume any orientation. Recall our physical interpretation of $D(f)$, however: $D(f)$ is the average tension associated with the mapping $f : N \rightarrow M$ which covers a marble range, M , by an elastic domain, N . For a fair comparison of kinematic distortion between two mechanisms that have the same joint space, therefore, the two workspace volumes should agree. One could alternatively formulate a normalized dexterity measure given by the ratio $D(f)/W(f)$, a distortion per volume measure, as a means of comparison. We have simply chosen to treat the kinematic distortion and workspace volume separately for clarity of exposition. In either case, the spherical mechanisms with larger workspace volumes should be favored, which for the 3R mechanism corresponds to the joint axes being orthogonal.

We now conclude this section by identifying the kinematic singularities of spherical chains. Intuitively it is clear that the singularities, or more precisely the critical points of the forward kinematic map, occur when the joint axes are coplanar. This result is now formally established.

Theorem 5.3 *An open-chain spherical mechanism is at a kinematic singularity if and only if the joint axes are coplanar.*

Proof: Since the geometric structure of an open-chain spherical mechanism is specified by the angles between adjacent joint axes, without loss of generality, the zero position of such a mechanism can be defined such that the joint axes are all coplanar. The corresponding forward kinematic mapping $f : T^n \rightarrow SO(3)$ is given by $f(x_1, \dots, x_n) = e^{A_1 x_1} \dots e^{A_n x_n}$, where each $A_i \in so(3)$ is of the form

$$A_1 = \begin{bmatrix} 0 & -1 & 0 \\ 1 & 0 & 0 \\ 0 & 0 & 1 \end{bmatrix}, \quad A_k = \begin{bmatrix} 0 & -\cos(\sum_{i=1}^{k-1} \alpha_i) & -\sin(\sum_{i=1}^{k-1} \alpha_i) \\ \cos(\sum_{i=1}^{k-1} \alpha_i) & 0 & 0 \\ \sin(\sum_{i=1}^{k-1} \alpha_i) & 0 & 0 \end{bmatrix}$$

for $k = 2, \dots, n$. Here α_i is the angle between joint axes A_i and A_{i+1} , satisfying $\langle A_i, A_{i+1} \rangle = \cos \alpha_i$. The point $x = (x_1, \dots, x_n)$ is a critical point of f if the derivative map df_x fails to be surjective. This condition is also equivalent to either the left differential $f^{-1} \cdot df$ or the right differential $df \cdot f^{-1}$ failing to be surjective. We henceforth work with the right differential of f , which is given explicitly by

$$df \cdot f^{-1} = A_1 dx_1 + \text{Ad}_1(A_2) dx_2 + \dots + \text{Ad}_1 \circ \dots \circ \text{Ad}_{n-1}(A_n) dx_n$$

where, as before, $\text{Ad}_k : so(3) \rightarrow so(3)$, $\Omega \mapsto e^{A_k x_k} \Omega e^{-A_k x_k}$ denotes the adjoint map associated with the element $e^{A_k x_k} \in SO(3)$. An equivalent condition for x to be a critical point of f is that the set

$$\{A_1, \text{Ad}_1(A_2), \dots, \text{Ad}_1 \circ \dots \circ \text{Ad}_{n-1}(A_n)\}$$

not span $so(3)$.

The proof now proceeds by induction. For the initial case $n = 3$, a simple calculation shows that the determinant of the matrix whose columns are formed by $\{A_1, \text{Ad}_1(A_2), \text{Ad}_1 \circ \text{Ad}_2(A_3)\}$ is $\sin \alpha_1 \sin \alpha_2 \sin x_2$. Excluding the permanently degenerate case $\alpha_1, \alpha_2 = 0, \pi$, the critical points of f occur when $x_2 = 0$ or π . Now, assume, as the induction hypothesis, that the set $S_k = \{A_1, \text{Ad}_1(A_2), \dots, \text{Ad}_1 \circ \dots \circ \text{Ad}_{k-1}(A_k)\}$ does not span $so(3)$ if and only if $x_i = 0$ or π , $i = 2, \dots, k-1$. We once again exclude the degenerate trivial case when $\alpha_i = 0$ or π , $i = 1, \dots, k-1$. Denote by M and \hat{M} the 3×3 matrices whose columns are

formed by $\{\text{Ad}_1 \circ \dots \circ \text{Ad}_{k-2}(A_{k-1}), \text{Ad}_1 \circ \dots \circ \text{Ad}_{k-1}(A_k), \text{Ad}_1 \circ \dots \circ \text{Ad}_k(A_{k+1})\}$ and $\{A_{k-1}, \text{Ad}_{k-1}(A_k), \text{Ad}_k(A_{k+1})\}$, respectively. Then $\det M = \det \hat{M} = \sin \alpha_{k-1} \sin \alpha_k \sin x_k$. It follows that S_{k+1} spans $so(3)$ if and only if $x_i = 0$ or π , $i = 2, \dots, k$, i.e., when all the joint axes are coplanar. \square

This result, also proven previously by Brockett (cited in Hollerbach[23]), establishes that for any given joint values for x_1 and x_n of an nR spherical mechanism, there exist exactly 2^{n-2} singular configurations.

5.1.3 Comparison with Other Dexterity Measures

We now analyze the dexterity of spherical mechanisms in terms of the other dexterity measures proposed in chapter 3. Once again, let $\alpha_1, \dots, \alpha_n$ denote the angles between adjacent joint axes of the spherical open chain. We first consider the second-order distortion measure based on the Ricci curvature tensor. On any compact semi-simple Lie group the Ricci tensor is

$$S(X, Y) = -\frac{1}{4}\text{Tr}(\text{ad } X \circ \text{ad } Y)$$

where X, Y are left-invariant vector fields and $\text{ad}(\cdot)$ denotes the adjoint representation (see Choquet-Bruhat[12]). S is proportional to the Killing form κ on the group, and hence can also be identified with the bi-invariant Riemannian metric. For spherical mechanisms the curvature-based distortion measure and the kinematic distortion are therefore the same.

On the other hand, if we now consider $V(f)$ as the performance measure, then for $n = 3$ it is clear that $V(f)$ is simply $2W(f)$, so that $\alpha_1 = \alpha_2 = \frac{\pi}{2}$ maximizes $V(f)$. A numerical study reveals that when $n = 4$, the angles $\alpha_1 = \alpha_2 = \alpha_3 = \frac{\pi}{2}$ maximizes $V(f)$. These results would seem to suggest that, for nR spherical mechanisms with $n \geq 3$, the joint axes should be orthogonal (i.e., $\alpha_i = \frac{\pi}{2}$, $i = 1, \dots, n-1$) in order to maximize $V(f)$ and fully utilize the available redundancy.

Gosselin and Angeles[18] also show that the 3R mechanism which maximizes the condition number-based measure $C(f)$ is given by $\alpha_1 = \alpha_2 = \frac{\pi}{2}$. A numerical analysis for the 4R wrist also shows that $C(f)$ is maximized when the twist angles are $\alpha_1 = \alpha_2 = \alpha_3 = \frac{\pi}{2}$, and is minimal when the four joint axes are colinear in space.

5.2 Spatial Mechanisms

We now analyze the workspace volume and kinematic distortion of general open-chain, revolute-joint, spatial mechanisms. The forward kinematics of these mechanisms are represented as mappings $f : T^n \rightarrow SE(3)$ given by the product-of-exponentials equations, expressed in body coordinates as

$$f(x_1, \dots, x_n) = M e^{A_1 x_1} \cdots e^{A_n x_n}$$

where $M \in SE(3)$, and each A_i is an element of $se(3)$. T^n is once again the flat torus given by \mathbb{R}^n modulo $2\pi\mathbb{Z} \times \cdots \times 2\pi\mathbb{Z}$ with the standard Euclidean metric $ds^2 = dx_1^2 + dx_2^2 + \cdots + dx_n^2$, and on $SE(3)$ we will take the usual left-invariant Riemannian metric parametrized by the length scale.

5.2.1 Workspace Volume

Since $SE(3)$ is six-dimensional group, a spatial chain must possess at least six degrees of freedom in order for its workspace to have nonzero volume. A particularly important 6R spatial chain design is the *elbow manipulator*, which can informally be described as any 6R chain satisfying the following requirements:

- The last three joint axes form an orthogonal-axes spherical mechanism.
- The first two joint axes are orthogonal and intersect at a common point.
- The third joint axis is parallel to one of the first two joint axes.

The standard example of an elbow manipulator is given by a 3R orthogonal axis wrist attached to the end of the 3R chain of figure 5.3; see Paden and Sastry[32] for a formal definition. Some prior studies on the workspace volume of 6R spatial open chains (*e.g.*, Roth[39]) have argued that the elbow manipulator has maximal workspace volume. Paden and Sastry[32] establish this result formally, by regarding the forward kinematics as a mapping from T^6 to $SE(3)$, and measuring the workspace volume in terms of the length scale-dependent, one-parameter family of bi-invariant volume forms on $SE(3)$. Denoting

such a volume form by Ω , the workspace volume of a manipulator $f : T^6 \rightarrow SE(3)$ is

$$W(f) = \int_{\text{Im}(f)} \Omega$$

In their analysis they first define the *length* of a manipulator as the length (in \mathbb{R}^3) of the shortest continuous, piecewise-linear curve passing through the joint axes in successive order. They then show that a manipulator with length L cannot have a workspace whose volume exceeds $\frac{4}{3}\pi L^3 \cdot 8\pi^2$: this upper bound corresponds intuitively to an end-effector's positioning volume in \mathbb{R}^3 (which forms a solid ball of radius L), multiplied by the orienting volume at each point (which is $8\pi^2$, the volume of $SO(3)$). This quantity is defined as the *maximal workspace volume* of a manipulator. Implicit in this formula is the choice of a length scale, which is determined by the units of length for L .

A manipulator is also defined to have a *well-connected workspace* if it is able to move between any two regular values in its workspace without passing through a critical value. Their main result states that *a 6R manipulator has well-connected workspace and maximal workspace volume if and only if the manipulator or its kinematic inverse¹ is an elbow manipulator.*

Note that for mechanisms with fewer than six degrees of freedom $W(f)$ will always be trivial, since the workspace $\text{Im}(f)$ does not form a set of positive measure in $SE(3)$. One might therefore be tempted to define the workspace volume for such mechanisms in terms of the volume form naturally induced from that on $SE(3)$, i.e., if $\text{Im}(f)$ is a compact n -dimensional subset of $SE(3)$, where $n < 6$, its volume can then be measured in terms of the volume form induced from the bi-invariant volume form Ω on $SE(3)$. Although geometrically this definition may appear natural, physically it is not meaningful; we illustrate this below in the example of the 3R spatial mechanism of figure 5.3. When the dimension of the workspace is less than six, some form of the reachable workspace volume (i.e., the volume of the set of reachable points in \mathbb{R}^3) is usually sufficient for quantifying the volume of the workspace.

¹A manipulator's kinematic inverse is obtained by numbering its links in opposite order.

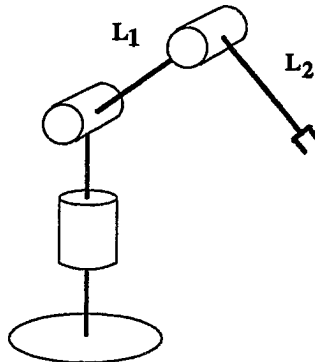


Figure 5.3: A 3R, two-link spatial chain.

5.2.2 Kinematic Distortion

While a great deal is known about harmonic maps into compact manifolds, relatively few assertions can be made when the range manifold is not compact. The Euler-Lagrange equations for harmonic maps, recall, form a second-order elliptic system of nonlinear differential equations, and there is no general theory that provides solutions to such systems. For this reason we find it difficult and impractical to attempt to find harmonic mappings from T^n to $SE(3)$ corresponding to revolute-joint spatial mechanisms. If prismatic joints are allowed, however, it is easy to see that a 3R spherical chain attached to a Cartesian positioning device (*i.e.*, three prismatic joints linked serially so that they form an orthogonal frame) is a six degree-of-freedom mechanism with minimum kinematic distortion; the Cartesian positioning device defines the identity mapping from \mathbb{R}^3 to \mathbb{R}^3 , which is clearly harmonic, and we showed earlier that all spherical open chains are harmonic maps. Since our focus throughout has been on revolute-joint mechanisms, we will consider in this section the kinematic distortion for some basic revolute-joint spatial chains.

We begin our analysis with the basic 3R, two-link spatial chain of figure 5.3. The forward kinematic equations are represented by the map $f(x_1, \dots, x_n) = M e^{A_1 x_1} \cdots e^{A_3 x_3}$, where

$$A_1 = \begin{bmatrix} 0 & 0 & 1 & 0 \\ 0 & 0 & 0 & 0 \\ -1 & 0 & 0 & -L_1 \\ 0 & 0 & 0 & 0 \end{bmatrix}, \quad A_2 = \begin{bmatrix} 0 & -1 & 0 & -L_2 \\ 1 & 0 & 0 & L_1 \\ 0 & 0 & 0 & 0 \\ 0 & 0 & 0 & 0 \end{bmatrix}, \quad A_3 = \begin{bmatrix} 0 & -1 & 0 & -L_2 \\ 1 & 0 & 0 & 0 \\ 0 & 0 & 0 & 0 \\ 0 & 0 & 0 & 0 \end{bmatrix}$$

and

$$M = \begin{bmatrix} 1 & 0 & 0 & L_1 \\ 0 & 0 & -1 & 0 \\ 0 & 1 & 0 & L_2 \\ 0 & 0 & 0 & 1 \end{bmatrix}$$

We determine the link lengths which minimize the kinematic distortion with respect to the left-invariant Riemannian metric $ds^2 = c(d\omega_1^2 + d\omega_2^2 + d\omega_3^2) + d(dv_1^2 + dv_2^2 + dv_3^2)$; the length scale in this case is $\frac{d}{c}$. We follow the same procedure outlined in the analysis of planar and spherical mechanisms. The left differential $J_L(x)$ of this mechanism is

$$J_L(x) = \begin{bmatrix} \sin(x_2 + x_3) & 0 & 0 \\ \cos(x_2 + x_3) & 0 & 0 \\ 0 & 1 & 1 \\ 0 & L_1 \sin x_3 - L_2 & -L_2 \\ 0 & L_1 \cos x_3 & 0 \\ -L_1 \cos x_2 + L_2 \sin(x_2 + x_3) & 0 & 0 \end{bmatrix}$$

The total distortion with respect to the left-invariant metric above then reduces to

$$D(f) = (3L_1^2d + 5L_2^2d + 6c) \cdot 4\pi^3$$

Given the reach constraint $L_1 + L_2 = L$, we can easily determine that the link lengths which minimize the kinematic distortion are

$$L_1 = \frac{5}{8}L, \quad L_2 = \frac{3}{8}L$$

Observe that these link lengths are independent of the choice of scales c and d . Moreover, if $d = 0$, so that the mechanism is regarded as a purely orienting device, the total distortion $D(f)$ is then independent of the link lengths, as expected.

Our usual definition of workspace volume assigns to this mechanism a volume of zero, since the dimension of $\text{Im}(f)$ is less than six. If instead $\text{Im}(f)$ is regarded as a three-dimensional compact subset of $SE(3)$, with a volume form naturally induced from the bi-invariant volume form Ω on $SE(3)$, one can then assign a nontrivial workspace volume to $\text{Im}(f)$. For this particular mechanism f is easily seen to be a 1-1 mapping into $SE(3)$.

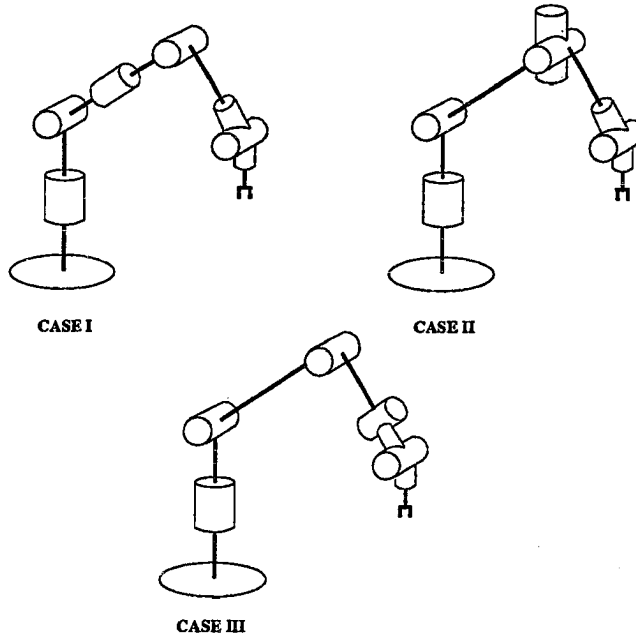


Figure 5.4: Three designs for a 7R manipulator.

By the degree formula, the induced volume of f is given by the integral $\int_{T^3} f^* \Omega$, and is proportional to $8\pi^3 L_1 cd$. In order to maximize the induced volume, L_2 should clearly be zero. If instead we utilized the reachable workspace volume (*i.e.*, the set of points reachable in \Re^3) as our measure, then obviously L_1 should equal L_2 in order for this volume to be maximized.

We now study the kinematic distortion of three particular 7R manipulator designs (see figure 5.4), first investigated by Hollerbach[23]. The three designs are formed by the addition of a revolute joint to a 6R elbow manipulator. All three designs have two principal links and identical workspaces. In case I the chain is obtained by adding a roll motion to the upper arm link of the elbow manipulator; the shoulder joint then becomes a 3R spherical joint, and the chain is kinematically equivalent to the human arm. In case II an additional degree of freedom is added to the elbow rather than the shoulder: only a yaw motion of the elbow results in a two-link design which does not duplicate the case I chain. Finally, in case III an additional degree of freedom is added to the wrist.

We determine numerically the kinematic distortion of these three chains. Assume the

link lengths L_1 and L_2 are both equal. We take the same left-invariant metric on $SE(3)$ parametrized by a length scale factor $\frac{d}{c}$ as before, but with d set to one, and determine the distortion $D(f)$ from the left differential of the forward kinematic map. The following observations can then be made. When c is made arbitrarily small, thereby emphasizing translational motion over rotational motion, the case III chain with the 4R wrist exhibits the smallest amount of kinematic distortion, followed by the case II chain with the elbow yaw, and then the case I chain with the upper arm roll. Intuitively this observation can be explained as follows. As c vanishes, the three chains can be regarded effectively as purely translating devices, so that the range of their forward kinematic map is now taken to be \mathbb{R}^3 . In case I and case II the translating of the end-effector is performed by the first four joints, whereas in case III only the first three joints are involved. Recalling the physical interpretation of the kinematic distortion as a measure of infinitesimal dispersion (see chapter 3), it is evident from dimensional considerations that mapping T^3 into \mathbb{R}^3 (corresponding to case III) should have less distortion than mapping T^4 into \mathbb{R}^3 (corresponding to cases I and II).

If on the other hand c is made arbitrarily large, so that we instead emphasize the rotational capability, the difference in kinematic distortion among the three chains eventually vanishes to zero. This observation also agrees with our intuition, since as strictly orienting devices the three chains are functionally equivalent; imagine L_1 and L_2 shrinking to zero, for example. Our analysis therefore suggests that, with respect to the harmonic mapping distortion, the case III chain with the 4R redundant wrist exhibits the least kinematic distortion for any choice of length scale.

Results of a numerical study with $C(f)$ as the dexterity measure also suggest the same conclusions as those for the kinematic distortion. If $V(f)$ is taken as our performance measure, numerical results then indicate that, independent of the scale factor c , the three cases all have identical values for $V(f)$. The workspace volume $W(f)$ is of course identical for the three cases.

In his analysis[23] Hollerbach proposes four criteria for evaluating the kinematic performance of these chains. They are (i) elimination of internal singularities, (ii) obstacle avoidance, (iii) simplicity of the kinematic equations, and (iv) mechanical constructability. Based on these considerations, he concludes that the case I chain with the spherical shoul-

der joint best satisfies the four criteria. Both the case II and case III chains suffer from poor mechanical constructability, and in addition the case III chain does not eliminate the shoulder singularity which occurs when the wrist lies along the first shoulder joint's axis.

One feature which the kinematic distortion $D(f)$ (or for that matter $V(f)$ and $C(f)$) fails to address is the ability of a mechanism to avoid obstacles in the workspace; it is clear that the case I and case II designs are superior to the case III design in this respect, although for kinematic distortion we saw that the case III design was best. In certain situations it may also be desirable to eliminate particular singularities of a mechanism (such as the case III chain's singularity mentioned above) at the cost of a degradation in a mechanism's overall global dexterity. These and other considerations suggest that in order to obtain a more complete picture of a mechanism's kinematic performance, it would be useful to augment the kinematic distortion criterion with measures for the well-connectedness of a mechanism's workspace, as well as a mechanism's ability to avoid workspace obstacles. In contrast to kinematic dexterity, it would seem that such measures are most naturally formulated as integrals over the workspace rather than the joint space.

5.3 Summary

In this chapter we have analyzed the workspace volume and kinematic dexterity of open-chain spherical and spatial mechanisms. A simple closed-form expression for the workspace volume of general nR spherical mechanisms is first derived. Using the kinematic distortion measure as our criterion for kinematic dexterity, it is shown that all open-chain spherical mechanisms with the same number of degrees of freedom have the same kinematic distortion, regardless of their geometry. We showed in fact that all product-of-exponentials mappings from T^n to $SO(3)$ are harmonic maps of minimum distortion within their homotopy class. The workspace volume would therefore appear to be the principal basis for evaluating the kinematic performance of spherical mechanisms. One can alternatively formulate a normalized dexterity measure, the distortion per volume, which is given by $D(f)/W(f)$: such a normalized measure provides a fair means of comparing the kinematic distortion between mechanisms with different workspace volumes.

For spatial mechanisms we briefly summarize results by Paden and Sastry on the 6R

manipulator geometry which maximizes workspace volume. We then determine the link lengths for a two-link, 3R open chain which minimize the kinematic distortion, and also compute the kinematic distortion for three basic 7R open chains, considered originally by Hollerbach[23]. Results of our analysis suggest that measures for obstacle and singularity avoidance are fundamentally different from measures for kinematic dexterity.

Chapter 6

Conclusions

6.1 Summary

In this thesis we have focused our attention on kinematic issues that arise in evaluating the performance of robotic mechanisms. The two fundamental performance criteria we have considered are the kinematic dexterity and workspace volume. While a number of mathematical measures for these two aspects of kinematic performance have been proposed and studied, we believe that our geometric approach provides a natural, coordinate-invariant means of quantifying kinematic performance. Obviously kinematic dexterity and workspace volume are intrinsic properties of a mechanism, independent of any particular coordinate representation of the kinematics. By regarding the forward kinematics of a mechanism as defining a mapping between Riemannian manifolds, we are able to use the coordinate-free language of geometry to investigate these intrinsic properties of mechanisms. The main contributions of each chapter are now summarized.

In chapter 2 we developed the necessary geometrical framework for studying the kinematics of mechanisms, and in particular reviewed the important geometric properties of Euclidean motions. The principal connection between kinematics and geometry was established by regarding the kinematics of a mechanism as defining a mapping between Riemannian manifolds. In addition to summarizing the more well-known facts about Euclidean motions, we also expressed many of the intrinsic quantities of $SE(3)$ in the coordinates of the *first* and *second kind*. The family of translation-invariant metrics on $SE(3)$ were then

discussed in terms of these coordinates.

The product-of-exponentials (POE) formula is a general representation for the forward kinematics of spatial open chains. While this representation is clearly of geometric appeal, we showed that it is also useful for practical applications, made even more attractive by some of its device-independent features. A scheme for computing the kinematics and Jacobian of a mechanism based on table lookup of the matrix exponentials, we showed, had computational requirements which were comparable with the more conventional recursive methods. Some recent findings on kinematic calibration methods also suggest that the POE equations may have certain advantages over the standard Denavit-Hartenberg four-parameter representation; this would seem to merit further investigation.

The two fundamental kinematic performance measures of interest considered in this thesis are the workspace volume and kinematic dexterity. In chapter 3 we formulated geometric measures for these performance features which are coordinate-invariant, and also take into account the topological and metric structure of $SE(3)$. Because $SE(3)$ admits a bi-invariant volume form there exists a natural notion of workspace volume. The integral functional of harmonic mapping theory also provides a natural means of characterizing a mapping's distortion, and we have shown that this functional is a physically meaningful measure of kinematic dexterity. This particular notion of kinematic distortion is a *global, first-order* dexterity measure; it is an integral measure which involves first derivatives of the kinematic map. After outlining a method for specifying coordinate-invariant functionals, we also proposed a number of alternative first-order kinematic dexterity measures, in particular the coordinate-invariant formulations of Yoshikawa's manipulability index[45] and Salisbury and Craig's condition number-based dexterity measure[41]. We also formulated a class of second-order kinematic dexterity measures based on the Ricci curvature tensor of the range manifold.

The definitions of distortion given here depend on the choice of Riemannian metrics on the configuration space and $SE(3)$. For this reason we discussed the physical implications of various metrics. In particular, for revolute-joint mechanisms, whose domain is the flat torus T^n , the particular choice of flat metric can be interpreted physically as the maximum allowable velocities of the joint actuators. Among the translation-invariant metrics on

$SE(3)$, we argued in chapter 2 that the left-invariant metrics were intrinsic, *i.e.*, defined with respect to a body-attached frame. For kinematic chains this has the desirable property that measures defined with respect to left-invariant metrics are invariant under rotations and translations of the base. A particular form of left-invariant metric on $SE(3)$ was therefore proposed which employs the bi-invariant metric on $SO(3)$, and also captures the isotropy and length-scale of \mathbb{R}^3 . These ideas were illustrated by a simple but nontrivial example of a 2R mechanism, regarded as a mapping from the two-torus to the two-sphere.

In chapter 4 we evaluated the performance of some basic planar mechanisms using these kinematic measures. The link lengths for a 3R open chain which maximize the workspace volume were found to be in the ratio $L_1 = L_2, L_3 = 0$, where L_1 is the base link. We also classified the singular configurations of planar n -link open chains. The link lengths for an n -link planar chain ($n \geq 3$) which minimize kinematic distortion were found to be in the ratio $(1, 1/2, \dots, 1/n)$, proceeding from the base to tip. An interesting observation is that the link lengths of human fingers more or less approximate this ratio. The peak actuator velocities which minimize kinematic distortion were also found to progressively decrease from the base outwardly to the distal joint. We then considered the kinematic distortion of a simple three degree-of-freedom closed chain, and showed that for a certain set of link parameters it exhibited less kinematic distortion than its open chain counterpart. All of these results were found to be independent of the choice of length scale.

In chapter 5 we considered the kinematic distortion and workspace volume of spherical and spatial mechanisms. The compactness of $SO(3)$ allows us to make particularly strong and concise statements about the kinematic properties of spherical mechanisms. We first derived a closed-form expression for the workspace volume of open-chain spherical mechanisms, defined with respect to its bi-invariant volume form. It was then shown that all open-chain spherical mechanisms with the same number of degrees of freedom also have the same kinematic distortion, regardless of its geometry. In fact, all product-of-exponentials mappings from T^n to $SO(3)$ were shown to be harmonic maps of minimum distortion within their homotopy class. We also showed that the second-order distortion measure based on the Ricci curvature coincides with the harmonic mapping distortion for spherical mechanisms. These results suggest that the workspace volume and singularities are the primary

kinematic criteria for robotic wrists. The singularities of general nR spherical open chains were also identified.

For spatial mechanisms we first determined that the link lengths which minimize kinematic distortion for a basic two-link, 3R spatial chain were in the ratio $L_1 = 5$, $L_2 = 3$, where L_1 is the base link length. A comparative analysis of three 7R manipulator designs, originally considered by Hollerbach[23], was then undertaken. While the workspace volumes of these three cases were identical, a numerical study revealed that the case III design with the redundant 4R wrist exhibited the least amount of kinematic distortion of the three designs. Apparently this can be traced to the informal observation that mapping a four-dimensional domain onto a three-dimensional range inherently has more distortion than mapping a three-dimensional domain onto the same range. This finding illustrates some of the kinematic properties not captured by our notion of kinematic dexterity and workspace volume, *e.g.*, a mechanism's ability to avoid workspace obstacles, or the well-connectedness of the workspace.

As a step toward obtaining a more complete picture of a mechanism's kinematic performance, a logical extension of our work could be to augment the kinematic distortion and workspace volume measures with measures for the well-connectedness of the workspace, as well as a mechanism's ability to avoid workspace obstacles. It seems that the primary advantages of redundant mechanisms over the nonredundant ones are precisely their ability to avoid obstacles and singularities, and their ability to overcome joint limits. At present it is not clear what the appropriate mathematical formulations of these performance features should be, although it is clear that for obstacle avoidance a snake-like arm is superior to other geometries. These issues merit further investigation.

6.2 Dynamics

In chapter 1 we observed that dexterity cannot be considered a purely kinematic property, since a mechanism's movement is determined by its dynamic equations of motion. A mechanism, from a kinematic viewpoint, can be regarded as an input-output device, whereby a given input joint velocity produces a velocity of the end-effector. This view afforded an interpretation of kinematic distortion as a measure of the uniformity of the velocity gain or,

alternatively, as the uniformity of the force-torque gain (since static force relationships obey the identity $\tau = J^T \mathcal{F}$, where τ is the joint torque vector, \mathcal{F} is the end-effector force vector, and J^T is the Jacobian transpose). From the perspective of dynamics a mechanism's inputs can instead be regarded as joint torques, and the corresponding outputs are end-effector accelerations. The internal state of the mechanism is determined by the joint positions and velocities. By an analogy with the kinematics, dexterity can be characterized as the uniformity of this torque-acceleration gain.

How might the mathematical formulation of this idea proceed? To begin, the dynamic equations of a manipulator are given according to the Lagrangian formulation by

$$\tau = M(\Theta)\ddot{\Theta} + V(\Theta, \dot{\Theta}) + G(\Theta)$$

where τ is the joint torque vector, Θ is the joint position vector, $M(\Theta)$ is the inertia matrix, and $V(\Theta, \dot{\Theta})$, $G(\Theta)$ are the Coriolis and gravity terms. $M(\Theta)$ can formally be regarded as a symmetric, positive-definite two-tensor on the configuration space, and the Coriolis term $V(\Theta, \dot{\Theta})$ is derived from the derivative of $M(\Theta)$. On the other hand, the kinematic equations imply that $\ddot{x} = J(\Theta)\ddot{\Theta} + \dot{J}(\Theta)\dot{\Theta}$, where x denotes the end-effector position and each dot denotes time differentiation. Combining these relationships, the torque-acceleration gain is given by

$$\ddot{x} = J(\Theta)M^{-1}(\Theta)\tau - [J(\Theta)M^{-1}(\Theta)(V(\Theta, \dot{\Theta}) - G(\Theta)) + \dot{J}(\Theta)\dot{\Theta}]$$

If one assumes that the manipulator is always at rest initially, the term in brackets can be ignored, and the linear torque-acceleration gain is given by $J(\Theta)M^{-1}(\Theta)$. This linear transformation assumes the role of the Jacobian in the expression for a dynamics-based distortion density, $\hat{d}(f)$:

$$\begin{aligned}\hat{d}(f) &= \frac{1}{2}\text{Tr}((JM^{-1})^T G (JM^{-1})H^{-1}) \\ &= \frac{1}{2}\text{Tr}(J^T G J (M^T H M)^{-1})\end{aligned}$$

H and G in this definition are again the Riemannian metrics on the domain and range of the forward kinematic map f , respectively. It is easily verified that this expression is invariant with respect to coordinate changes. Note that $\hat{d}(f)$ is obtained by simply replacing the

metric H in the usual definition of the distortion density $d(f)$ by $M^T H M$, so that it now reflects the manipulator's inertia.

As a simple example consider a basic two-link planar open chain, regarded as a map into \mathbb{R}^2 , whose inertia tensor is

$$M(\Theta) = \begin{bmatrix} m_1 L_1^2 + m_2(L_1^2 + L_2^2 + 2L_1 L_2 \cos \theta_2) & m_2(L_2^2 + L_1 L_2 \cos \theta_2) \\ m_2(L_2^2 + L_1 L_2 \cos \theta_2) & m_2 L_2^2 \end{bmatrix}$$

where m_i and L_i are the mass and length of link i , respectively. This inertia tensor models the link mass as a point mass situated at the end of the link. Suppose the dexterity measure is taken to be the integral $\int_{T^2} \hat{d}(f) dx$, where we take the usual Euclidean metric on \mathbb{R}^2 . If the m_i are set equal (a reasonable assumption for direct-drive arms, since the actuator masses dominate), the optimal link lengths which minimize this measure are in the ratio $L_1 = 1, L_2 = 2$. If the m_i are assumed to vary linearly with L_i , the optimal link lengths are then found to be in the ratio $L_1 = 2, L_2 = 3$. In contrast to the kinematic distortion results, we find that the base link is shorter than the outer link for both cases.

This particular measure of dexterity, which we call the *dynamic distortion*, measures the ease with which the end-effector can, starting at rest, accelerate (or apply forces) in arbitrary directions. If the assumption of starting at rest were suspended, then in general the Coriolis and gravity terms of the dynamics equations cannot be ignored. In [22] Hollerbach gives several examples of trajectories for general manipulators, in which all the dynamic terms are significant relative to each other. Unlike the kinematic case, where the velocity gain is given by a simple linear transformation (the Jacobian), the situation in dynamics is nonlinear and considerably harder. Moreover, for many manipulators the actuator dynamics are often significant. Unfortunately there does not appear to be a natural way of including actuator dynamics, Coriolis and gravity terms into a simple dynamic dexterity measure which also assumes arbitrary initial velocities.

A geometrical framework for considering dynamics problems of this nature might be constructed as follows. Because work is the time-integral of force and linear velocity (or torque and angular velocity), forces and torques are most naturally thought of as belonging to a linear algebraic dual of the velocity space. The kinematics and dynamics can then be considered within a common framework based on pullbacks of vector bundles. More

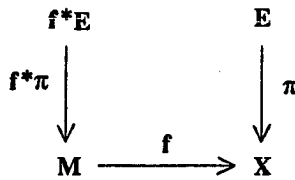


Figure 6.1: The pullback of a vector bundle.

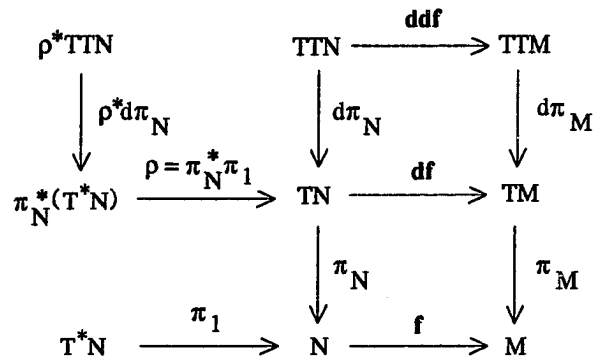


Figure 6.2: A mechanical system.

specifically, if $\pi : E \rightarrow X$ is a vector bundle and $f : M \rightarrow X$ is a smooth map, one can then construct a vector bundle over M , called the pullback bundle and denoted by $f^*\pi : f^*E \rightarrow M$; the base space is M , and the fibers are $\pi^{-1}(f(m))$ (see figure 6.1).

For mechanisms we then have the picture given in figure 6.2, where N is the configuration space, M is the group of Euclidean motions, f is the forward kinematic map, π_1 , π_N , and π_M are the standard projections, and the dynamic equations define a section on the vector bundle $\rho^*d\pi_N : \rho^*(TTN) \rightarrow \pi_N^*(T^*N)$. One might attempt to formulate within this framework a dexterity measure based on a suitable mapping from $\pi_N^*(T^*N)$ to TTM . It is not at all clear what the metrics should be, however, and any such criterion would also be a third-order measure. At this point it seems appropriate to pause and ask what the important dynamic performance criteria really are. One possible notion could be in terms of a manipulator's "efficiency": given a set of end-effector trajectories, which manipulator design executes these trajectories in the most efficient manner possible? One possibility might be the total energy expended by the mechanism. The complexity of the dynamic equations clearly makes the task of formulating dexterity in this context much harder, and

a wide range of related questions deserving further attention are raised.

6.3 Concluding Remarks

In this thesis we have investigated a geometric approach to understanding the kinematic performance of mechanisms. By focusing on the two specific but fundamental criteria of kinematic dexterity and workspace volume, we have provided a set of analytical tools for optimal kinematic design. In this regard a novel application of harmonic mapping theory to kinematic dexterity is presented. Although we have formulated the workspace volume and kinematic dexterity in a natural way, it appears that other measures are needed to describe other facets of kinematic performance, such as a mechanism's ability to avoid obstacles. It is hoped that ultimately these geometric methods will fit into an integrated theory of mechanical design, one that includes other design factors like control, actuation, and material properties.

Bibliography

- [1] R. Abraham and J. E. Marsden, *Foundations of Mechanics*. Reading, Massachusetts: The Benjamin/Cummings Publishing Co., 1978.
- [2] V. I. Arnold, *Mathematical Methods of Classical Mechanics*. New York: Springer-Verlag, 1978.
- [3] H. Asada, “A geometrical representation of manipulator dynamics and its application to arm design,” *Journal of Dynamic Systems, Measurement, and Control*, vol. 105, pp. 131–135, 1983.
- [4] P. Baird, *Harmonic Maps with Symmetry, Harmonic Morphisms and Deformation of Metrics*. Vol. 87 of *Research Notes in Mathematics*, Boston: Pitman, 1984.
- [5] R. W. Brockett, *Finite Dimensional Linear Systems*. New York: J. Wiley & Sons, 1970.
- [6] R. W. Brockett, “Robotic manipulators and the product of exponentials formula,” in *Proceedings MTNS-83 International Symposium*, (Beer Sheba, Israel), pp. 120–129, 1983.
- [7] R. W. Brockett, “On the computer control of movement”, in *1988 IEEE Conference on Robotics & Automation*, (Philadelphia), April 1988.
- [8] R. W. Brockett, “Some mathematical aspects of robotics”, in *Robotics*, vol. 41 of AMS Short Course Lecture Notes, Providence:American Mathematical Society, 1990.

- [9] R. W. Brockett and J. Loncaric, "The geometry of compliance programming," in *Theory and Application of Nonlinear Control Systems*, C. I. Byrnes and A. Lindquist, Eds., Amsterdam: North Holland, 1986.
- [10] S. S. Chern and S. I. Goldberg, "On the volume-decreasing property of a class of real harmonic mappings," *American Journal of Mathematics*, vol. 97, pp. 133–147, 1975.
- [11] C. Chevalley, *Theory of Lie Groups*. Princeton: Princeton University Press, 1946.
- [12] Y. Choquet-Bruhat, C. DeWitt-Morette, & M. Dillard-Bleick, *Analysis, Manifolds and Physics: Part I*. Amsterdam: North Holland, 1982.
- [13] J. Duffy, *Analysis of Mechanisms and Robot Manipulators*. New York: Halsted Press, 1980.
- [14] J. Eells and J. H. Sampson, "Harmonic mappings of Riemannian manifolds," *American Journal of Mathematics*, vol. 86, pp. 109–160, 1964.
- [15] J. Eells and L. Lemaire, "A report on harmonic maps," *Bulletin London Mathematical Society*, vol. 10, pp. 1–68, 1978.
- [16] J. Eells and L. Lemaire, "Another report on harmonic maps," *Bulletin London Mathematical Society*, vol. 20, pp. 385–524, 1988.
- [17] G. Golub and C. F. Van Loan, *Matrix Computations*. Baltimore: The Johns Hopkins University Press, 1983.
- [18] C. Gosselin and J. Angeles, "A new performance index for the kinematic optimization of robotic manipulators," in *20th ASME Mechanisms Conference*, (Kissimmee, Florida), pp. 441–447, 1988.
- [19] V. W. Guillemin and A. Pollack, *Differential Topology*. Englewood Cliffs, New Jersey: Prentice-Hall, Inc., 1974.
- [20] K. C. Gupta, "On the nature of robot workspace," *The International Journal of Robotics Research*, vol. 5, no. 2, pp. 112–121, 1986.

- [21] S. A. Hayati, "Robot arm geometric link parameter estimation," in *22nd IEEE Conference on Decision and Control*, (San Antonio), pp. 1477–1483, December 14–16, 1983.
- [22] J. M. Hollerbach, "Dynamics", in *Robot Motion: Planning and Control*, edited by J. M. Brady, J. M. Hollerbach, T. Lozano-Perez, and M. T. Mason. Cambridge: MIT Press, 1982.
- [23] J. M. Hollerbach, "Optimum kinematic design of a seven degree of freedom manipulator", in *Robotics Research: The Second International Symposium*, edited by H. Hanafusa and H. Inoue. Cambridge: MIT Press, 1985.
- [24] J. M. Hollerbach, "A survey of kinematic calibration", in *The Robotics Review I*, edited by O. Khatib, J. J. Craig, and T. Lozano-Perez. Cambridge: MIT Press, 1989.
- [25] K. Hunt, *Kinematic Geometry of Mechanisms*. Oxford: Oxford University Press, 1978.
- [26] C. A. Klein and B. E. Blaho, "Dexterity measures for the design and control of kinematically redundant manipulators," *The International Journal of Robotics Research*, vol. 6, no. 2, pp. 72–83, 1987.
- [27] A. Kumar, and K. J. Waldron, "The workspaces of a mechanical manipulator," *ASME Journal of Mechanical Design*, vol. 103, pp. 665–672, 1981.
- [28] J. Loncaric, *Geometric Analysis of Compliant Mechanisms in Robotics*. PhD thesis, Division of Applied Sciences, Harvard University, 1985.
- [29] O. Ma and J. Angeles, "The concept of dynamic isotropy and its applications to inverse kinematics and trajectory planning," in *1990 IEEE International Conference on Robotics and Automation*, (Cincinnati), pp. 481–486, April 1990.
- [30] J. M. McCarthy, *Introduction to Theoretical Kinematics*. Cambridge: MIT Press, 1990.
- [31] D. Orin and W. Schrader, "Efficient computation of the jacobian for robot manipulators," *The International Journal of Robotics Research*, vol. 3, no. 4, 1984.
- [32] B. Paden and S. S. Sastry, "Optimal kinematic design of 6R manipulators," *The International Journal of Robotics Research*, vol. 7, no. 2, 1988.

- [33] F. Park and R. Brockett, "Harmonic maps and the optimal design of mechanisms", in *1989 IEEE Conference on Decision and Control*, (Tampa), December 1989.
- [34] F. Park, "On the optimal kinematic design of spherical and spatial mechanisms", in *1991 IEEE International Conference on Robotics and Automation*, (Sacramento), April 1991.
- [35] F. Park, "Motion control using the product-of-exponentials kinematic equations", in *1991 IEEE International Conference on Robotics and Automation*, (Sacramento), April 1991.
- [36] R. P. Paul, *Robot Manipulators: Mathematics, Programming, and Control*. Cambridge: MIT Press, 1981.
- [37] A. I. Pluzhnikov, "Some properties of harmonic mappings in the case of spheres and Lie groups," *Soviet Mathematics Doklady*, vol. 27, pp. 246–248, 1983.
- [38] B. Roth, "Performance evaluation of manipulators from a kinematic viewpoint," in *Performance Evaluation of Programmable Robots and Manipulators*, Bethesda, Maryland: National Bureau of Standards, pp. 39–61, 1975.
- [39] B. Roth, "Kinematic design for manipulation," in *NSF Workshop on Research Needed to Advance the State of Knowledge in Robotics*, University of Rhode Island, pp. 110–118, 1980.
- [40] F. Salam and C. Yoon, "On the computational aspect of the matrix exponentials and their use in robot kinematics," *IEEE Transactions on Automatic Control*, vol. 3, no. 4, 1986.
- [41] J. K. Salisbury and J. J. Craig, "Articulated hands: force control and kinematic issues," *The International Journal of Robotics Research*, vol. 1, no. 1, pp. 4–17, 1982.
- [42] M. Spivak, *Calculus on Manifolds*. Menlo Park, California: The Benjamin/Cummings Publishing Co., 1965.
- [43] M. Spivak, *A Comprehensive Introduction to Differential Geometry, Vol. 1 & 2*. Berkeley, California: Publish or Perish, Inc., 1979.

- [44] G. Toth, *Harmonic and Minimal Maps with Applications to Geometry and Physics*. Chichester, England: Ellis Horwood, Ltd., 1984.
- [45] T. Yoshikawa, "Manipulability of robotic mechanisms," *The International Journal of Robotics Research*, vol. 4, no. 2, pp. 3-9, 1985.
- [46] T. Yoshikawa, "Dynamic manipulability of robot manipulators," in *1985 IEEE International Conference on Robotics and Automation*, (St. Louis), pp. 1033-1038, March 1990.